**Nanooptics with Surface Plasmons
and Resonant Nanoparticles**

**Nanooptik mit Oberflächenplasmonen
und Resonanten Nanopartikeln**

Der Fakultät für Mathematik und Physik
der Leibniz Universität Hannover
zur Habilitation
für das Fachgebiet Physik
vorgelegte wissenschaftliche Arbeit von

Professorial Dissertation for Habilitation of

– Dr. rer. nat. Carsten Reinhardt –
geboren am 08. März 1972
in Gronau / Leine

2014

Titel image:

The upper image shows an electron microscopy image of gold nanoparticles generated and arranged in the form of the word "NANO" on a gold film covered glass substrate.

The second image from the top is a dark-field image recorded with an optical microscope, showing the far-field scattering of the particles.

The third image from the top shows the same particles as above, acting as local scattering centers for surface plasmon-polaritons. The image is recorded by leakage radiation microscopy

The bottom image is a numerical simulation of the surface plasmon excitation and propagation on the nanoparticles using a Green's function approach.

Contents

Kurzzusammenfassung (German)

Die Entwicklung der Nanooptik und Nanophotonik als Wissenschaften der Wechselwirkung von Licht mit nanostrukturierter Materie ist eng an die Fortschritte der Mikro- und Nanotechnologie zur Herstellung metallischer oder dielektrischer Strukturen gebunden. Sie erfordert anspruchsvolle Detektions- und Visualisierungstechniken sowie neue theoretische Methoden, um Einblicke und Verständnis in das Verhalten von elektromagnetischen Feldern auf der Subwellenlängen-Ebene zu erhalten. Ziele der Arbeiten zu dieser Habilitationsschrift sind die Erforschung laserbasierter Herstellungsverfahren für nanooptische Systeme in den Bereichen Plasmonik und Metamaterialien, deren Charakterisierung mit modernen und teilweise neuentwickelten optischen Methoden und die Verbesserung numerischer Simulationen zur Beschreibung der experimentellen Resultate.

Im Rahmen dieser Arbeit wurde ein Zweiphotonen-Laserfertigungsverfahren zur schnellen und flexiblen Herstellung von mikromechanischen und mikrooptischen Systemen mit Auflösungen unter 100 nm entwickelt. Gleichzeitig wurden neuartige biodegradierbare Polymere, Hybridpolymere mit hohem Brechungsindex und selektiv metallisierbare Kunststoffe für die Zweiphotonenstrukturierung synthetisiert und erprobt. Aus den anfänglich experimentellen Versuchsaufbauten wurde ein heutzutage kommerziell erhältliches Gerät entwickelt.

Weiterhin wurde die Anwendbarkeit dieser Technologie zum Prototyping von plasmonischen Komponenten und Wellenleitern untersucht, wobei erste polymerbasierte dielektrische Wellenleiter für Oberflächenplasmonen demonstriert werden konnten. Anregung, Ausbreitung und Wechselwirkung propagierender Oberflächenplasmonen wurden mit modernen Methoden der Leckstrahlungsmikroskopie und Photoelektronen-Emissions-Mikroskopie studiert. Mit den hergestellten Strukturen konnten effiziente Licht-Plasmon-Kopplung, verschiedene Fokussierungsschemata und Steuerung der Oberflächenplasmonenausbreitung gezeigt werden. Zur Abbildung lokalisierter plasmonischer Anregungen und optischer Nahfeldverteilungen innerhalb und außerhalb von stabförmigen und chiralen metallischen Nanopartikeln, die als optische Antennen dienen, wurden neuartige Methoden auf Basis resonanter Vierphotonenabsorption und ultraschneller Schmelzdynamik untersucht.

Insbesondere sind sphärische Nanopartikel von großem Interesse für die Nanooptik, da sich ihre optischen Eigenschaften in einer homogenen Umgebung analytisch beschreiben lassen. Zur schnellen Herstellung von Goldnanopartikeln mit kontrollierbarem Durchmesser und kontrollierbarer Position auf einem Substrat wurde der laserinduzierte Materialtransfer durch ultrakurze Laserpulse entwickelt. Die optischen Eigenschaften und die Anregung höherer elektrischer Multipolmomente dieser Partikel wurden mittels spektroskopischer Methoden und Leckstrahlungsmikroskopie von Plasmonenstreuung untersucht. Als Demonstratoren für ihren Einsatz als Grundelemente von Metamaterialien wurden hochsensible, einfach zu handhabende Sensorflächen realisiert, mit denen bei

einem Detektionslimit von 10^{-7} RIU nahezu Empfindlichkeiten von kommerziellen Oberflächenplasmonresonanz-Sensoren erreicht werden konnte.

Zusätzlich konnte erstmals eine kontrollierte Herstellung von sphärischen Siliziumnanopartikeln in Bezug auf Größe und Position auf einer Substratoberfläche demonstriert werden. Mit den produzierten sphärischen Nanopartikeln konnte magnetische Dipolstreuung bei optischen Frequenzen mit Einzelpartikelspektroskopie nachgewiesen werden. Es wurde weiterhin gezeigt, dass die Anregung des magnetischen Dipols direkt auf die Wirkung des magnetischen Feldes des Lichts zurückzuführen ist, was sie besonders als Bausteine für rein dielektrische Metamaterialien interessant macht.

Die Streueigenschaften von Nanopartikeln wurden neben Finite-Differenzen-Simulationen in der Zeitdomäne mit der Methode der Greenschen Funktion in der diskreten Dipolnäherung berechnet. Für diese wurde eine Umformulierung eingeführt, womit es erstmals möglich wurde Zugang zu den einzelnen Streumultipolmomenten auch für beliebig geformte Partikel zu erhalten.

Abstract (English)

The development of nanooptics and nanophotonics as the sciences of light interactions with nanostructured matter is closely linked to progress in micro- and nanostructuring technologies for the fabrication of suitable metallic and dielectric structures. Sophisticated detection and visualization techniques as well as novel theoretical methods are further required, in order to obtain insights into and knowledge about the behaviour of electromagnetic fields at subwavelength scales. The goals of the work for this professorial dissertation are investigations of laser-based fabrication technologies for nanooptical systems in the fields of plasmonics and metamaterials, the characterization of these systems with modern and newly developed optical methods, and the improvement of numerical techniques for the description of experimental results.

In the frame of this work, two-photon laser fabrication has been developed for fast and flexible fabrication of micromechanical and microoptical systems with spatial resolutions in the sub-100 nm region. At the same time, novel biodegradable, high refractive index, and selectively metallizable polymer materials have been synthesized and tested for two-photon structuring. The initial experimental setups have been improved into nowadays commercially available systems.

Furthermore, the application of this technology for prototyping of plasmonic components and waveguides has been investigated and first dielectric polymer waveguides for surface plasmons have been demonstrated. Excitation, propagation, and interactions of propagating surface plasmons have been studied using novel methods of leakage radiation microscopy and photoelectron emission microscopy. With the fabricated structures efficient light-plasmon-coupling and different schemes for their focussing and routing have been presented. Novel methods for imaging plasmonic excitations and near-field distributions inside and outside of rod-like and chiral metallic nanoparticle, acting as optical antennas, based on resonant four-photon absorption and ultrafast melt dynamics have been investigated.

Of special interest for nanooptics are spherical nanoparticles, since their optical properties in homogeneous environments can be described analytically. Laser-induced material transfer using ultrashort laser pulses has been developed for fast production of spherical gold nanoparticles with controlled sizes and positions on receiver substrates. The optical properties and the occurrence of higher electric multipole excitations of the generated particles have been investigated by optical spectroscopy and leakage radiation microscopy of surface plasmon scattering. As demonstrators for their use as basic elements of metamaterials novel highly sensitive and easy to use sensor planes have been realized, achieving with their detection limit of 10^{-7} RIU nearly the responsivity of commercially available surface plasmon resonance sensors.

Additionally, a controlled production of spherical silicon nanoparticles, with respect to sizes and positions, has firstly been demonstrated. With the realized particles it has been

possible to show magnetic dipole scattering at optical frequencies using single particle spectroscopy. It has further been verified that the excitation of the magnetic dipole of a silicon particle is a direct reaction on the magnetic field of light, opening new ways for the realization of all-dielectric metamaterials.

The scattering properties of nanoparticles have been calculated using finite-difference time-domain simulations and the Green's function method in the discrete dipole approximation. For the latter, a reformulation has been introduced, with which it became possible for the first time to obtain contributions of individual multipole moments to the total scattering for arbitrary shaped particles.

1 Introduction

Nanooptics with surface plasmons (SPs), i.e. propagating surface plasmons-polaritons (SPPs) on plane and structured metal films and localized surface plasmons (LSPs) in resonant metallic nanoparticles, has attracted a lot of attention during the last years due to the unique properties of metals at optical frequencies. These properties arise from the negative permittivity of metals in certain regions of the electromagnetic spectrum. Examples of important plasmonic applications are metal film surface plasmon resonance (SPR) sensors, the gold nanoparticle based home pregnancy test, surface enhanced Raman scattering, and scanning near-field optical microscopes. All these devices are already commercially available and draw their functionality from the excitation of SPPs and LSPs by optical fields.

The linear scattering properties of metallic nanoparticles due to LSP excitations provide persistent and non-bleaching colorants. Large area metallic nanoparticle arrays may open new ways to the design of novel sensor concepts and plasmonic-enhanced photovoltaic cells. The field enhancement connected with plasmonics and the localization of electromagnetic fields to metallic surfaces is the basis for advanced sensing applications and strong nonlinear effects. Propagating SPPs in plasmonic waveguiding structures provide further potential for chip-scale optical data transport as an alternative to or in combination with silicon photonics, due to the high field confinement, which is achievable with metallic structures. In addition, they resemble a model system for a two dimensional optics, allowing investigating propagation effects, phase shifts, and electromagnetic fields in spaces with varying refractive indices.

Plasmonic excitations in complex metallic nanostructures with non-spherical building blocks can further lead to resonant response to magnetic fields at optical frequencies. The metal's permittivity in such artificial 3D metamaterials or 2D metasurfaces together with the magnetic permeability, which can substantially deviate from unity at resonance, can result in unusual optical properties, e.g. designable and even negative refractive indices.

However, the drawback of metallic nanostructures is their inherent Ohmic loss. To overcome this limitation, initially amplification schemes have been suggested for SPPs, SP waveguides, nanoparticles, and metamaterials. During the last years, the focus has been set more on avoiding losses by use of all-dielectric metamaterials composed of submicron and nanoscale particles of high refractive index. Materials such as silicon and silicon carbide have been investigated within the last years. They provide a valuable alternative to metal structures, as they exhibit high quality electric and magnetic dipole Mie resonances in the visible and near-infrared spectral ranges.

Development of advanced plasmonic and metamaterial structures and future progress in nanooptics requires advanced fabrication technologies, innovative optical near- and far-field characterization methods, and theoretical and numerical simulations of electromagnetic fields inside the realized functional metallic or dielectric nanostructures.

Connected to these requirements, the work presented in this thesis has been focussed

on the application of advanced laser technology for the realization of plasmonic excitation and waveguiding structures as well as metallic and dielectric nanoparticles, potentially serving as building blocks for metamaterials. For characterization of the fabricated plasmonic components and particles, novel near- and far-field methods have been applied and newly developed. To understand the behaviour of light in these nanostructures, existing numerical methods have been applied and novel theoretical approaches have been developed.

This thesis covers the following topics:

- **Development of fabrication technologies for rapid prototyping of photonic and plasmonic components and nanoparticle structures**

- **Optical near- and far-field characterization of nanophotonic structures and plasmonic waveguides**

- **Theoretical and numerical simulation of light in nanostructures**

Novel ultrashort pulse laser fabrication technologies for photonic and plasmonic micro- and nanostructures as well as for metallic and dielectric nanoparticles have been investigated. A prototyping technology for microoptic, micromechanic, and microfluidic components based on two-photon polymerization (2PP) has been set up and developed into a commercially available product. This fabrication method has been applied to prototyping of plasmonic structures for excitation and manipulation of SPPs, and first dielectric polymer SPP waveguides have been realized.

Laser-induced transfer (LIT) technology has been developed for the generation of metallic meso- and nanoparticles, with diameters >200 nm and <200 nm, respectively. It has further been improved for the first controlled production of spherical silicon nanoparticles. These particles can serve as building blocks for metal-dielectric and all-dielectric metamaterials and metasurfaces. They further can be combined with polymer micro- and nanostructures realized by 2PP, providing potential for novel nanooptical systems, plasmonic components, and highly efficient plasmonic metamaterial sensors. Optical properties of the produced nanoparticles have been investigated by surface enhanced Raman scattering (SERS) and single particle spectroscopy (SPS).

The properties of plasmonic excitation and waveguiding components as well as of metallic and dielectric nanoparticles and nanoparticle systems have been investigated using near- and far-field methods. Scanning near-field optical microscopy (SNOM) and leakage radiation microscopy (LRM) have been applied to a first demonstration of SPP waveguiding in polymer ridges and time-resolved SPP excitation, propagation, and focussing have been investigated by two-photon photoelectron emission microscopy (2PPEEM). Novel nonlinear absorption processes in polymers and ultrafast hydrodynamics in metals have been used for high-resolution imaging of optical near-fields in and around metallic nanostructures. Magnetic response of silicon nanoparticles in the visible spectral range has been demonstrated by SPS.

Significant progress has been achieved in the development of theoretical and numerical methods. The Green's function method in the discrete dipole approximation (DDA) has been reformulated for describing scattering properties of arbitrary shaped nanoparticles.

It has firstly been shown that scattering and absorption cross sections can be decomposed into individual multipole contributions.

A combination of 2PP and LIT fabrication, LRM characterization, and DDA simulations has been used for a first demonstration of multipole SPP scattering from spherical gold particles. Time-resolved interaction of SPPs with a nanoparticle has been investigated by 2PPEEM. The SPP-LSP interaction has been analyzed with DDA and finite-difference time-domain (FDTD) simulations, showing an instantaneous response of the particle's electric dipole and the coherent control of the generated field hotspots.

1.1 Context and Outline of this work

In 2009, photonics has been identified as one of the key enabling technologies for European industry over the next 5 to 10 years [1]. In the same year, the *Nanophotonics Europe Association* has been established [2], in order to promote the European science and technology in the emerging area of nanophotonics [3] and to provide input to roadmap activities for photonics research within the *Horizon2020* framework programme of the European Commission in partnership with the *Photonics21* platform [2, 4, 5].

In 2011, the *Nanophotonics Europe Association* has identified 10 nanophotonics research areas, being expected to have impact on photonic industries [3]. Along with these independent identifications, several contributions to the highlighted research areas have been made within the work related to this thesis. The nanophotonic research highlights, published in the report of the *Nanophotonics Foresight Workshop 2010* are listed below together with the relevant author's contributions, which are arranged in this habilitation treatise:

- *Nanoscale Quantum Optics:*
  Imaging of coherent SPP-LSP interactions [6] and SPP pulse propagation [7]
  Phase singularities in plasmonic metamaterials [8]
  Nonlinear plasmonic enhanced EUV generation [9, 10]

- *All Optical Routing:*
  Direct laser writing of plasmonic components and waveguides [11–20]
  SPP focussing and routing in plasmonic devices [6, 17, 21–23]

- *Plasmonics for Enhanced Magnetic Storage - Near-Field Antennas:*
  Nonlinear near-field characterization of nanoantennas [24]
  Localized heating of plasmonic nanostructures [25, 26]

- *Diagnosis, Therapy, and Drug Delivery using Light:*
  Laser fabrication of microvalves for biomedical applications [27] and microcapsules for drug release [28] using two-photon polymerization
  Biodegradable material synthesis and laser structuring [29]
  Laser fabrication of metallic nanoparticles [30–32]

- *Nanoscale Imaging:*
  Near-field microscopy of SPP waveguides [11]

Aluminium-based plasmonic superlens for deep UV radiation [33]
Imaging of plasmonic near-fields [24–26]

- *Chemical and Biological Sensors at the Molecular Scale:*
  Fabrication of highly ordered nanoparticle arrays for advanced sensing applications
  [8, 31] (Sensitivity 5×10^4 deg./RIU, detection limit 10^{-7} RIU)

- *NanoTagging:*
  Fabrication of nanoparticles and nanoparticle Arrays by laser-induced transfer [8,
  30–32]

- *Manipulation of Light Distribution at the Nanoscale:*
  SPP directing and focussing [6, 22, 34]
  Study of optical response of silicon nanoparticles and silicon nanoparticle arrays
  [35–39],

- *New Processing Technologies for Prototyping:*
  Realization and prototyping of photonic components by 3D direct laser writing
  using two-photon fabrication [40–47]
  Nanoimprint technology for plasmonic waveguides [48–50]

- *Nanophotonic Materials with Tailored Optical Properties:*
  Demonstration of magnetic resonances of silicon nanoparticles [35–37]
  Demonstration of response of silicon nanoparticles to the magnetic field of light [38]
  Control and manipulation of light scattering from silicon nanocylinders [39]

In addition to these application oriented research topics a novel theoretical approach
for the description of light scattering from arbitrary shaped nanoparticles has been es-
tablished [51–53].

The habilitation treatise is structured in the following way:

The development of the fields of photonics and nanooptics and the emergence of the
research areas of plasmonics and optical metamaterials as they are relevant to the present
thesis are reviewed in chapter 2. The efforts which have been made for compensating
Ohmic losses are briefly pointed out and the development towards all-dielectric metama-
terials is outlined
    In chapter 3, the laser direct write two-photon fabrication method with emphasis on the
developed materials is introduced. Realization of two- and three-dimensional polymeric
structures using nonlinear laser direct writing is reviewed.
    In chapter 4, the characteristics of SPPs and SPP waveguides on a semi-infinite metal-
dielectric interface and on thin metal films are given. SPP waveguiding is focussed on
polymeric dielectrically-loaded surface plasmon-polariton waveguides (DLSPPWs) and
polymer-based large mode surface plasmon anti-resonant reflecting optical waveguides
(SPARROWs) for sensing applications. Fabrication methods based on nonlinear laser
direct writing and nanoimprint are presented.

In chapter 5, the optical properties of nanoparticles are summarized within maps for the corresponding scattering efficiencies in dependence on particle size and incident wavelengths using Mie theory. The main focus is put on spherical gold and silicon particles, serving as building blocks for metamaterials and metasurfaces. The novel fabrication methods for metallic and silicon nanoparticles by laser-induced transfer are presented and applications of gold particle metasurfaces for advanced sensing purposes are pointed out.

Chapter 6 summarizes the characterization methods applied in this work, covering scanning near-field optical microscopy (SNOM), leakage radiation microscopy (LRM), two-photon photoelectron emission microscopy (2PPEEM), surface enhanced Raman scattering (SERS), and single particle spectroscopy (SPS). The last section within this chapter deals with field enhancement effects, which have been used for imaging of optical near-fields in plasmonic structures and for the nonlinear generation of extreme ultraviolet radiation.

The theoretical methods used in this thesis are presented in chapter 7, including finite-difference time-domain (FDTD) simulations, the finite element method (FEM), Mie theory, and the Green's function method in the discrete dipole approximation (DDA). Substantial progress has been obtained to improve the DDA for the calculation of scattering properties of arbitrary shaped nanoparticles. Using the newly developed decomposition approach for the scattering moments, it has firstly been possible to obtain quantitative results for the individual contributions of the electric dipole, magnetic dipole, and the electric quadrupole moments of arbitrary shaped particles.

The relevant publications are listed within the chapters 3 to 7.

The work is concluded in chapter 8 and an outlook together with recent developments is given in chapter 9.

2 Nanooptics: Plasmonics and Metamaterials

Optics is perhaps the oldest discipline in natural sciences, beginning with the development of first lenses about 4600 years ago [54]. An early treatise on geometrical optics and reflection of light rays from mirrors has already been given by Euclid 300 BC [55, 56]. A pioneering discovery has been the law of refraction by Ibn Sahl in the year 984, mathematically formulated by Snellius in the 17th century [57, 58], leading to the construction of the microscope around 1590 and 1595, credited to Janssen [55, 59, 60]. This ingenious invention firstly opened the view into the world at micrometer scales and is an important pillar of modern photonics and nanooptics.

Light as an electromagnetic wave has been described mathematically in 1861 to 1865 by Maxwell [61, 62]. The equations, as they are nowadays widely used in optics and photonics, have been given by Heaviside, Gibbs, and Hertz 1884 until 1901 [63–66]. Together with two vectorial constitutive relations, connecting electric and magnetic fields with the material's permittivity and permeability, respectively, Maxwell's equations [67] are the basis for modern electromagnetic engineering and the development of optical imaging systems, operating at the resolution limit.

Photonics has emerged in the 1960th in order to emphasize the aspects of optical engineering, optical data transport, and optical data storage and processing. In analogy to electronics, the term *photonics* has been introduced by Agrain in 1967 for the science of generation, detection, and management of light through guidance, manipulation, and amplification [68]. The development of photonics has been linked to the invention and development of lasers [69], transistors [70], and optical fibers [71, 72], merging concepts of optics and electronics. The achievements of modern photonics are already present in data transport through optical fiber networks, semiconductor lasers in entertainment media, and optical data storage and readout. This development is based on the control of optical fields in microscale dimensions and efforts have been made to further miniaturize and integrate optical components and systems down to the nanometer scale [73–76]. An artistic vision of a fiber-coupled photonic integrated circuit with waveguides, filters, switches, and amplifier components is depicted in Fig.2.1.

Fast progress in photonics is strongly connected to rapid advances in micro- and nanostructuring technologies [77, 78]. To confine light to dimensions below half its wavelength is at first glance not trivial as Bethe [79] and Bouwkamp [80] have shown by calculating the transmission of light through subwavelength holes. Diffraction sets a lower limit to the confinement of free propagating light and is the reason for the limited resolution of optical systems such as the microscope, as has been analyzed by Abbe [81] and Rayleigh [82] in 1873 and 1879, respectively.

Overcoming the diffraction limit inevitably leads to optics in the non-propagating near-field regime. The appearance of optical near-fields with imaginary wave vector components and the limited resolution of optical devices turns out as a direct consequence of Heisenberg's uncertainty principle [83]. However, exploiting the near-field interactions
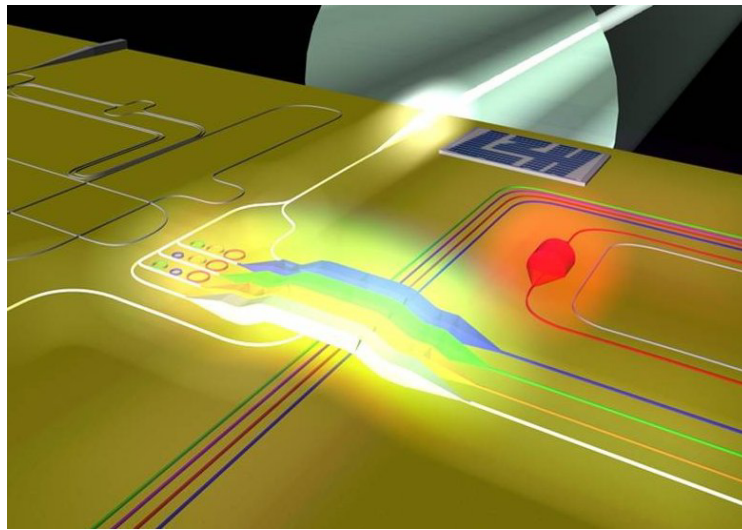
Figure 2.1:
  Vision of photonic circuitry with passive filters, amplification sections, optically controlled switches, and fiber coupling ports to the exterior world.

has led to a new concept for improving optical microscopy. The idea of a near-field optical microscope operating in a scanning mode has been suggested in 1928 by Synge [84] and experimentally realized in 1984 by Pohl et al. [85].

Downscaling the concepts of photonics, e.g. waveguiding components, sensors, and light sources, to the nanometer scale has resulted in the development of *nanophotonics* [1,3,86–88]. Similar like photonics is related to optics, nanophotonics can be regarded as the special discipline in nanooptics, dealing with engineering of light-matter interactions at wavelength or subwavelength scales with naturally or artificially nanostructured matter and the coherent controle of fields inside the nanostructures [89,90]. Metal optics plays an important role for the confinement of light to these dimensions by supporting LSPs or propagating SPPs, which can circumvent the diffraction limit [91–93].

The science of SPs and SPPs can be dated back to the observation of anomalous diffraction properties of gratings by Wood in 1902 [94] and to the theoretical explanation of optical properties of colloidal gold nanoparticles of spherical shape by Mie in 1908 [95]. The breakthrough of surface plasmon physics came in 1998 by the discovery of unusual high light transmission through arrays of subwavelength holes in an optically thick gold foil, sparking a world wide interest in this field of science [96]. It has been found that even more light has been transmitted through the perforated area than light impinging onto the area occupied by the holes themselves, which has been attributed to the excitation and coupling of SPs and SPPs on both sides of the foil. This important observation is shown in Fig.2.2.

Nanophotonics, being viewed initially as a mainly academic field, has nowadays developed into an application driven research area, with potential new products, such as improved solar cells [1,97], high-efficient sensors [8,98], and SP enhanced light sources [99,100].
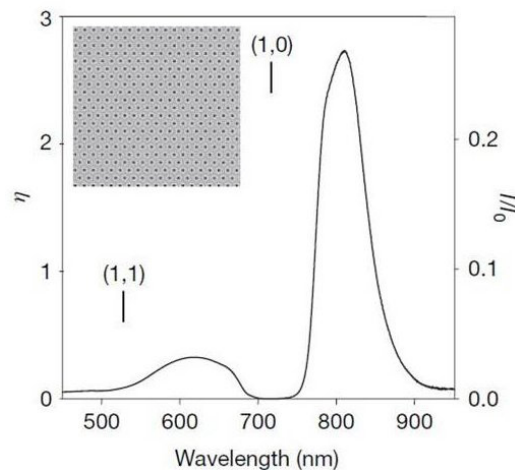
Figure 2.2:
  Extraordinary light transmission through subwavelength holes. Nearly three times more light is transmitted than hitting the holes. (From [96])

Two main research fields, related to this thesis, shall be introduced in the following: Surface-Plasmon Nanophotonics or Plasmonics [101] and Optical Metamaterials [102]. However, the separation between these fields is not strict.

Surface Plasmon Nanophotonics:

The field of surface plasmon nanophotonics deals with the manipulation and guiding of light with nanoscale metallic structures, exploiting the action of the optical near-fields. The research topics, as they have been summarized in [101], cover the investigation of optical properties of nanoparticles and nanoparticle arrays as well as nanoapertures and periodic nanoaperture structures, optical superlensing, field enhancement effects in metal nanostructures, near-field imaging, SPP excitation and detection, and advanced sensing applications. To emphasize the aspect of optical engineering using SPs or SPPs, the term *plasmonics* has been introduced in 1999 in analogy to photonics [103]. In this context, waveguiding of SPPs and SPP integrated optics have been extensively investigated [104–106]. Within the work presented in this thesis, prototyping of plasmonic components and waveguides by nonlinear laser lithography [11,13–20] and nanoimprint [48–50] has been introduced. The use of metal nanostructures for SPP waveguiding further allows transporting simultaneously both, optical and electric signals, providing the possibility to merge photonics and electronics on similar length scales [107–109]. Here it should be mentioned that high refractive index materials can also have advantages for confining and guiding light. A well known concept is that of silicon waveguides based on silicon-on-insulator (SOI) technology [110, 111]. Investigations have been made to merge these two concepts to benefit from the individual advantages [105, 112]. A review on plasmonic research in the last few years until 2007 is provided in the textbook from Maier [113]. Coupling of light into nanoscale plasmonic systems and the efficient

conversion of propagating light into strongly enhanced near-fields has further led to the conception of optical antennas [114–117]. Field enhancement inside the gap of rod-type dipole antennas in the optical range has been investigated and strong nonlinear white-light emission from the gap region has been observed [118]. Downscaling the concept of antennas from the radio frequency to the optical region has been systematically studied in [119], taking into account the excitation of localized SPs and SPPs in a nanorod structure. Field enhancements in the order of 10^3 have been achieved with bow-tie antennas [120]. These structures have recently been discussed for the generation of high-order harmonic and extreme ultraviolet radiation from ultrashort pulse laser oscillators, making use of the plasmonic field enhancement [121–126]. The recent advances in optical antenna theory are reviewed in [127]. Present and possible future applications of nanoplasmonics have been discussed in [128].

Optical Metamaterials:

The excitation of plasmonic modes in metallic nanostructures has additionally created new interest in the field of artificially structured materials with novel optical properties, exploiting also, but not exclusively, the interaction with the optical magnetic field. The aim of metamaterial research is the development of material composites with not naturally occurring refractive indices, chirality, absorption, and scattering properties by designing their electric permittivity and magnetic permeability [102]. The term *meta-materials* for these kinds of composites has been coined in 2000 by Smith et al. [129]. Historically, the research on electrodynamic properties of artificially structured materials dates back to 1898, when Bose investigated the microwave transmission properties of twisted jute as an artificial chiral medium [130]. A further artificial chiral medium consisting of wire helices has been discussed by Lindemann in 1914 [131]. Tailoring of the effective index has been demonstrated in 1948 by Kock [132] and an artificial dielectric with a refractive index of less than unity has been presented in 1953 by Brown [133]. These initial investigations have mainly been restricted to material actions on the electrical field, leading to media with specially designed permittivity. At microwave and optical frequencies only a negligible response of natural matter to the magnetic field exists, and the refractive index is only determined by the electric permittivity $n = \sqrt{\epsilon_r}$ [102, 134]. In contrast, magnetic response of split-ring resonators (SRRs) around 1 GHz has firstly been demonstrate in 1980 by Hardy [135], giving the possibility to also achieve effective permeabilities which substantially can deviate from unity or assume even negative values. The consequences of simultaneously negative permittivity and permeability, resulting in a negative refractive index, have systematically been studied theoretically by Veselago in 1968 [136]. An experimental study on negative index materials has been presented by Smith et al. in 2000, using SRRs driven in resonance by the magnetic field in the microwave region [129]. Further efforts have been made to realize negative index materials in the visible spectral range. The development of nanostructuring technologies has recently allowed achieving magnetic responses in the visible spectral range around 530 nm using aluminium SRRs [137] and 604 nm using silver SRRs [138]. While large SRRs can still be realized by optical lithography, the fabrication of SRRs for the visible spectral range requires high resolution and expensive electron beam lithography. Fig.2.3
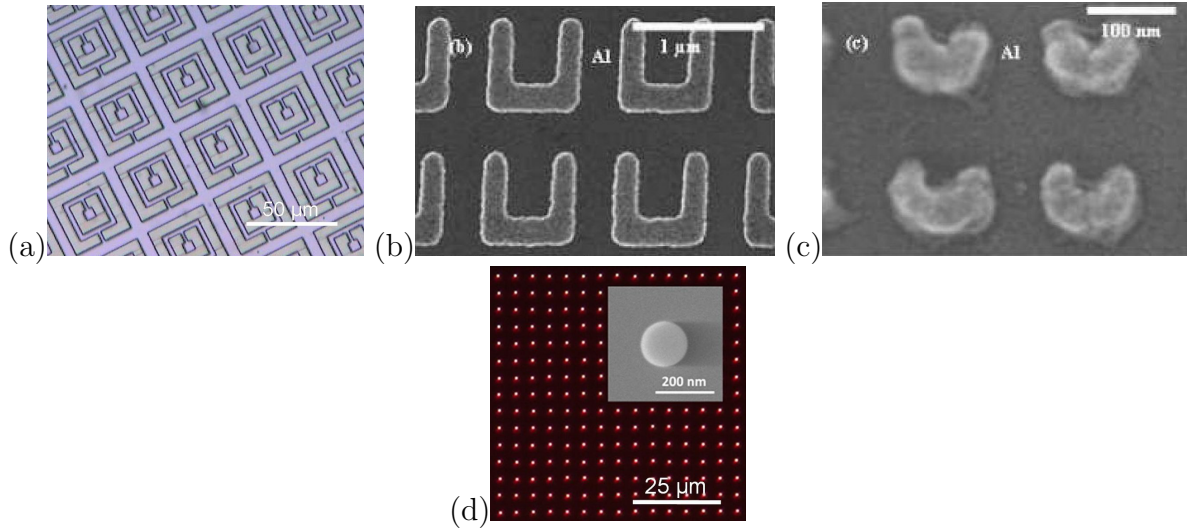
Figure 2.3:
Magnetic resonant structures for different spectral ranges: (a) Double-SRRs for the THz region, (b) 700 nm × 700 nm SRRs with a response at 7 µm wavelength, (c) particle-like SRR with magnetic resonance at 530 nm. (d) Comparison to silicon particles with low-loss magnetic resonance at 700 nm. (Images (b) and (c) from [137]).

shows a comparison of magnetic resonant structures arranged in a 2D *metasurface* for different wavelengths from the THz to the visible region.

A further approach to obtain response to the magnetic field of light is the use of pairs of gold nanoparticles in the visible spectral ranges [139–141]. However, the main drawback of metallic building blocks or *meta-atoms* used to obtain magnetic response are their inherent resistive losses [102]. Therefore, two different alternatives have emerged: First, the application of gain media to compensate the losses, and second, the avoidance of losses by all-dielectric meta-atoms. The efforts made to compensate plasmonic losses by gain media and the developments of dielectric metamaterial building blocks are discussed in subsequent sections. In contrast, spherical dielectric particles of high refractive index materials, exhibiting low-loss magnetic dipole Mie resonances, would allow novel and cost effective fabrication approaches to be used, without the need for gain media. This possibility is discussed in this thesis in chapters 5 and 7. As a comparison to the metallic magnetic resonant SRRs and particles, an array of silicon nanoparticles with magnetic Mie resonances around 700 nm, fabricated by comparatively low priced laser transfer, is shown in Fig.2.3(d).

Loss Compensation in Plasmonic Systems:

The losses of metallic nanosystems are the reason for strong damping of metallic particle resonances [142,143] and the finite propagation length of plasmonic surface and waveguide modes [17, 144]. The application of gain media for loss compensation has widely been discussed and demonstrated for metamaterials with metallic building blocks [145],

nanoparticle systems [146], SPPs [147], and SPP waveguides [148, 149]. The acronym *spaser* in analogy to laser for an SP or SPP amplifying system has been introduced in 2003 by Bergman and Stockman [150]. A first proof of stimulated emission of SPPs has been given in 2005 by Seidel et al. [151], using Rhodamin 101 and Cresyl Violet dye solutions. The concept has been refined by Noginov et al., demonstrating a spaser-based nanolaser [152]. An overview on the current research is provided in [153]. Although the Ohmic losses have been shown to be efficiently compensated, the gain media have additionally to be incorporated into the plasmonic systems or metamaterials, making their fabrication more difficult. A further requirement is the need for suitable pump sources, resulting in an enhanced complexity of the experimental work.

All-Dielectric Metamaterials:

Recently, there has been a growing interest in metamaterials with all-dielectric building blocks to avoid the Ohmic losses connected with metallic structures. [35, 154, 155]. The basis for this development is the occurrence of Mie or Mie-type resonances in nanoparticles of high refractive index materials. The use of spherical dielectric particles as building blocks for such metamaterials has been theoretically investigated in 2005 by Wheeler et al., showing the existence of a negative effective permeability [156]. In 2007, experimental investigations on chemically grown silicon carbide nanorods have shown that for these structures magnetic modes exist [157]. A further theoretical study of metamaterials using dielectric spheres and disks has been presented by Ahmadi in 2008, where the possibility for double negative materials with simultaneously negative effective permittivity and effective permeability has been pointed out [158]. The comparison of scattering properties of the classic SRR structure with a rectangular dielectric particles has has been studied in 2008 by Popa et al. [159]. It has been shown that the dielectric particle has an identical behaviour but without Ohmic losses, resulting in a 3-fold increase of the quality factor. However, these results have been obtained in the GHz range.

In this work, an important contribution to this field has been made and fabrication approaches for high quality spherical silicon nanoparticles as meta-atoms with strong electric and magnetic dipole resonances have been presented [36–38]. These results have sparked a world wide interest in the use of semiconductor nanostructures as building blocks for low loss metamaterials [160–163] and might contribute to the further development of silicon nanophotonics [164–166].

3 Two-Photon Fabrication

Growing interest in downscaling electronic, optical, and mechanical components and devices as well as the demand of their integration has pushed the development of micro- and nanofabrication methods in the last years [77, 78]. UV and X-ray lithography [167, 168], electron beam lithography [169], focused ion beam (FIB) etching [170], and nanoimprint lithography (NIL) [171] are widely used in industrial applications. These methods, however, are suffering a lack of flexibility and/or cost efficiency and are mainly limited to 2D fabrication. A method for the generation of 3D structures in rapid prototyping is the UV stereolithography, developed in 1986 by Hull [172]. This technology, although flexible and cost efficient, is limited in resolution down to several micrometers and in fabrication speed [173].

To overcome these limitations, nonlinear light-matter interactions can be used in true 3D structuring. The method of nonlinear laser structuring has been demonstrated to be a promising candidate regarding flexibility, cost efficiency, and the ability to generate arbitrary complex 3D structures.

The process of nonlinear laser-writing is based on two-photon absorption. This nonlinear effect has theoretically been investigated by Göppert-Mayer in 1930 and 1931 [174, 175]. It has been demonstrated experimentally by Kaiser and Garret in 1961 after the invention of the laser by two-photon excitation of $CaF_2 : Eu^{2+}$ [176]. Two-photon excitation in dyes has been shown in laser scanning fluorescence microscopy in 1991 [177]. The potential of this mechanism for 3D laser structuring has been suggested one year later in 1992 by Wu et al. with the idea for applications in microelectronics [178]. 3D microstructures with a resolution down to 500 nm have already been demonstrated. Further investigations of two-photon induced polymerization processes in carbon disulfide clusters and by use of azobenzene dyes have been reported subsequently in 1995 and 1997, respectively [179, 180]. These developments are linked to the availability of commercial titanium:sapphire short pulse laser systems [181, 182].

Three dimensional microfabrication has later been introduced by Maruo et al. in 1997, using a standard polymer SCR-500 [183]. The potential for subwavelength resolution has been pointed out. Since the laser radiation can be focussed directly into the material volume and is only absorbed in the focal region of the beam, the process speed can be much faster compared to conventional 3D stereolithography and the fabricated structures can have a much higher complexity.

The term two-photon polymerization (2PP), which has been given to this technology, has been introduced in 2003, when this technique has been applied to a new class of organic-inorganic hybrid materials [184]. This method has one year later in 2004 independently been used for the realization of 3D photonic crystals by Deubel [185] and Serbin [186]. Three-dimensional micro structuring of photosensitive materials by 2PP can achieve repeatable resolutions down to 100 nm. A detailed overview about this technology up to 2004 is given in [187]. The developments of two-photon polymerization
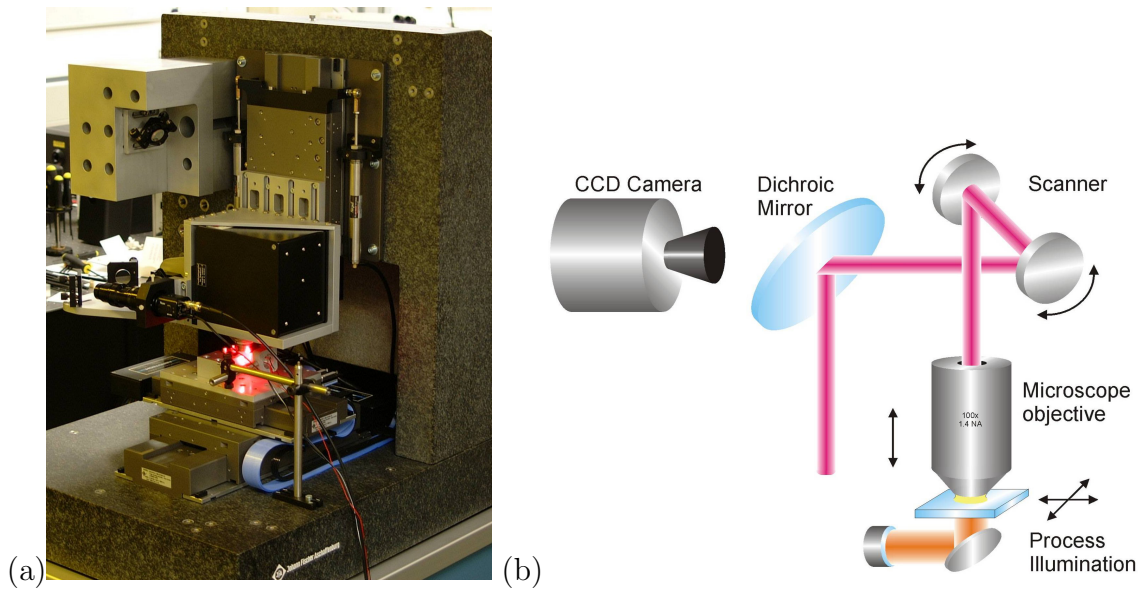
Figure 3.1:
  (a) Photo of the 2PP structuring system developed within this work. (b) Principle optical setup.

within the last 10 years are reviewed in [188].

3.1 Laser-Writing of 3D Structures

Within the work for this thesis, the initial experimental setups for generating 3D structures by 2PP have been developed into commercially available systems [40], using titanium:sapphire or frequency-doubled ytterbium laser oscillators with emission wavelength around 780 nm and 520 nm, respectively. An early version of the 2PP structuring system together with the principle optical setup is shown in Fig.3.1.

3D microstructure fabrication has been demonstrated in different photosensitive materials for applications in micromechanics and microfluidics [27, 28], biology [29], chemistry [42, 43], and microoptics [47]. Woodpile structures have been used as test structures for 3D microfabrication by 2PP for determining the achievable resolutions in different materials, e.g. SU8, ORMOCER®, TiO_2 resist [41], polyethylene glycol biodegradable polymer [29], titanium sol-gel materials with adjustable refractive index [44], and zirconium sol-gel material with selective metal binding affinity [45]. Structure resolution has been improved down to 82.5 nm [46].

This section provides an overview about the materials used in laser-based photofabrication of photonic and plasmonic structures. The materials can be divided into photoresist and photopolymers. As photoresist shall be denoted materials, which change their solubility in basic aqueous solutions or organic solvents after illumination due to bond cleavage or crosslinking, but they remain generally soluble after illumination in certain solvents. The mixture of crosslinkable polymers, polymerizable monomers, or oligomers,
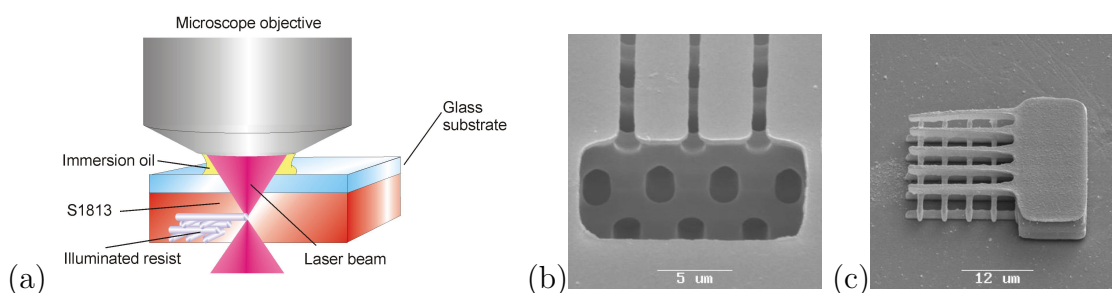
Figure 3.2:

(a) Laser-writing scheme in positive resist materials. (b) Inverted woodpile structure in positive tone resist S1813. (c) Casting with a photocurable arcylate and removing the resist in acetone yield the internal structure.

which become insoluble in organic solvents are denoted as photopolymers.

3.1.1 Positive Tone Photoresist

3.1.1.1 Novolac Photoresist

One well known class of materials are photoresists, as they are used in lithographic processing of microelectronics components. The most widely used materials nowadays are Novolacs. Solid Novolac polymers are synthesized without crosslinking to remain soluble in basic aqueous solutions. The rate of dissolution can be enhanced by suitable additives. For the use as photoresists, these additives are generated by a photochemical reaction. One of the most common additives is diazonaphthaquinone, resulting in a positive tone photoresist [189]. Examples of commercially available spin-coatable materials used in this work are the S1800 class from *Shipley* and maP-1200 class from *microresist technology GmbH*, both having absorption maxima at 350 nm and 405 nm [190, 191]. Typical developers are aqueous solutions of sodium hydroxide or tetramethylammonium hydroxide. The two-photon structurability has been demonstrated in [28]. An example of a woodpile structure in S1813 photoresist together with its inverted replication in photopolymerizable acrylate monomer is shown in Fig.3.2.

3.1.1.2 PMMA Photoresist

Poly (methyl methacrylat) (PMMA) is commonly used as e-beam and deep UV resist for wavelength below 250 nm. Upon illumination with high energetic electrons or photons the polymer chains break and the material can be dissolved in a mixture of methyl isobutyl ketone (4-methyl 2-pentanone, MIBK) and isopropanol. The mixing ratio can be varied depending on the desired resolution from 1:1 to 1:3 [33]. PMMA has turned out to be not directly structurable with ultrashort pulse irradiation at 520 nm and 780 nm using a two-photon absorption. In the present work, PMMA has been used as imaging material for an aluminium superlens at a wavelength of 157 nm, and a four-photon illumination process in the optical near-field of rod type gold nanoantennas has been demonstrated [24].

3.1.2 Negative Tone Photoresist

Negative tone photoresins are realized from Novolac together with phenyl azides [192]. Hydrogen cleavage upon irradiation forms reactive nitrene which results in an immediate crosslinking of the Novolac [193]. This modification increases the solubility in basic aqueous solutions. Typical developers are aqueous solutions of sodium hydroxide or tetramethylammonium hydroxide. In this work, the negative tone photoresist maN-1400 from *microresist technology GmbH* dissolved in organic solvent [194] has been used for the fabrication of plasmonic waveguides. In the dilution maN-1405 this material can be spin coated to a layer thickness of 500 nm at 3000 rpm and has been applied for the prototyping of plasmonic waveguides, see chapter 4.2.3.

3.2 Negative Tone Epoxy Photopolymers

3.2.1 Epoxy Based SU8

The amplified epoxy Novolac SU8, available from *microchem* [195], has been developed for the fabrication of high aspect ratio structures with submicrometer resolution [196]. It has found many applications in fabrication of micro-electro-mechanical systems (MEMS) and microfluidics [197, 198]. The unilluminated regions of the materials can be dissolved by 1-methoxy-2-propyl acetate. The structuring process is based on a cationic polymerization reaction, leading to crosslinking of the polymer. As photosensitive starter usually triarylium-sulfonium salts with spectral sensitivity around 365 nm are added, generating a strong acid upon illumination [198]. Triarylium-sulfonium salts can efficiently be used with titanium:sapphire lasers. The polymerization reaction requires heating of the sample after the laser writing process is necessary. The material has been used to demonstrate the complex 3D structurability [28].

3.2.2 Epoxy Based mr-NIL 6000

A similar material as SU8 is the chemically amplified photocurable phenol epoxy nanoimprint polymer mr-NIL 6000 from *microresist technology GmbH* [199]. The solid photosensitive polymer is dissolved in γ-butyrolactone and can be spin coated to heights between 100 nm and 500 nm. Although designed for nanoimprint lithography, this material can be structured directly by laser direct-writing using ultrashort laser pulses at a central wavelength of 520 nm. The unilluminated regions of the materials can be dissolved by 1-methoxy-2-propyl acetate. The photostarter is not known. Structuring is efficient with frequency-doubled ytterbium lasers. The material has been applied for the prototyping of plasmonic waveguides, see chapter 4.2.3.

3.3 Negative Tone Organic-Inorganic Photopolymers

3.3.1 Organically Modified Ceramics

Organically modified ceramics (ORMOCER®s) from *microresist technologies GmbH* [200] under the brand names ORMOCER® b59, ORMOCER® USS4, OrmoCore, and
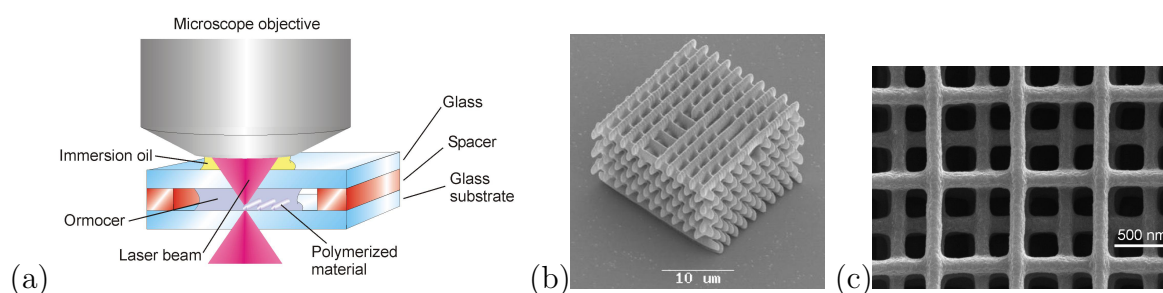
Figure 3.3:
 (a) Structuring scheme for photopolymers. (b) Woodpile structure as photonic crystal with 90°-bend waveguide defects. (c) Demonstration of 100 nm line width in titanium sol-gel.

OrmoClad have been used within this work. ORMOCER®s are synthesized from silicon alcoxides together with organic groups in a sol-gel process. The material is liquid and does not contain any solvent. It can directly be structured and is polymerized in a radicalic chain reaction. A convenient solvent for development is MIBK, which can be diluted with isopropanol. Details of this material and its structuring properties are described in [201].

3.3.2 Own Developments: Titanium and Zirconium Photopolymers

The sol-gel process has been used in the synthesis of two novel hybrid photopolymers, providing high refractive indices and giving the possibility for selective electroless plating. The first material features a co-polymerization of titanium isopropoxide (TIP) with 3-methacryloxypropyltrimethoxisilane (MAPTMS). The organic group is methacrylic acid (MAA). Depending on the relative content of MAPTMS and TIP the refractive index of this material has experimentally been determined to be adjustable between 1.5 and 1.65 [44].

The second material uses zirconium propoxide (ZPO) instead of ITP together with MAPTMS to form the inorganic network. The polymerizable organic group is again MAA. In the basic form, the material has been used for the fabrication of microaxicons with high surface quality [47].

Although the material is quite rigid, structures with characteristic dimensions below 100 nm are getting washed away during the development. To circumvent this problem an additional crosslinker, 2 dipentaerythritol penta-methacrylate (DPMA), has been added. With this amplified polymer structures with 82.5 nm diameter have been demonstrated [46].

The addition of 2-(diethylamino)ethyl methacrylate (DEMAEMA) provides metal binding moieties. The material can be selectively covered with a metal layer by electroless plating. Materials and procedures are described in [45].

A different kind of material which is not prepared by a sol-gel process is based on titanium *n*-butoxide. The material has been prepared by forming a chelate complex with the enol form of benzoylacetone. It has been designed as a hybrid polymer for electron
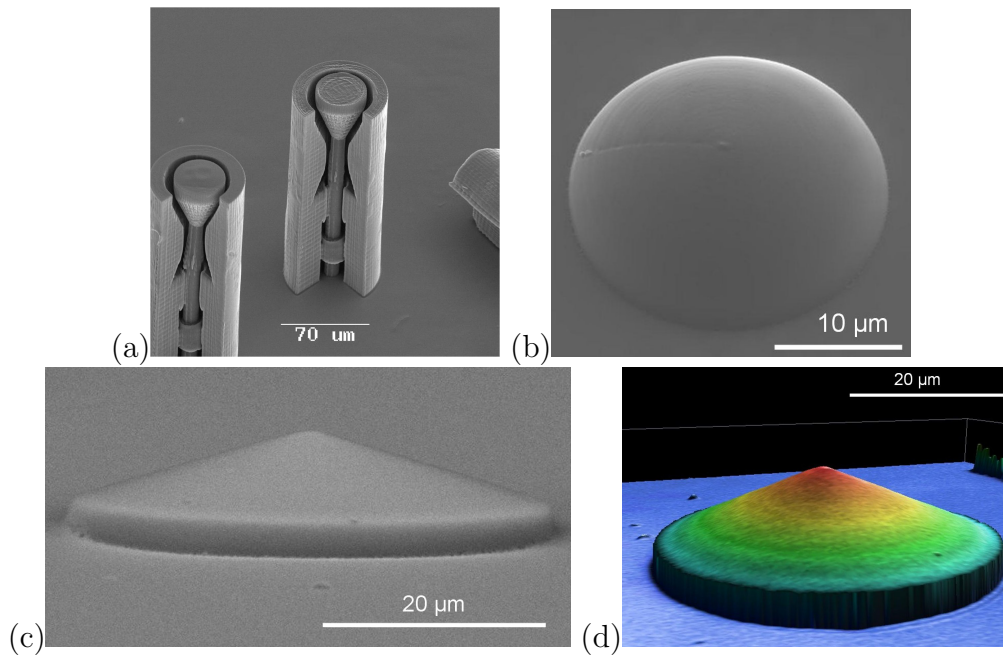
Figure 3.4:
  (a) Model of movable microvalve after one-step fabrication. (b) Microlens from zirkon-polymer. (c,d) Microaxicon. The height in (d) is color coded to show the high surface quality.

beam lithography. However, it has been demonstrated that the material can directly be structured by femtosecond laser radiation. The structuring properties for 2PP have been investigated in [41].

Radicalic photostarters that have mostly been used are Irgacure369 and Michler's Ketone. Irgacure369 is 2-benzyl-2-diethylamino-(4-morpholinophenyl)-butanone-1 [202]. The UV absorption of Irgacure 369 is in the range of 320 nm to 340 nm [203] and can be used with titanium:sapphire lasers and frequency-doubled ytterbium lasers.

Michler's Ketone [204] is 4,4-bis(dimethylamino)benzophenone. It has been introduced as a photostarter for chemical reactions in 1966 [205]. The molecule absorbs strongly from below 300 nm to above 400 nm with a maximum sensitivity around 360 nm to 370 nm [206]. It is a very efficient photostarter for use with titanium:sapphire lasers.

The absorption bands given above refer to single-photon absorption. Two-photon absorption cross sections for different Irgacure and Darocure initiators have been measured by Schafer et al. [207]. For Irgacure369 it has been shown that both, single- and two-photon absorption cross sections show the same spectral absorption. The results from 2PP experiments indicate a similar behaviour for Michler's Ketone.

3.4 Functional 3D Microstructures

The principle structuring scheme for photopolymers and some examples of woodpile photonic structures of SU8 with 90°-bend waveguide defects and titanium sol-gel with
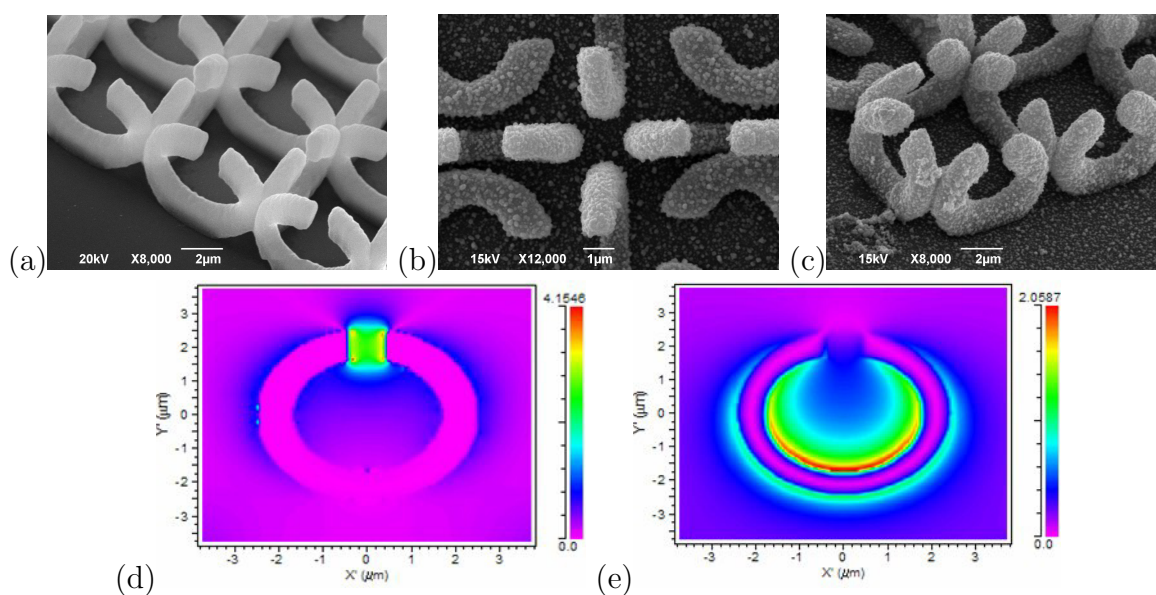
Figure 3.5:
 (a) (a-c) Metallized 3D SRRs standing on a substrate surface fabricated by 2PP and possibilities for 2D arrangement. FDTD simulation of the electric (d) and magnetic (e) fields around the structure at an incident wavelength of 8 µm.

rod diameters of 100 nm are schown in Fig.3.3.

The huge potential of this technology is demonstrated by readily assembled micromechanical and microfluidic structures, acting as microvalves for biomedical applications inside blood vessels [27]. No other technology can fulfill this performance today.

The achievable good optical quality and the high transparency in the visible spectral range further open new possibilities for realizing microoptical elements. In [47], the structure of an axicon has been chosen, since no other approach for their realization on the microscale exists. The examples are given in Fig.3.4.

To further emphasize the possibilities of this technology, structuring of zirconium polymer with metal binding affinity has been applied to the fabrication of 3D standing split-ring resonators (SRRs). The ring diameter is 5 µm and the gap width and wire diameter are 800 nm, respectively, in order to provide a magnetic resonance at 12 µm incident wavelength. The initial polymer structures can be arranged in 2D and 3D arrays for 2D or 3D isotropic magnetic response. Measurements of the conductivity of the metal coverage are presented in [45]. First examples, outlining the potential for future investigations, are shown in Fig.3.5, together with FDTD simulations.

Important main contributions:

- **Development of a two-photon structuring system for industrial application, commercially available at http://lzh.de/en/departments/nanotechnology/nanolithography**

- **Improvement of structure resolution down to 82.5 nm**

- **Development and structuring of high-refractive index titanium-based sol-gel with adjustable index between 1.50 and 1.65**

- **Development and structuring of sol-gel polymer for electroless plating**

- **Fabrication of high-quality microvalves and microoptical conical lenses**

The relevant literature is:

- *Recent progress in direct write 2D and 3D photofabrication technique with femtosecond laser pulses*
  J. Koch, T. Bauer, C. Reinhardt, B. N. Chichkov
  in Recent Advances in Laser Material Processing, chapter **8**, Elsevier, pp. 472 - 495 (2006)

- *Direct 3D Patterning of TiO_2 Using Femtosecond Laser Pulses*
  S. Passinger, M. S. Saifullah, C. Reinhardt, K. R. V. Subramanian, B. N. Chichkov, M. E. Welland
  Advanced Materials **19**, pp. 1218 - 1221 (2007)

- *Three-Dimensional Biodegradable Structures Fabricated by Two-Photon Polymerization*
  F. Claeyssens, E. A. Hasan, A. Gaidukeviciute, D. S. Achilleos, A. Ranella, C. Reinhardt, A. Ovsianikov, X. Shizhou, C. Fotakis, M. Vamvakaki, B. N. Chichkov, M. Farsari
  Langmuire **25**, pp. 3219 - 3223 (2009)

- *Microstructured templates produced using femtosecond laser pulses as templates for the deposition of mesoporous silicas*
  F. Heinroth, I. Bremer, S. Münzer, P. Behrens, C. Reinhardt, S. Passinger, C. Ohrt, B. Chichkov
  Microporous and Mesoporous Materials **119**, pp. 104 - 108 (2009)

- *Three-dimensional titania pore structures produced by using a femtosecond laser pulse technique and a dip coating procedure*
  F. Heinroth, S. Münzer, A. Feldhoff, S. Passinger, W. Cheng, C. Reinhardt, B. Chichkov, P. Behrens
  Journal of Materials Science **44**, pp. 6490 - 6497 (2009)

- *On the design and fabrication by two-photon polymerization of a readily assembled micro- valve*
  C. Schizas, V. Melissinaki, A. Gaidukeviciute, C. Reinhardt, C. Ohrt, V. Dedoussis, B. N. Chichkov, C. Fotakis, M. Farsari, D. Karalekas
  International Journal of Advanced Manufacturing Technology **48**, pp. 435 - 441 (2010)

- *Two-photon polymerization of titanium-containing sol-gel composites for three-dimensional structure fabrication*
  I. Sakellari, A. Gaidukeviciute, A. Giakoumaki, D. Gray, C. Fotakis, M. Farsari, M. Vamvakaki, C. Reinhardt, A. Ovsianikov, B. N. Chichkov
  Applied Physics A **100**, pp. 359 - 364 (2010)

- *3D conducting nanostructures fabricated using direct laser writing*
  K. Terzaki, N. Vasilantonakis, A. Gaidukeviciute, C. Reinhardt, C. Fotakis, M. Vamvakaki, M. Farsari
  Optical Materials Express **1**, pp. 586 - 597 (2011)

- *Development of functional sub-100 nm structures with 3D two-photon polymerization technique and optical methods for characterization*
  V. Ferreras-Paz, M. Emons, K. Obata, A. Ovsianikov, S. Peterhänsel, K. Frenner, C. Reinhardt, B. Chichkov, U. Morgner, W. Osten
  Journal of Laser Application **24**, pp. 042004-1 - 042004-7 (2012)

- *Closely packed hexagonal conical microlens array fabricated by direct laser photopolymerization*
  A. Zukauskas, M. Malinauskas, C. Reinhardt, B. N. Chichkov, R. Gadonas
  Applied Optics **51**, pp. 4995 - 5003 (2012)

4 Plasmonics - Surface Plasmon-Polaritons

The occurrence of surface plasmon wave excitations in planar geometries has been observed by Wood in the diffraction features from ruled metallic gratings in reflection mode in 1902 [94]. In the same publication, the influence of different dielectric media on top of the grating have been discussed, causing a shift of the anomalous reflection features. This observation could be termed the first sensing application for surface plasmons.

A mathematical description has been given in 1941 by Fano [208], providing the first expression for the dispersion relation of surface plasmon-polaritons by relating the damping of the superficial waves to the finite conductivity of the metal. He concluded that the propagation length of the waves could be significantly enhanced by reducing the resistive losses in the metal. Superficial waves have also been introduced by Sommerfeld [209]. Together with Zenneck, he investigated the propagation of electromagnetic waves over sea water [209, 210]. The theoretical description is analogue to that of Fano, except for the difference that the medium is characterized by a positive real part of the complex dielectric function.

The optical properties of metals are linked to the possibility to excite plasma oscillation in the free electron gas. Excitation of plasma oscillations in the volume of metals by inelastic electron scattering has been suggested by Bohm and Pines in 1952 and 1953 [211, 212]. The plasma frequency of these oscillations is given by $\omega_p = \sqrt{ne^2/m\epsilon_0\epsilon_\infty}$, where n is the electron density, e is the electron charge, m is the effective electron mass, ϵ_0 is the vacuum permittivity, and ϵ_∞ represents a real valued background permittivity [213]. First evidence for their excitation has been observed by Watanabe in 1955 [214]. The term *plasmon* for the quanta of electron oscillations has been introduced by Pines in 1956 [215]. One year later 1957, Ritchie has predicted in a theoretical article the existence of longitudinal plasma oscillations at the surface of a thin metal film [216], which has been experimentally confirmed in 1959 by Powell and Swan for aluminium films [217]. The term *surface plasmon* has been introduced one year later in a paper by Stern and Ferrell about surface plasma oscillations in a degenerate electron gas [218].

The surface plasmon oscillations predicted by Ritchie have been obtained in the electrostatic approximation, which is valid only for the surface plasmon resonance at $\omega_{SP} = \omega_p/\sqrt{1+\epsilon}$, where ϵ is the dielectric function for the material above the metal surface. Retardation effects have been neglected so far. At optical frequencies these surface plasmons have spatially fast varying charge density oscillations and are necessarily coupled to an electromagnetic field, which is exactly the superficial wave on a metallic surface as introduced by Fano.

When electromagnetic fields propagate through a medium, metal or dielectric, they couple to internal degrees of freedom of the material. These are the induced polarization, the magnetization, the optical phonons in ionic crystals, or charge density oscillations in the valence electrons or the free electron gas in metals. These coupled modes are generally called *polaritons* [219]. According to this definition, the coupled mode of a surface plasma

oscillation with a photon is termed *surface plasmon-polariton (SPP)*. This terminology is not always followed in the literature and often the shorter term *surface plasmon* is used instead.

To open ways for practical applications of SPPs, an optical excitation scheme using a prism coupling method has been suggested by Otto [220] for bulk metal surfaces and subsequently by Kretschmann and Raether [221, 222] for thin metal films.

When SPPs are excited in the Kretschman-configuration on a metallic film covered glass substrate, the reflected light intensity shows a characteristic dip for a certain angle of incidence, representing the resonance of the SPPs with the incoming light. The angular position of this dip depends on the metal, the film thickness, and the dielectric constant of the medium above the metal film in its closest vicinity. By measuring the angular dip position the dielectric constant of the covering medium can be determined with a very high accuracy. The potential of SPPs for sensing application has been demonstrated from 1976 to 1978 by measuring optical properties of overcoatings of silver films with silver sulfide, lithium fluoride, and carbon [223, 224] as well as organic monolayers on gold and silver films [225, 226]. These observations have resulted in the development of the first commercial sensing device based on the surface plasmon resonance (SPR), being on the market since 1990. Sensitivities down to 10^{-7} refractive index units (RIU) are typically achieved [227].

4.1 The SPP dispersion relation of a semi-infinite system and on thin metal films

The properties of SPPs at a single metal-dielectric interface are described by their analytic dispersion relation [208, 228]. Both media are assumed to extend to infinity away from the interface and to be isotropic in directions parallel to the interface. The metal and the dielectric are characterized by their individual dielectric functions ϵ_m and ϵ_d, respectively. The permeability of the media at optical frequencies is neglected and set to unity.

SPP surface modes exist for TM polarization only and only if the real part of the permittivity ϵ_m of the metal is smaller than the negative modulus of the permittivity of the dielectric ϵ_d, i.e. $\epsilon_m < -\epsilon_d$. This condition is fulfilled for noble metals like gold and silver in the visible and near-infrared spectral ranges. In contrast, aluminium represents a low-loss plasmonic material in the spectral range of 100 nm to 400 nm [33]. The dispersion relation of an SPP in the semi infinite system is given by [93, 113]

$$k_{\mathrm{SPP}} = k_x = k_0 \sqrt{\frac{\epsilon_m \epsilon_d}{\epsilon_m + \epsilon_d}} \quad . \tag{4.1}$$

A derivation of this expression in terms of the resonances of the Fresnel reflection coefficient can be found in [93]. An alternative solution, using directly Maxwell's equations, is given in [113]. From this expression the SPP wavelength λ_{SPP} and the SPP propagation length L_{SPP}, defined as the $1/e$-intensity decay, can be obtained.

(a)

(b)
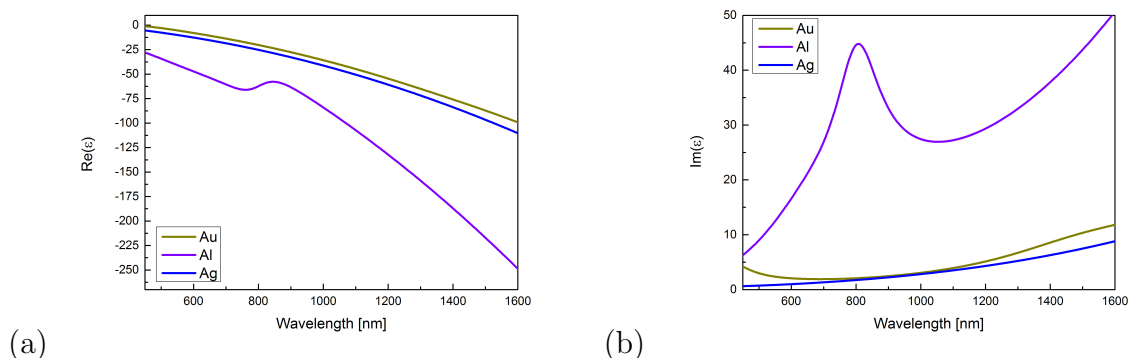
Figure 4.1:
(a) Real $Re(\epsilon)$ and (b) imaginary $Im(\epsilon)$ parts of the permittivity as functions of the excitation vacuum wavelength.

$$\lambda_{\mathrm{SPP}} = \frac{2\pi}{Re(k_{\mathrm{SPP}})} \qquad (4.2)$$

$$L_{\mathrm{SPP}} = \frac{1}{2Im(k_{\mathrm{SPP}})} \qquad (4.3)$$

The dielectric functions of gold, silver, and aluminium, shown in Fig.4.1, have been modelled by an extended Drude-Lorentz model, taking into account interband transitions, which are of importance for gold for vacuum wavelength below 650 nm and aluminium around 780 nm. The dielectric functions can be found in [213]. The background permittivity and the collision length are matched to the experimentally measured dielectric functions of gold and silver by Johnson and Christy [229]. Data for Drude model parameters for aluminium are provided at [230].

In the experiments, presented in the next chapter, mostly gold has been used as metal. The choice is based on the chemical stability of gold films. Aluminium as plasmonic material has been considered for realization of a plasmonic superlens for deep UV radiation [33] and provides huge potential in the visible spectral rage. Together with silver, it will be considered in future work, see chapter 9. A comparison of plasmonic properties of aluminium, gold, and silver is further given in [231]. The SPP wavelengths λ_{SPP} and the SPP propagation lengths L_{SPP} at the metal-air interface in the visible spectral range for these three metals as functions of the vacuum excitation wavelength are given in Fig.4.2.

However, the system, which has been used in SPP experiments, is a rather a thin gold films deposited onto a glass substrate. The dispersion of SPPs on thin metal films and in multilayer systems has been studied by Kretschmann and Economou [222, 232].

The system consists of a metallic film (layer 2) with dielectric function ϵ_2 deposited on a dielectric substrate (layer 1, semi-infinite) with dielectric constant ϵ_1 and covered with a superstrate (layer 3, semi-infinite) with dielectric constant ϵ_3. For convenience, the z-direction is chosen perpendicular to the interfaces. Mode propagation is considered along the positive x-direction.

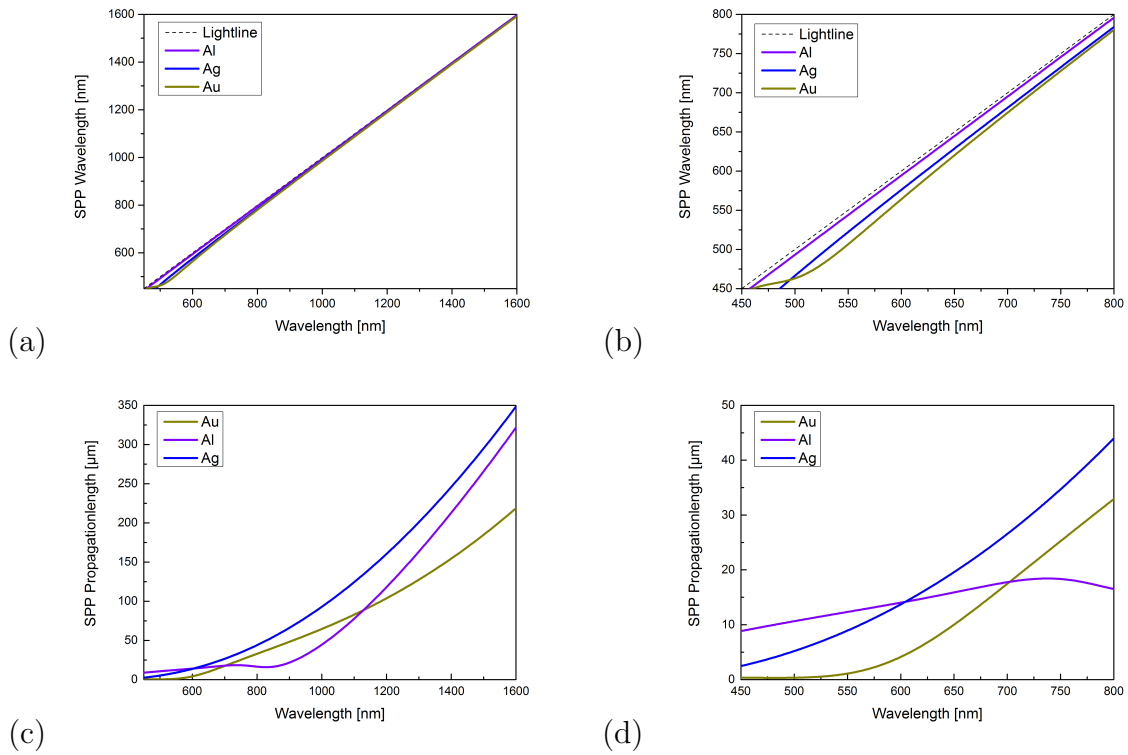**Figure 4.2:**
SPP wavelengths λ_{SPP} (a,b) and the SPP propagation lengths L_{SPP} (c,d) at the metal-air interface for gold (gold), silver (blue), and aluminium (violet) as functions of the vacuum excitation wavelength.
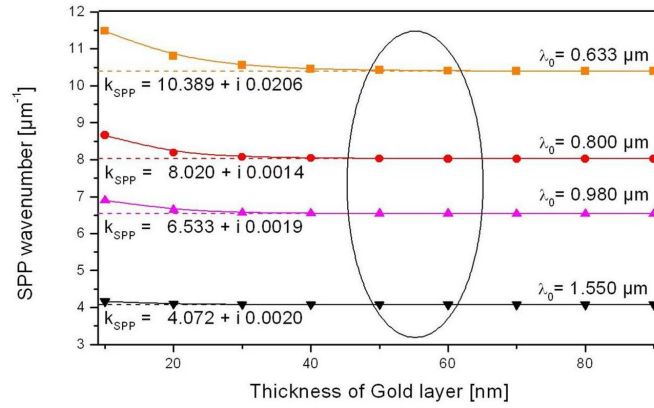
Figure 4.3:

 Comparison of real parts of SPP wave vectors (wave numbers) calculated according to equations 4.1 and 4.4 for the semi-infinite and the two interface systems, respectively. Only below 50 nm film thickness significant deviations occur. Equation 4.1 remains a good approximation for the experimentally used metal film thicknesses marked by the ellipse.

The SPP properties of the system are described by the resonances of Fresnel reflection coefficient for the two-interface system for p-polarized light of frequency $\omega = ck_0$ [33,143,151], with k_0 being the modulus of the wave vector in vacuum, and c is the speed of light in vacuum,

$$r^p_{123} = \frac{r^p_{12} r^p_{23}}{1 + r^p_{12} r^p_{23} \exp 2k_{z,2}d} \quad , \tag{4.4}$$

where the reflection coefficients are given by

$$r^p_{ij} = \frac{\frac{k_{zi}}{\epsilon_i} - \frac{k_{zj}}{\epsilon_j}}{\frac{k_{zi}}{\epsilon_i} + \frac{k_{zj}}{\epsilon_j}} \quad . \tag{4.5}$$

The wave vector components k_{zi} perpendicular to the interface are calculated in terms of the wave vector component k_x parallel to the interface.

$$k^2_{zi} = \epsilon_i k^2_0 - k^2_x \quad . \tag{4.6}$$

It has been shown that for the experimentally relevant film thickness around 50 nm the difference of the real parts of the SPP wave vector is in the order of 10^{-2} and can be neglected in most cases [233]. In a good approximation, the real part of the SPP dispersion evaluated from equation 4.4 can be described with the analytic expression 4.1, as it is shown in Fig.4.3.

This geometry allows coupling of the SPP electromagnetic field to propagating modes in the glass substrate. Although, this is an additional loss mechanism, which adds to the resistive losses in the metal and reduces the propagation length, it enables optical

microscopic methods for the visualization of SPP propagation, i.e. the leakage radiation microscopy, described in section 6.2.

4.2 Surface Plasmon-Polariton Waveguides

Waveguiding of SPPs turns out as a compromise between mode confinement and propagation distances. Additionally, the metal, which is responsible for the mode confinement, introduces unavoidable losses. The first SPP waveguide concept from 1997 has been based on scaling down concepts of electronics, e.g. metal wires, hollow metallic waveguides, and coaxial cables. Numerical investigation has been performed for silver rods of 20 nm diameter embedded in a dielectric, showing that the electric field can be concentrated down to 33 nm for an excitation vacuum wavelength of 633 nm, but with huge propagation losses of 3 dB/410 nm [234]. In 1999, Weeber et al. have investigated plasmon excitation on metallic nanowires [235]. It has been demonstrated in 2005 that a local excitation can be guided along such a nanowire, which can act as nanoresonator. [236]. SPP waveguiding along nanowires has in 2009 been demonstrated with wire diameters down to 60 nm [237], however, the propagation length was only 5 µm for a vacuum wavelength of 1550 nm.

To overcome the huge losses of nanowires, the use of chains of closely spaced resonant nanospheres has been considered due to a reduced metal content in the waveguide. When the particles are resonantly excited, their near-fields can couple and a local excitation can be guided along the chain, having been demonstrated for silver particles of 50 nm diameter with a particle spacing of 25 nm [238]. The corresponding propagation length has been determined to 900 nm, which has been attributed to increased scattering losses of the nanoparticles. This concept has been transferred to closely spaced silver nanorods, enabling the transport of a local plasmonic excitation to a localized detector over 500 nm [239], demonstrating subwavelength energy transport by SPs.

Another approach for realizing SPP waveguiding has been based on band gap structures on metal surfaces. The first demonstration by angular and wavelength resolved reflectivity measurements has been reported for a periodically corrugated silver film for a wavelength of 782 nm using scanning near-field microscopy [240]. The propagation of SPPs in a 3.2 µm wide and 18 µm long channel free from corrugations has been observed [241].

The most intuitive approach for realizing SPP waveguides is to reduce the width of a metal film used for SPP propagation. The stripe remains more extended in width to avoid to high confinement. It can be placed on top of a glass substrate [242] or embedded into a dielectric [243]. For very thin films the plasmons on both sides of the film couple, resulting in two fundamental SPP modes with symmetric and asymmetric electric field distributions perpendicular to the metal film, corresponding to the long- and short-range plasmons, respectively [101]. It should be noted that also higher modes are supported by this structure, which is therefore not single-mode. Theoretical [243–245] and experimental [246–249] studies have been performed on this type of plasmonic waveguide with different aspect ratios of height and width of the metal and different surrounding dielectrics. The longest propagation length, which have been reported, is 0.3 dB/mm, corresponding to a $1/e$ intensity decay length of 1.5 *cm* for silver stripes

on glass with an index-matched polymer overcladding. The field confinement, however, is comparable to that of single mode optical fibers. Nevertheless, this approach allows the integration of SPP-based optical components on one optical chip, e.g. Y-splitter, couplers, Mach-Zehnder-interferometers (MZI), and thermooptically controlled switches, see chapter 15 in [101].

One further concept to achieve SPP waveguiding is the use of metal-insulator-metal (MIM) structures in a slab geometry, for which negative refraction has been reported [250]. A case study has shown that also in other geometries and even on thin films negative refraction can be achieved [251].

Special cases of this concept are V-shaped channels fabricated by focused ion-beam etching. This type of plasmonic waveguide modes have been denoted channel SPPs (CPPs) [252]. It has been demonstrated that single-mode operation of a sub-wavelength V-groove plasmonic waveguide can be achieved by adjusting the depth and angle of the groove. The power of confined CPPs modes is concentrated near the bottom of the groove with the electric field parallel to the sample surface [253]. Sub-wavelength confinement and propagation lengths in the order of hundreds of micrometers in straight waveguides have been demonstrated using near-field microscopy, and several wavelength selective components such as MZIs and ring resonators have been realized [254, 255].

4.2.1 Dielectrically-Loaded Surface Plasmon-Polariton Waveguides

Confinement of SPPs in dielectrically-loaded SPP waveguides is realized analogous to conventional integrated optics [256]. The configuration for SPP waveguiding consists of a dielectric ridge on top of a metal surface, where the lateral SPP confinement is achieved analogue to optical waveguides [11, 257]. The concept of dielectric waveguides for SPPs has independently introduced by Steinberger et al. [257] and Reinhardt et al. [11] in 2006, using silicon dioxide and polymer waveguides, respectively.

Analog to integrated optics, this waveguide configuration has been termed dielectric-loaded SPP waveguide (DLSPPW) [258, 259]. The first experimental investigations have already indicated that the DLSPPWs can be used for efficient guiding of SPP modes. The SPP mode is mostly confined to the dielectric ridge, and by properly designing the dimensions of the ridge, one can achieve single-mode operation with sub-wavelength confinement and propagation lengths comparable those of CPPs.

One of the great advantages of this concept is that it is technologically simple to realize, especially when using polymer materials instead of oxides, where photolithographic methods can be used for fabrication. The application of direct-write nonlinear laser lithography has been investigated in the present work for fast prototyping of plasmonic waveguides and components. The extension to large scale industrial fabrication using mask lithography has been investigated and reported in [260–263].

The use of polymers has furthermore the advantage that different types of dielectrics with specialized properties can be applied, e.g. nonlinearity, thermooptical, or electrooptical activity. This allows realizing different active components such as plasmonic switches, which have been reported recently [112].

Moreover, there exists the possibility of structuring the underlying metal film to form electrodes, allowing electrical heating of the polymer [264] or additional data transport

[265].

DLSPPW have been characterized by SNOM and leakage radiation microscopy, see sections 6.1 and 6.2.

Very recently, Holmgaard et al. have extended the DLSPPW concept to long-range surface plasmons. The continuous metal layer used for DLSPPWs is structured in stripes of 500 nm width and 15 nm height, surrounded by a polymer ridge of 850×850 nm^2 cross section. Propagation length of up to 3.1 mm have already been reported, with a mode width of 1.6 µm [266].

4.2.2 Surface Plasmon Anti-Resonant Reflecting Optical Waveguides

This type of SPP waveguide comprises a narrow strip-like region of a metal surface of a few micrometers in width, confined by a periodic sequence of straight dielectric ridges. These periodic ridges constitute a Bragg reflector and SPP waves can be confined to the metallic region between two reflectors. Due to the reflecting behaviour the waveguide forms the plasmonic analogue of an anti-resonant reflecting optical waveguide (Surface Plasmon ARROW, SPARROW) [267, 268]. The SPPs guided inside the waveguide core of a SPARROW are low-order modes of the corresponding large diameter plasmonic waveguide. This system provides single mode operation with a large mode area for direct fiber-coupling and direct access to the plasmonic field, making them interesting for sensing applications [19, 20].

4.2.3 Laser-Writing of Plasmonic Components, Excitation Structures, and Waveguides

Nonlinear laser-writing has been applied to fabrication of plasmonic waveguides for telecommunication wavelength around 1.5 µm in 2006, using ORMOCER® b59 [11]. The functionality has been demonstrated using SNOM characterization, see section 6.1. Tapered waveguides have been fabricated to improve the excitation of guided modes when laser beams with large spot sizes are used. Some examples of SPP waveguides are shown in Fig.4.4.

Spin coatable materials provide the advantage that the height of the waveguides can be determined and limited before the structuring process. In first experiments the photoresist maN-1405 has been used [13]. In recent experiments, mrNIL-6000.5 has been applied due to its insolubility in organic solvents. For both materials a layer thickness of 500 nm has been realized at a spinning speed of 3000 rpm [17]. The modes of the waveguiding structures can easily be excited by focussing p-polarized laser light on one end of the waveguides. Characterization has been performed using leakage radiation microscopy, see section 6.2. This method has firstly been demonstrated within the work for this habilitation treatise for DLSPPWs in 2006 and 2007 [12, 13]. An example is provided in section 6.2.

Polymer structures are also well suited for efficient excitation of SPPs. Nanodots as well as straight and curved ridges for SPP excitation have been fabricated using ORMOCER®. SPP focussing and directing has been demonstrated [15, 16].
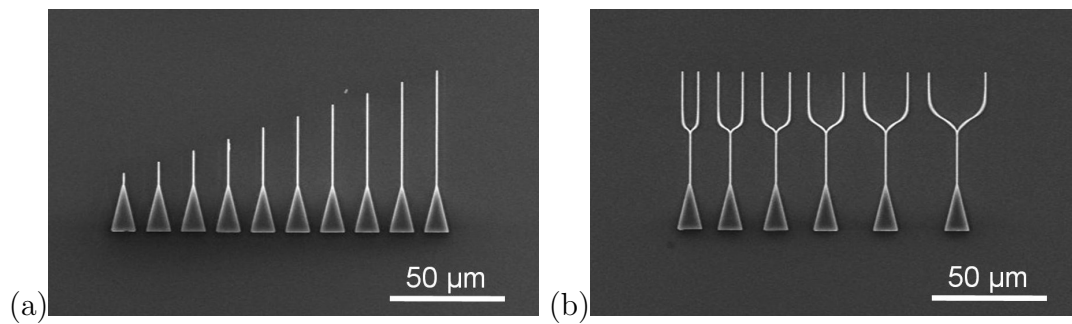
Figure 4.4: Straight (a) and Y-splitter (b) DLSPPws with tapered incoupling regions.

The Novolac maN-1405 has additionally been applied for local restructuring of nanorod arrays. The addition of polymer on the nanorods allows controlling their resonant wavelength and the effective index of the SPs supported by the system [14].

Important main contributions:

- **Realization of first polymer-based dielectrically-loaded SPP waveguides**

- **Development of nonlinear direct laser-writing for prototyping of plasmonic waveguides and excitation components**

The relevant literature is:

- *Laser-fabricated dielectric optical components for surface plasmon polaritons*
  C. Reinhardt, S. Passinger, B. N. Chichkov, C. Marquart, I. P. Radko, S. I. Bozhevolnyi
  Optics Letters **31**, pp. 1307 - 1309 (2006)

- *Restructuring and modification of metallic nanorod arrays using femtosecond laser direct writing*
  C. Reinhardt, S. Passinger, B. N. Chichkov, W. Dickson, G.A. Wurtz, P. Evans R. Pollard, and A. V. Zayats
  Applied Physics Letters **89**, pp. 231117-1 - 231117-3 (2006)

- *Rapid laser prototyping of optical components for surface plasmon polaritons*
  R. Kiyan, C. Reinhardt, S. Passinger, A. L. Stepanov, A. Hohenau, J.R. Krenn, and B. N. Chichkov
  Optics Express **15**, pp. 4205 - 4215 (2007)

- *Rapid laser prototyping of plasmonic components*
  C. Reinhardt, R. Kiyan, S. Passinger, A. L. Stepanov, A. Ostendorf, and B. N. Chichkov
  Applied Physics A **89**, pp. 321 - 325 (2007)

- *Direct laser-writing of dielectric-loaded surface plasmon-polariton waveguides for the visible and near infrared*

C. Reinhardt, A. Seidel, A. B. Evlyukhin, W. Cheng, R. Kiyan, B. N. Chichkov
Applied Physics A **100**, pp. 347 - 352 (2010)

4.2.4 Nanoimprinting of Plasmonic Waveguides

The nonlinear laser writing of plasmonic components has advantages for prototyping and optimization. But once the optimized structures are found, mass production steps are more efficient, e.g. when SPP waveguides shall be implemented within optical or electronic circuitry. As one possibility for fast replication of such structures a nanoimprint process for SPP components has been developed using polydimethoxysiloxane (PDMS) [48]. Master structures of SPP waveguides have been fabricated by 2PP on glass substrates. PDMS has been casted onto the master structure, and after thermal polymerization, the PDMS mold is removed from the master structure. Replica of the initial structures can be produced by pressing the PDMS mold into liquid imprint resin mrNIL-6000.5. After illumination with UV light, the mold can be released from the imprinted sample and is ready for further use [49].

This approach not only allows 2D waveguide structures to be reproduced, but also structures with a varying height profile can be imprinted. This enables the fast production of waveguides together with 3D tapers for light incoupling via optical fibers. The fabrication and transmission measurements are described in detail in [50].

Important main contributions:

- **Development of a nanoimprint process for fast replication of dielectrically-loaded SPP waveguides**

- **Nanoimprinting of 3D tapered SPP waveguides allowing fiber coupling for enhanced integration**

The relevant literature is:

- *Replica molding of picosecond laser fabricated Si microstructures*
  C. Reinhardt, S. Passinger, V. Zorba, B. N. Chichkov, and C. Fotakis
  Applied Physics A **87**, pp. 673 - 677 (2007)

- *Nanoimprinting of dielectric loaded surface plasmon-polariton waveguides from masters fabricated by 2-photon polymerization technique*
  A. Seidel, C. Ohrt, S. Passinger, C. Reinhardt, R. Kiyan, B. Chichkov
  Journal of the Optical Society of America B **26**, pp. 810 - 812 (2009)

- *Fiber-Coupled Surface Plasmon Polariton Excitation in Imprinted Dielectric-Loaded Waveguides*
  A. Seidel, J. Gosciniak, M. U. Gonzalez, J. Renger, C. Reinhardt, R. Kiyan, R. Quidant, S. I. Bozhevolnyi, and B. N. Chichkov
  International Journal of Optics **2010**, pp. 897829-1 - 897829-6 (2010)

5 Metallic and Dielectric Nanoparticles as Building Blocks for Metamaterials and Metasurfaces

Novel fabrication methods and optical characteristics of metallic [30–32] and dielectric silicon nanoparticles [35–38] are introduced. Due to electric and magnetic multipole resonances, these particles provide huge potential as building blocks for metamaterials and metasurfaces. Applications of gold particle metasurfaces for sensing purposes have been investigated within this work. The appearance of Fano resonances in these metasurface structures leads to high sensitive response to refractive index changes [8, 31].

5.1 Scattering Properties of Spherical Metallic Nanoparticles

The first spectroscopic measurement of the extinction spectrum of colloidal gold was published in 1898 by Zsigmondy, showing for the first time the plasmon resonance of gold nanoparticles [269]. The correct scattering behaviour is obtained from Mie theory, allowing separating the cross sections into different multipole contributions [95]. The method is described in chapter 7.3.

Fig.5.1 shows color coded plots of the extinction efficiencies of gold and silver nanoparticles as a function of particle radius and incident wavelength in vacuum environment. For particles with radii larger than 100 nm for gold and 60 nm for silver, a contribution of the electric quadrupole is present.

The influence of the electric quadrupole on the scattering of SPPs on spherical gold particles placed on top of a gold film have experimentally been demonstrated in [30], showing up as a reduced backscattering. The experiment is described in section 6.6.

5.1.1 Laser-Induced Transfer of Gold Nanoparticles

The method of laser-induced transfer (LIT) has been developed to generate spherical nanoparticles and to arrange them on a surface or even combine them with polymeric 2D plasmonic and 3D photonic structures [30, 31].

LIT of bunches of material after irradiation of thin films of various metals and oxides has been shown as early as 1986 using an ArF excimer laser [273]. Schemes of forward and backward transfer, where the ablated material is ejected into and opposite to the laser beam direction, respectively, have been investigated in 1999 for the fabrication of laser generated high-resolution holograms [274].

The occurrence of a hydrodynamic process on gold films prior to ablation has already been shown in 2004 [28, 275]. The formation, ejection, and deposition of single nanodroplets of the molten material have been observed and reported subsequently in 2005 and 2006 [276–278]. The laser energy is first absorbed in the electron gas and then slowly transferred to the ion lattice. The coupling between the electron oscillations and
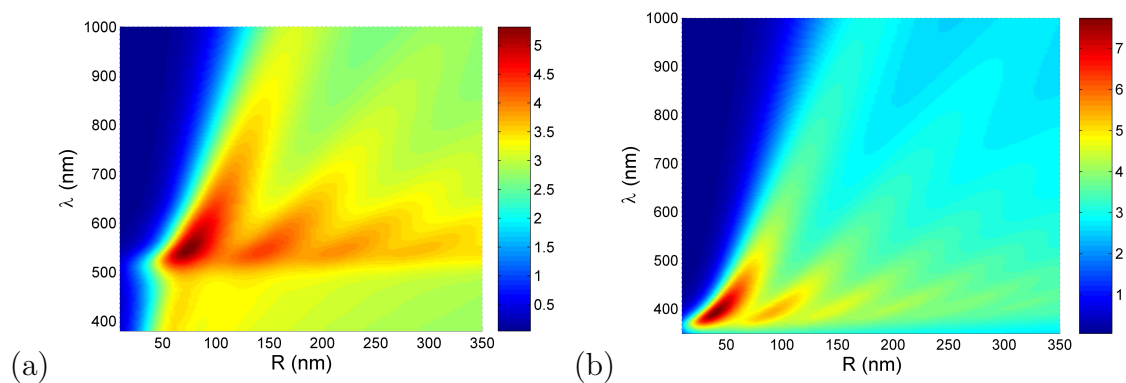
Figure 5.1:
  Extinction efficiencies for gold(a) and silver (b) nanoparticles as a color coded 2D plot in dependence on wavelength and particle radius.
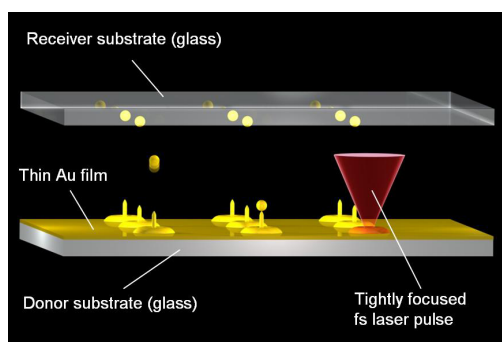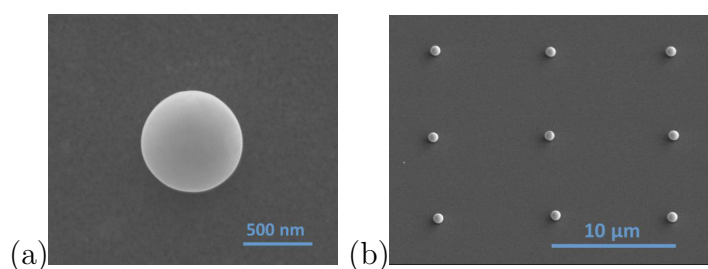

Figure 5.2:
  Schematic of the laser-induced transfer process for the production of gold nanoparticles.

Figure 5.3:
(a) Single particle with 600 nm diameter. (b) Particle array from LIT-particles.

the lattice oscillations, i.e. the phonons, is described by the electron-phonon coupling constant [279]. The energy transfer from the electrons to the lattice occurs on a time scale in the picosecond range, leading to a transient liquid phase. This liquid phase can be created by absorption of one single laser pulse with an energy of a few nanojoules. This leads to built up of temperature and pressure gradients in thin films of the material. When the material increases its volume during melting, the process can be compared to the dynamics initiated by a drop of liquid falling into a liquid surface. A back jet of the material is driven upwards. If the laser pulse energy is increased a droplet is ejected away from the structure. These droplets can be captured on a second glass plate, acting as a receiver substrate [30]. The schematic is shown in Fig.5.2. The nanojet remains on the donor substrate. It can further serve as nanoscale electron source due to the field enhancement and lightning rod effect at the very sharp tip with curvature radius of a few nanometers. Produced nanoparticles are shown in Fig.5.3.

The diameter of the generated particles is limited in size down to 250 nm [30]. The SPP scattering properties of such gold particles deposited on a gold film have been investigated, showing the emergence of a quadrupole scattering moment with increasing diameter. Properties of particle arrays with electric dipole and quadrupole resonances of the individual particles have been investigated in [52].

A reduction of the particles size has been achieved when the film is structured before the LIT process. Pre-structuring has been accomplished by means of nanosphere lithography, where one monolayer of monodispersed colloidal spheres is deposited onto a glass substrate. After anisotropic evaporation of gold onto the sample and subsequent lift-off a hexagonal array of plane triangular nanoparticles remains on the glass surface. The material can be melted by ultrashort laser pulses. During melting the triangle contracts into a sphere due to the surface tension of the liquid material, leading to an elevation of the center-of-mass of the material volume. The generated momentum drives the particle towards the receiver substrate. Examples of the generated highly ordered nanoparticle arrays are given in Fig.5.4.

5.1.2 Sensing Properties of Gold Nanoparticle Arrays

Recently, it has theoretically been investigated that spectrally narrow resonances occur in the transmission spectra of metal nanoparticle chains and arrays [270]. These Fano
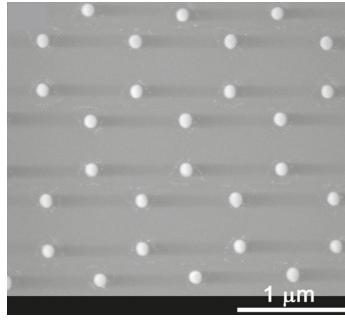
Figure 5.4:
   Array of gold particles as metasurface for sensing application. The particle diameter is 80 nm.

type spectral transmission profiles are caused by coupling of the broad individual particle plasmon resonances with the spectrally diffraction orders of the particle array, when certain diffractive orders propagate nearly parallel to the array plane. Fano resonances further occur in two or more closely spaced nanoparticles, coupled by near-field interactions leading to interference of the hybridized collective superradiant and subradiant plasmon modes [271, 272]. The plasmon resonance of the particles strongly depends on the refractive index of the medium above the sample surface, on which the particles are deposited. Using the method described above, spherical gold particles with diameters of 80 nm have been deposited on a PDMS surface in a hexagonal array as shown in Fig.5.4. This prototype of a metamaterial layer has been applied for sensing the refractive index of water-glycerine solutions and immersion oil with refractive indices between 1.333 and 1.518. The spectral measurement of the minimum transmission of the Fano profile and the corresponding width revealed a sensitivity of 365 nm/RIU [31]. In comparison, with thin-film surface plasmon resonance sensors sensitivities in the order of 1000 nm/RIU can be reached [227].

   If larger metallic particles are arranged in an array, also their electric quadrupole resonances can be coupled with the diffractive modes of the array, leading to a second Fano resonance. This possibility for gold nanoparticles with radii between 100 nm and 140 nm has been considered theoretically within the present work [52].

   The sensitivity can be significantly enhanced by several orders of magnitude by additionally measuring the phase shift that occurs in the resonance of the Fano profile, being different for p- and s-polarized light under 57° incidence. Using s-polarized light as a reference, the phase shift of the p-polarized light in the vicinity of the resonance is 175° for a refractive index difference of 0.0035. This result directly yields a sensitivity of 5×10^4 $deg./RIU$. According to this value, the lower detection limit can be estimated to 10^{-7} RIU, which is comparable to or even slightly better than achievable with commercial amplitude sensitive surface plasmon resonance sensors [8].

   Important main contributions:

- **Development of the laser-induced transfer technology for generation of spherical, monodisperse metal meso- and nanoparticles with determined**

size and position

- **Generation of large-scale ordered arrays of metal nanoparticles**

- **Realization of advanced sensor arrays: Sensitivity 5×10^4 deg./RIU, detection limit 10^{-7} RIU, comparable to existing SPR sensors**

The relevant literature is:

- *Laser-induced transfer of metallic nanodroplets for plasmonics and metamaterial applications*
  A. I. Kuznetsov, A. B. Evlyukhin, C. Reinhardt, A. Seidel, R. Kiyan, W. Cheng, A. Ovsianikov, B. N. Chichkov
  Journal of the Optical Society of America B **26**, pp. B130 - B138 (2009)

- *Laser Fabrication of Large Scale Nanoparticle Arrays for Sensing Applications*
  A. I. Kuznetsov, A. B. Evlyukhin, M. R. Goncalves, C. Reinhardt, A. Koroleva, M. L. Arnedillo, R. Kiyan, O. Marti, B. N. Chichkov
  ACS Nano **19**, American Chemical Society, pp. 4843 - 4849 (2011)

- *Optical properties of spherical gold mesoparticles*
  A. B. Evlyukhin, A. I. Kuznetsov, S. M. Novikov, J. Beermann, C. Reinhardt, R. Kiyan, S. I. Bozhevolnyi, B. N. Chichkov
  Applied Physics B **106**, pp. 841 - 848 (2012)

- *Laser-ablative engineering of phase singularities in plasmonic metamaterial arrays for biosensing applications*
  A. I. Aristov, U. Zywietz, A. B. Evlyukhin, C. Reinhardt, B. N. Chichkov, A. V. Kabashin
  Applied Physics Letters **104**, pp. 071101-1 - 071101-5 (2014)

5.2 Scattering Properties of Spherical Silicon Nanoparticles

In order to provide suitable meta-atoms for the visible spectral range, silicon nanoparticles have been suggested in 2010 within the work for this thesis, due to existence of magnetic dipole resonances [35]. Experimentally, the occurrence of these resonances has firstly been demonstrated in [36], where the spherical silicon particles have been realized by laser ablation from bulk silicon surfaces. Fabrication approaches of monodisperse spherical silicon particles with controllable positioning have been suggested in [37, 38]. These are summarized in the next section 5.2.1.

As in the previous case it is helpful to generate a map for the extinction efficiency in dependence on the particle radius and the incident wavelength using Mie theory, Fig.5.5. The dielectric function of crystalline silicon can be evaluated from the complex refractive index data provided in [280, 281]. The map shows the electric dipole, magnetic dipole, and total extinction efficiency.
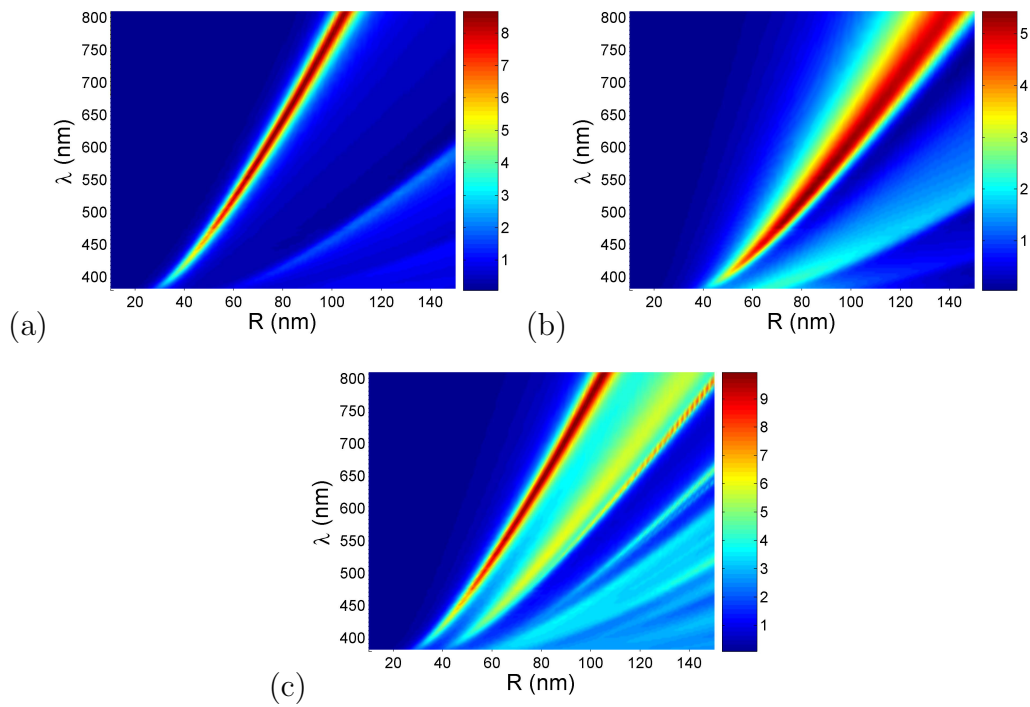
Figure 5.5:
   Extinction efficiency of silicon nanoparticles in dependence on radius and incident
   wavelength: (a) Magnetic dipole contribution only. (b) Electric dipole contribution
   only. (c) Total extinction using electric and magnetic Mie coefficients.
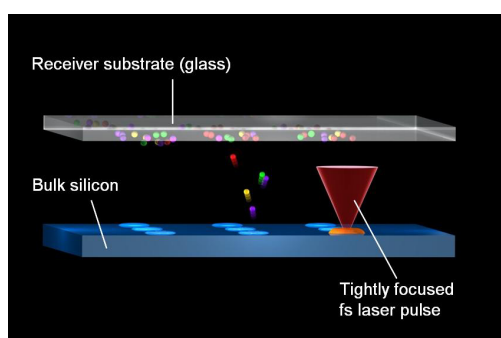
Figure 5.6: Schematic of laser-induced transfer from bulk silicon wafer surfaces.
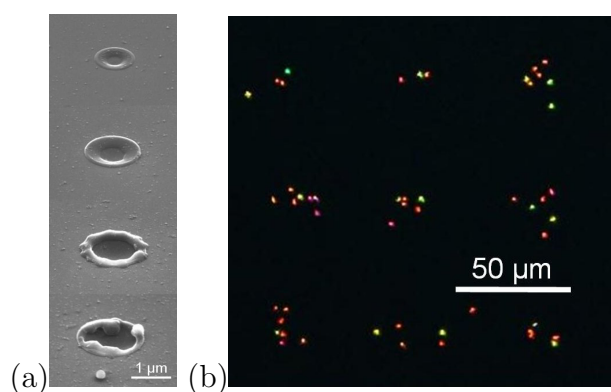

(a)   (b)

Figure 5.7:
(a) SEM image from silicon wafer surface. (b) Dark field image of the particles captured on the receiver substrate. No controlled production of particles, different colors indicate different diameters

5.2.1 Laser-Induced Transfer of Silicon Nanoparticles

In the work for this professorial dissertation, it has firstly been demonstrated that spherical silicon nanoparticles can be realized from laser ablation processes from silicon wafers. However, the laser-transfer from silicon wafers does not lead to controlled positioning of single particles. Instead, numerous particles are ejected and deposited uncontrollably onto a receiver glass substrate. The schematic is shown in Fig.5.6.

Silicon reduces its volume during transit from the solid to the liquid phase. This leads to a pressure gradient dragging the liquid material to the outside rim of the molten zone. Due to the Rayleigh instability [37], the material starts to form several numbers of nanoparticles, see Fig.5.7.

To control the melting process and to produce only one single particle per laser pulse, a laser beam with a ring shaped intensity can be applied. The minimum particle diameters in this case are in the range of 350 nm to 500 nm. Details can be found in [37].

A controlled deposition of single silicon nanoparticles with smaller diameters, however, can be achieved using silicon-on-insulator (SOI) wafers as a donor substrate, as schemat-
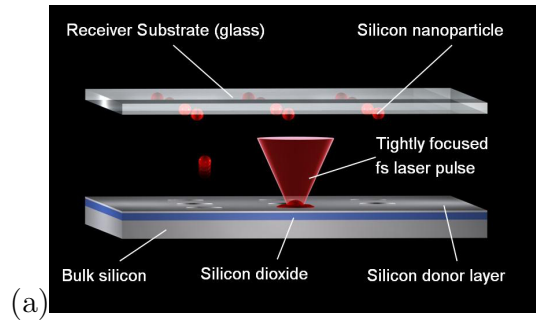
(a)

Figure 5.8: Schematic of laser-induced transfer from SOI wafer surfaces.
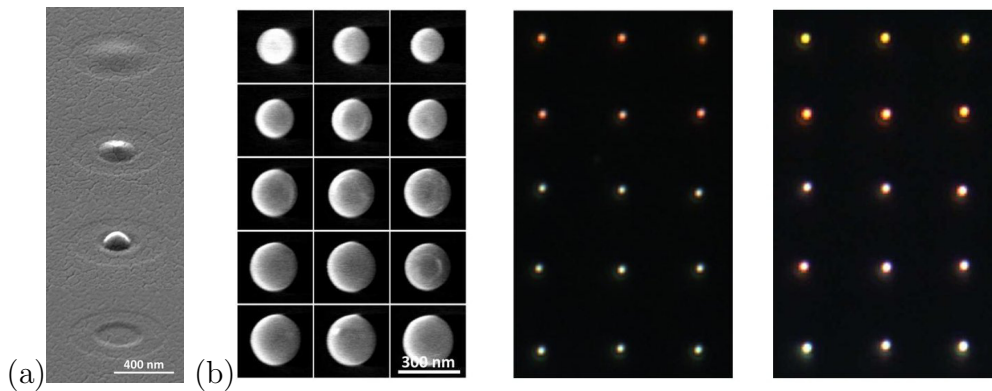

(a)   (b)

Figure 5.9:

(a) SEM image from SOI wafer surface. (b) SEM (left) and dark field (right) images of particles captured on the receiver substrate. Different sizes had been adjusted by laser pulse energy, position control on the receiver is possible. The dark field images show the same particles before (left) and after (right) recrystallization.

ically shown in Fig.5.8. Wafers used in the present experiments have a 50 nm thick crystalline silicon layer. One single laser pulse can melt the silicon film, and the molten disk-shaped material contracts into a sphere, driven by the surface tension of the liquid material. This leads to an elevation of the center-of-mass of the material volume which moves the particle towards the receiver substrate. The particles cool down rapidly on the receiver substrate, resulting in an amorphous phase, as it has been shown by spectrally resolved light scattering, see Fig.5.9.

To confirm the amorphous phase from the spectral measurements the experimental results are compared to Mie theory using the dielectric function for amorphous silicon [281]. After further irradiation and heating, each single particle can selectively re-crystallized. The crystalline particles have lower absorption and thus stronger resonances which can be seen as a brighter scattering in the dark-field microscopy image in Fig.5.9b

The fabrication process for spherical silicon nanoparticles using SOI and the control of the crystallographic phase have been demonstrated for the first time. A detailed investigation of the fabrication process, the optical measurements, and the theoretical

modelling of the silicon particle optical properties is published in [38].

Important main contributions:

- **First demonstration of spherical silicon nanoparticles with magnetic resonances in the visible spectrum**

- **Development of novel fabrication technology for spherical silicon particles with determined position from bulk silicon wafers and SOI wafers**

- **Laser-induced recrystallization of amorphous silicon particles**

The relevant literature is:

- *Demonstration of Magnetic Dipole Resonances of Dielectric Nanospheres in the Visible Region*
  A. B. Evlyukhin, S. M. Novikov, U. Zywietz, R. L. Eriksen, C. Reinhardt, S. I. Bozhevolnyi, B. N. Chichkov
  Nano Letters **12**, pp. 3749 - 3755 (2012)

- *Generation and patterning of Si nanoparticles by femtosecond laser pulses*
  U. Zywietz, C. Reinhardt, A. B. Evlyukhin, T. Birr, B. N. Chichkov
  Applied Physics A **114**, pp. 45 - 50 (2014)

- *Laser printing of silicon nanoparticles with resonant optical electric and magnetic responses*
  U. Zywietz, A. B. Evlyukhin, C. Reinhardt, B. N. Chichkov
  Nature Communications **5**, pp. 4402-1 - 4402-7 (2014)

6 Optical Characterization Methods

In this chapter, optical characterization methods for surface plasmon-polaritons and nanoparticles are summarized. The techniques to visualize SPP propagation and their interaction with surface nanostructures and nanoparticles include initial investigations of the first polymer-based dielectrically-loaded SPP waveguides by scanning near-field optical microscopy (SNOM) and leakage radiation microscopy (LRM). Two-photon photoelectron emission microscopy (2PPEEM) has been applied for time resolved imaging.

Near-field and far-field characterization of nanoparticles and nanoparticle structures has been accomplished by surface enhanced Raman scattering (SERS) and single particle spectroscopy (SPS), respectively.

At the end of the chapter, recent investigations of field enhancement effects are presented, showing further possibilities for near-field imaging in and around nanoantennas and utilization of high field strengths in nonlinear optics.

6.1 Scanning Near-Field Optical Microscopy (SNOM)

The original idea of performing microscopy by scanning optical near-field over a sample surface has been suggested by Synge in 1928 using evanescent light transmission through a sub-wavelength hole [84]. He also suggested the use of piezoelectric crystals for fast and precise positioning [282]. SNOM has been introduced to nanooptics applications in 1981 by Pohl [85,283] in analogy to scanning raster force microscopy, using an extruded optical fiber covered with silver or aluminium. The method allows detection of SP near-fields in different geometries and on semi-infinite systems. It has also been applied in combination with heterodyne detection for temporally resolved tracking of SPP propagation [284].

In the experiment performed within this work, SPPs on the gold film have been excited by prism coupling using a laser wavelength of 1520 nm. Near-field images have been recorded in the collection mode. Tip diameters of the fiber have been in the range of 100 nm. The setup is described in [285].

To enhance the incoupling into the waveguides, a taper structure has been added to the simple polymer line. The length of the taper has to be chosen as a trade-off between the finite decay length of the SPP and the back-reflection and scattering losses. The near-field distribution and the topography of the tapered waveguides for different taper lengths is shown in Fig.6.1, indicating the advantage of a small taper angle.

Important main contributions:

- **First demonstration of functionality of dielectrically loaded SPP waveguides from polymer**

- **Tapered waveguides for improved incoupling**
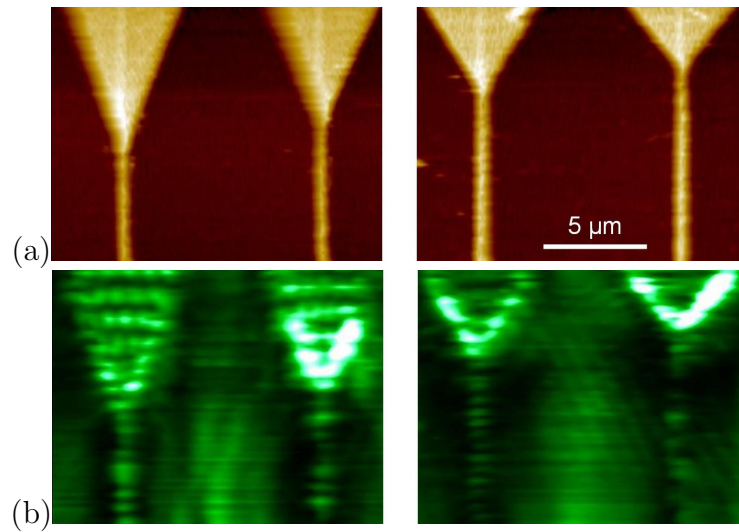
The relevant literature is:

Figure 6.1:
  Surface topography (a) and optical near-field distribution (b) for tapered DLSPPWs
  with different taper length.

- *Laser-fabricated dielectric optical components for surface plasmon polariton*
  C. Reinhardt, S. Passinger, B. N. Chichkov, C. Marquart, I. P. Radko, S. I.
  Bozhevolnyi
  Optics Letters **31**, pp. 1307 - 1309 (2006)

6.2 Leakage Radiation Microscopy (LRM)

A first observation of SPP leakage radiation from thin metal films has been reported in
1971 by Kr"oger and R"ather [286], using SPP excitation by electrons, and later by [287],
using light scattering on rough metallic films for SPP excitation. Optical imaging using
immersion oil microscope objectives has been suggested 1996 by Hecht et al. using SPPs
excitation by local light scattering from a SNOM tip [288]. This detection assembly
represents first LRM for investigation of SPPs on metallic films. In addition to the
surface image, it has been shown that an optical Fourier transform can be performed
by imaging of the back focal plane (BFP) of the microscope objective. The BFP image
allows distinguishing between scattered light and SPP leakage radiation. The leakage
radiation is emitted under sharp angles with respect to the surface normal, forming two
sharp crescent shaped features in the BFP image, whereas scattered light from the surface
defects or local excitation points appears under a broad angular distribution, showing
as a band in the BFP image. In 2006, Drezet et al. have shown that first producing
an image of the BFP and then performing a subsequent optical Fourier transform to
obtain the surface image on a camera provides the unique possibility to filter out noise
signals [289]. A detailed review about the technique is given in [290].

  LRM has been applied to imaging SPP excitation and propagation properties on gold
films and it has been demonstrated that this method can also be applied for investigation
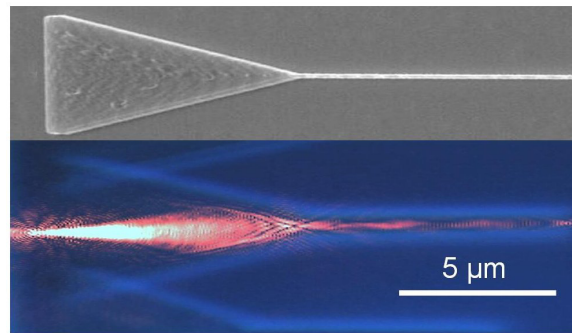
Figure 6.2:
  Example of a LRM image of two interfering SPPs. (a) Experimental results. (b) Theoretical simulation using 2D Gaussian beams.

of waveguiding in polymer DLSPPWs [12,13]. Focussing and directing of two-dimensional Gaussian SPP beams and SPP waveguiding have been investigated in details in [15–18, 22, 49, 50]. Mode-selective excitation and switching operation in Y-splitters has been demonstrated firstly within the work for this thesis [17, 23].

As a novel approach for characterization of optical properties of gold nanoparticles on thin gold films, LRM images of SPP scattering have been evaluated to demonstrate the relevance of quadrupole moments for particle diameters exceeding 100 nm [30]. This method is discussed in section 6.6.

An example of SPP excitation and guiding in a tapered waveguide made from maN-1405 photoresist is given in Fig.6.2.

Important main contributions:

- **Excitation and focussing of SPP Gaussian beams on curved and straight ridges**

- **Demonstration of functionality of laser-written DLSPPWs in the visible and infrared spectral ranges**

- **Mode-selective excitation of multimode DLSPPWs**

- **Demonstration of excitation dependent routing and switching in DL-SPPW Y-splitters**

- **First demonstration of quadrupole contributions for SPP scattering on gold nanoparticles**

The relevant literature is:

- *Rapid laser prototyping of optical components for surface plasmon polaritons*
  R. Kiyan, C. Reinhardt, S. Passinger, A. L. Stepanov, A. Hohenau, J.R. Krenn, and B. N. Chichkov
  Optics Express **15**, pp. 4205 - 4215 (2007)

- *Rapid laser prototyping of plasmonic components*
  C. Reinhardt, R. Kiyan, S. Passinger, A. L. Stepanov, A. Ostendorf, and B. N. Chichkov
  Applied Physics A **89**, pp. 321 - 325 (2007)

- *Focussing and directing of surface plasmon polaritons by curved chains of nanoparticles*
  A. B. Evlyukhin, S. I. Bozhevolnyi, A. L. Stepanov, R. Kiyan, C. Reinhardt, S. Passinger, B. N. Chichkov
  Optics Express **15**, pp. 16668 - 16680 (2007)

- *Nanoimprinting of dielectric loaded surface plasmon-polariton waveguides from masters fabricated by 2-photon polymerization technique*
  A. Seidel, C. Ohrt, S. Passinger, C. Reinhardt, R. Kiyan, B. Chichkov
  Journal of the Optical Society of America B **26**, pp. 810 - 812 (2009)

- *Mode-selective excitation of laser-written dielectric-loaded surface plasmon polariton Waveguides*
  C. Reinhardt, A. Seidel, A. B. Evlyukhin, W. Cheng, B. N. Chichkov
  Journal of the Optical Society of America B **26**, pp. B55 - B60 (2009)

- *Laser-induced transfer of metallic nanodroplets for plasmonics and metamaterial applications*
  A. I. Kuznetsov, A. B. Evlyukhin, C. Reinhardt, A. Seidel, R. Kiyan, W. Cheng, A. Ovsianikov, B. N. Chichkov
  Journal of the Optical Society of America B **26**, pp. B130 - B138 (2009)

- *Direct laser-writing of dielectric-loaded surface plasmon-polariton waveguides for the visible and near infrared*
  C. Reinhardt, A. Seidel, A. B. Evlyukhin, W. Cheng, R. Kiyan, B. N. Chichkov
  Applied Physics A **100**, pp. 347 - 352 (2010)

- *Demonstration of Laser-Fabricated DLSPPW at Telecom Wavelength*
  A. Seidel, C. Reinhardt, T. Holmgaard, W. Cheng, T. Rosenzveig, K. Leosson, S. I. Bozhevolnyi, B. N. Chichkov
  IEEE Photonics Journal **2**, pp. 652 - 658 (2010)

- *Photonic bandgap plasmonic waveguides*
  A. Markov, C. Reinhardt, B. Ung, A. B. Evlyukhin, W. Cheng, B. N. Chichkov, M. Skorobogatiy
  Optics Letters **36**, pp. 2468 - 2470 (2011)

- *Bandgap-confined large-mode waveguides for surface plasmon-polaritons*
  C. Reinhardt, A. B. Evlyukhin, W. Cheng, T. Birr, A. Markov, B. Ung, M. Skorobogatiy, B. N. Chichkov
  Journal of the Optical Society of America B **30**, pp. 2898 - 2905 (2013)

6.3 Photoelectron Emission Microscopy (PEEM)

The principle of PEEM has been shown in 1933 by Brüche [291]. PEEM analyzes directly the spatial photoelectron yield with high resolution. In the case that the photon energy is lower than the work function, the simultaneous absorption of two or more photons can lead to photoelectron emission. Due to the short free path length of electrons in a solid material this effect is presumably surface sensitive [292] and the local photoelectron current is a function of the local electric fields at the surface and the work function [293–295]. This current is proportional to the square of the local surface intensity of the electric field for two-photon photoemission [295].

The electric field at the sample surface is a superposition of the electric laser field and the SPP electric field having different phase velocities. Hence, the excitation and propagation of SPPs appears indirectly as an interference of these two field contributions to the electron emission, leading to a contrast in the PEEM image [296]. The work function of the usually used gold surfaces is typically about 5.4 *eV* [297], which would require at least a three-photon absorption in the spectral region around 633 nm up to a four-photon absorption at 800 nm and a five-photon absorption around 1000 nm. To lower the work function to allow two-photon photoemission at 800 nm, less than one monolayer of caesium is deposited on the gold surface [298].

In the experiments, a PEEM from *Focus GmbH* with an electrostatic lens system has been used [299]. A maximum magnification of about 3500 times can be obtained and the achievable resolutions is estimated to about 40 nm. Ultrashort SPPs are excited by p-polarized laser radiation at 800 nm wavelength and pulse durations around 18 fs from a titanium:sapphire oscillator-amplifier system from *KMLabs*. The chirp induced by the entrance window to the PEEM vacuum chamber and the focussing lens has been compensated by a prism compressor [300]. Laser radiation has been focussed onto the sample with a 500 mm focal length lens under an angle of 65° with respect to the sample surface normal on a 3 µm wide and 100 nm high gold ridge. The ridge is orientated perpendicular to the incoming laser radiation. Details of the imaging process for SPPs are described in [301, 302].

Photoemission electron microscopy (PEEM) has been applied to investigations of focussing properties of parabolic metal edges and 2D Fresnel lens structures [6] as well as to the study of SPP interactions with LSPs on nanodot structures [7]. Time-resolved measurements of the SPP propagation have been performed in pump-probe experiments. The interference of the SPP excited by the first pulse and its interference with the second pulse for a time delay of 60 fs is shown in Fig.6.5 as an example (from [302]). The static PEEM image obtained for the case of zero delay is provided as comparison.

Important main contributions:

- **Spatially and temporally resolved investigation of ultrashort SPP propagation**

- **Time resolved imaging of SPP-LSP interactions**
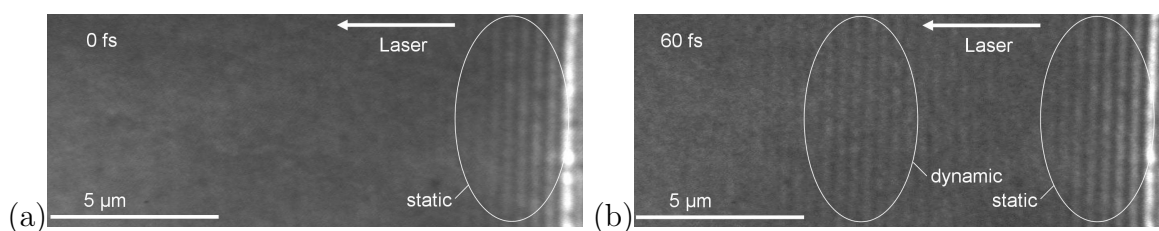
The relevant literature is:

Figure 6.3:
   Interference pattern imaged by PEEM for the static (a) and the dynamic (b) case, recorded for a time delay between the two excitation pulses of 60 fs. The additional interference pattern can be seen in the middle of (b). (from [302])

- *Spatiotemporal Characterization of SPP Pulse Propagation in Two-Dimensional Plasmonic Focussing Devices*
  C. Lemke, C. Schneider, T. Leissner, D. Bayer, J. W. Radke, A. Fischer, P. Melchior, A. B. Evlyukhin, B. N. Chichkov, C. Reinhardt, M. Bauer, M. Aeschlimann
  NANO Letters **13**, pp. 1053 - 1058 (2013)

- *The Interplay between Localized and Propagating Plasmonic Excitations Tracked in Space and Time*
  C. Lemke, T. Leissner, A. B. Evlyukhin, J. W. Radke, A. Klick, J. Fiutowski, J. Kjelstrup-Hansen, H.-G. Rubahn, B. N. Chichkov, C. Reinhardt, M. Bauer
  NANO Letters, DOI 10.1021/nl500106z (2014)

6.4 Surface Enhanced Raman Scattering (SERS) on Gold Nanoparticles

Detailed information about SERS can be found in [213]. SERS has been applied for investigation of field distribution and enhancement in gold mesoparticle pairs with radii of 325 nm and spacing between the particles of about 20 nm [32]. The measurements have been performed using a commercial confocal scanning Raman microscope, model *Alpha300 R* from *Witec*. Raman images have been recorded for an excitation wavelength of 532 nm. The samples have been covered with Rhodamine 6G (R6G) dye in an 10^{-6} M aqueous solution and subsequent drying.

   Raman spectra are recorded with a 600 lines/mm diffraction grating and a 100× microscope objective with an NA of 0.9. The pump laser beam is focussed by the same objective and has been raster scanned over the sample surface, resulting in 25×25 points in a scanned area of 3 µm × 3 µm.

   The Raman images are formed by mapping the spatial dependence of SERS intensity integrated over the main R6G Raman peak within a shift range of 1345 cm^{-1} to 1390 cm^{-1} and a time of 400 ms for each of the 25×25 points. These scan parameters represent a compromise between minimum bleaching of the R6G dye molecules, significant signal-to-noise ratio, and a sufficient step size of 120 nm compared to the spatial resolution of 350 nm of the focussed pump beam. Reference Raman spectra have been recorded at the
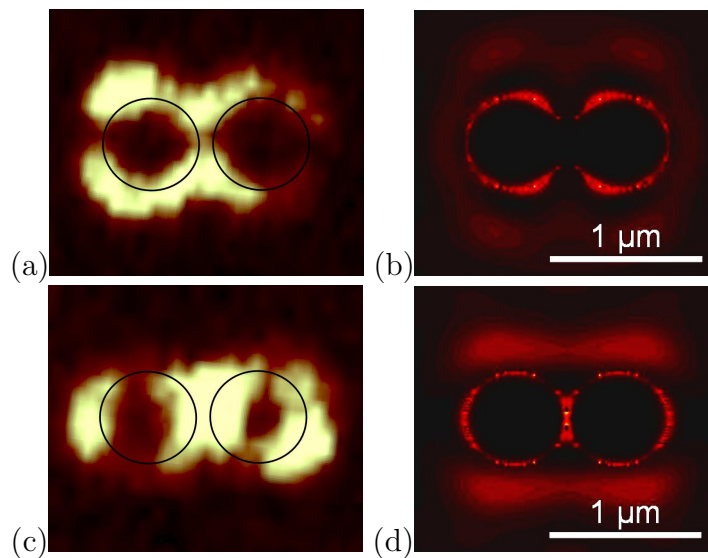
Figure 6.4:

Raman signal for mesoparticle pair: Experimental measurements for electric field direction perpendicular (a) and parallel (c) to the pair axis compared to electric field density calculations (b,d) using FDTD.

smooth gold surface about 50 µm away from the particles using the same parameters. This reference is independent of the polarization of the pump light. Field concentration between the particles is observed for polarization of incident laser light parallel to the particle pair axis [32]. The results in comparison with FDTD simulations are shown in Fig.6.4.

Important main contributions:

- **Demonstration of field concentration in nanoparticle pairs generated by LIT**

The relevant literature is:

- *Optical properties of spherical gold mesoparticles*
  A. B. Evlyukhin, A. I. Kuznetsov, S. M. Novikov, J. Beermann, C. Reinhardt, R. Kiyan, S. I. Bozhevolnyi, B. N. Chichkov
  Applied Physics B **106**, pp. 841 - 848 (2012)

6.5 Single Particle Spectroscopy (SPS)

SPS has been performed in backward [32, 36, 39] and forward directions [37, 38] with respect to the illumination direction. Measurements of scattering properties of gold particles in reflection mode have been performed using a commercial microscope with a 60× infinity-corrected microscope objective with an NA of 0.85. A standard 50 W halogen lamp has been used as illuminating light source. The reflected light from the

sample has been separated from the illumination light by means of a beam splitter. Light from an area of 30 µm diameter has been collected for spectral measurements.

For measuring scattering spectra of silicon particle in the forward direction, an experimental setup has been designed using a dark-field condenser with an NA of 0.9 from *Mueller Optronic* in the illumination beam path. A broad and smooth spectrum for illumination is provided by a high-pressure xenon lamp. The light scattered by individual nanoparticles has been imaged by an infinity-corrected 50× microscope objective with an NA of 0.55 simultaneously on a CCD camera and an optical fiber facet with an aperture of 200 µm. This combination collects light from a circular area with a diameter of 4 µm from the sample surface. Spectra have been recorded using a HR 2000 spectrometer from Ocean Optics.

Important main contributions:

- **Demonstration of multipole contributions in light scattering on gold mesoparticles up to the hexadecapole**

- **First demonstration of electric and magnetic dipole Mie resonances in the visible spectral range for spherical silicon particles**

- **Determination of the crystallographic phase of silicon nanoparticles**

- **Control of directional light scattering from silicon nanocylinders**

The relevant literature is:

- *Optical properties of spherical gold mesoparticles*
  A. B. Evlyukhin, A. I. Kuznetsov, S. M. Novikov, J. Beermann, C. Reinhardt, R. Kiyan, S. I. Bozhevolnyi, B. N. Chichkov
  Applied Physics B **106**, pp. 841 - 848 (2012)

- *Demonstration of Magnetic Dipole Resonances of Dielectric Nanospheres in the Visible Region*
  A. B. Evlyukhin, S. M. Novikov, U. Zywietz, R. L. Eriksen, C. Reinhardt, S. I. Bozhevolnyi, B. N. Chichkov
  Nano Letters **12**, pp. 3749 - 3755 (2012)

- *Generation and patterning of Si nanoparticles by femtosecond laser pulses*
  U. Zywietz, C. Reinhardt, A. B. Evlyukhin, T. Birr, B. N. Chichkov
  Applied Physics A **114**, pp. 45 - 50 (2014)

- *Laser printing of silicon nanoparticles with resonant optical electric and magnetic responses*
  U. Zywietz, A. B. Evlyukhin, C. Reinhardt, B. N. Chichkov
  Nature Communications **5**, pp. 4402-1 - 4402-7 (2014)

- *Laser-ablative engineering of phase singularities in plasmonic metamaterial arrays for biosensing applications*
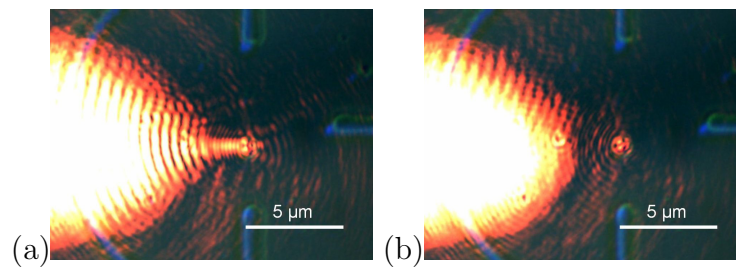
Figure 6.5:
(a) SPP excited on dielectric curved ridge interacting with a nanoparticle. (b) SPP leakage radiation is blocked. Scattering pattern from the nanoparticle shows the superposition of electric dipole and quadrupole.

A. I. Aristov, U. Zywietz, A. B. Evlyukhin, C. Reinhardt, B. N. Chichkov, A. V. Kabashin
Applied Physics Letters **104**, pp. 071101-1 - 071101-5 (2014)

- *Optical spectroscopy of single Si nanocylinders with magnetic and electric resonances*
A. B. Evlyukhin, R. L. Eriksen, W. Cheng, J. Beermann, C. Reinhardt, A. Petrov, S. Prorok, M. Eich, B. N. Chichkov, S. I. Bozhevolnyi
Scientific Reports **4**, 4126 (2014)

6.6 SPPs as Tool for Characterizing Nanoparticles

The combination of 2PP and LIT allows the fabrication of dielectric SPP excitation and focussing structures together with spherical gold meso- and nanoparticles on one sample. This possibility has been investigated in [30].

The different experimental and theoretical methods have been combined for determining multipole contributions of gold particles for SPP scattering. The particles have been positioned in a certain distance to SPP excitation structures to enable interaction with Gaussian SPP beams excited on the polymer ridges. SPP scattering properties have been investigated using LRM, see Fig.6.5. Together with numerical simulations based on the discrete dipole approximation, a significant quadrupole contribution for SPP scattering has been observed for increasing particle diameter, resulting in reduced SPP backscattering. The comparison between experiment and theoretical simulation, summarizing the different topics in this thesis, is provided in Fig.6.6, showing LRM images of SPP scattering on gold particles with diameters of 200 nm and 400 nm. The reduced backscattering appears as a reduced interference contrastin the direction of the incoming SPP beam.

6.7 Field Enhancement Effects

Ultrashort laser pulse illumination of metallic nanostructures has been used to create enhanced electromagnetic fields inside and outside of the structures. A precise knowl-
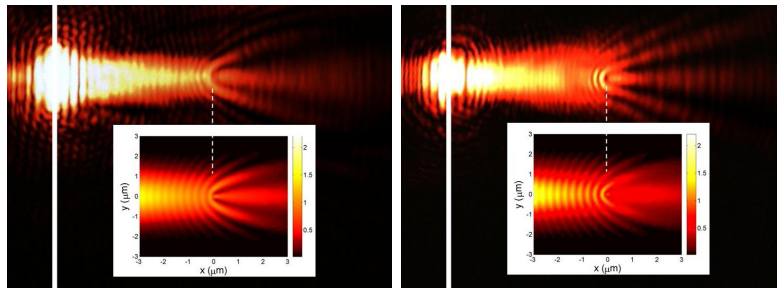
Figure 6.6:
 Reduced backward SPP scattering for gold mesoparticles with 400 nm diameter. The right images show the SPP scattering from a 200 nm particle.

edge about plasmonic excitations, the localization of field hotspots, and the near-field distributions around nanoantennas is of huge importance for the understanding of properties of plasmonic metamaterials as well as for the investigation and explanation of nonlinear effects, which occur due to the strong electromagnetic fields, and their possible applications, e.g. second- or higher-order harmonic generation [272].

For mapping the local near-fields around plasmonic nanostructures, nonlinear illumination of PMMA photoresist has been studied. The principle approach has been suggested in 2005 by Hubert et al. to image dipolar near-fields around metallic nanoparticles using mass transport in azobenzene dye [305]. In contrast, PMMA reacts on deep UV exposure with the fraction of polymer chains into smaller molecules, which provides higher resolution. It has been shown for the first time that using laser radiation around 860 nm wavelength for excitation of the gold nanoantennas leads to a four-photon resonant absorption in PMMA. It should be noted that this nonlinear absorption does not result in evaporation or burning of the polymer. The illuminated material can be removed by the standard developer as described in [33]. Rod-type nanoantennas with resonances ranging from $\lambda/2$ up to $5\lambda/2$ have been demonstrated with resolution of 10 nm using scanning electron microscopy [24].

In order to map the field hotspots inside chiral metallic structures [25] and straight nanorod antennas [26], the laser-induced melt dynamic has been applied. This technique allows mapping the plasmonic field patterns inside metallic nanostructures with the resolution of scanning near-field microscopy and concentrating optical energy down to subwavelength scales [303]. For illumination, strong ultrashort 50 fs laser pulses at 800 nm central wavelength with intensities around 10^{12} W/cm^2 from an titanium:sapphire amplifier system have been used. The laser system consists of a femtosecond oscillator *Tsunami* together with an amplifier *Spitfire* from *Newport-Spectra Physics*, operating at 1 kHz repetition rate. In the experiments, the structures have been illuminated by single laser pulses. The beam profile on the sample has a square cross section with dimensions of 5×5 µm^2 and a flat-top intensity distribution. Although the intensity of 10^{12} W/cm^2 is not sufficient to directly melt the metal, local molten features on the nanostructures become visible at the positions of the current hotspots, see Fig.6.8. It has been found that the position of the field hotspots is linked with the position of the induced
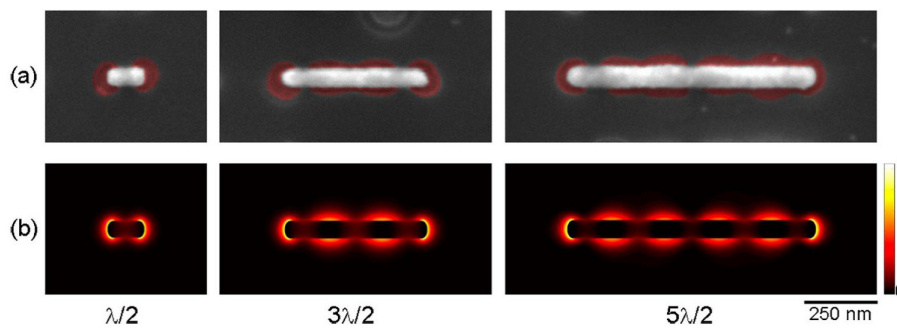
Figure 6.7:
Near-field pattern around gold nanoantennas with different length excited at 860 nm. The field patterns indicating the fundamental (left), third- (middle), and fifth-order (right) resonance have been imaged into PMMA by a four-photon process. Experimentally obtained field patterns (a) have been supported by FDTD simulations (b).(From [24])

magnetic fields [26] and the induced electric currents inside the metal nanostructures. Since high electric field enhancements occur at the same positions, these locations on the nanostructures act as sources for second-harmonic generation [304].

A possible application of near-field enhancement effects in plasmonic nanostructures that has been discussed in recent years is the generation of high-order harmonics (HHG) directly from femtosecond laser oscillators [121–126]. A possible scheme consists of resonant bow-tie antennas placed on a transparent substrate. The structures are placed in vacuum and are illuminated by ultrashort laser pulses through the substrate. Xenon gas, used as the nonlinear medium for HHG, is being injected into the bow-tie gaps through a vacuum nozzle [9, 10, 121].

It has been found that the nanostructures are easily melted, before a comparable field enhancement to that reported in [121] can be reached [9, 10, 25, 26]. It could be shown that slight detuning of the laser frequency helps avoiding melting but only xenon plasma lines have been observed. The investigation of HHG from resonant nanostructures still remains a topic for future investigations.

Important main contributions:

- **Imaging of plasmonic hotspots inside metallic nanostructures**

- **Surface plasmon induced nanojet formation and nanoparticle ejection**

- **Near-field imaging around metallic rod nanoantennas using resonant 4-photon absorption in PMMA**

- **Demonstration of plasmonic enhanced EUV generation in bow-tie antennas using femtosecond oscillators**
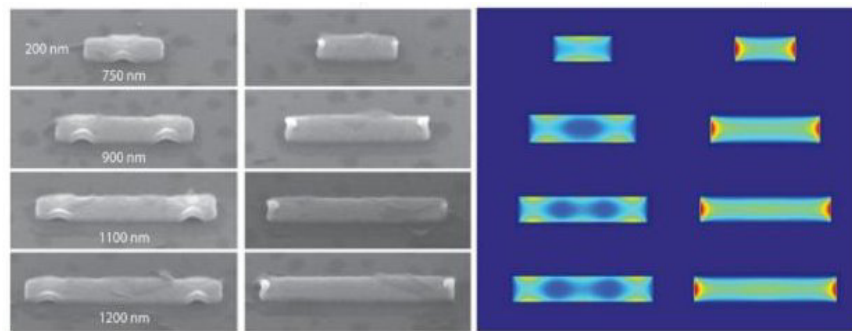
The relevant literature is:

Figure 6.8:
Melting pattern in nanorod antennas indicating field hotspots. The incident wavelength is 800 nm. The direction of the electric field is parallel to the long antenna axis for the left column and perpendicular for the right column of the electron microscopic images. FDTD calculations show the corresponding current hotspots. (From [26])

- *Near-Field Mapping of Plasmonic Antennas by Multiphoton Absorption in Poly (methyl methacrylate)*
  G. Volpe, M. Noack, S.S. Acimovic, C. Reinhardt, R. Quidant
  NANO Letters **12**, pp. 4864 - 4868 (2012)

- *Plasmon-Enhanced Sub-Wavelength Laser Ablation: Plasmonic Nanojets*
  V. K. Valev, D. Denkova, X. Zheng, A. I. Kuznetsov, C. Reinhardt, B. N. Chichkov, G. Tsutsumanova, E. J.Osley, V. Petkov, B. DeClercq, A. V. Silhanek, Y. Jeyaram, V. Volskiy, P. A. Warburton, G. A. E. Vandenbosch, S. Russev, O. A. Aktsipetrov, M. Amelo, V. V. Moshchalkov, T. Verbiest
  Advanced Materials **24**, pp. OP29 - OP35 (2012)

- *Nanostripe length-dependence of plasmon-induced material deformation*
  V. K. Valev, W. Libaers, U. Zywietz, X. Zheng, M. Centini, N. Pfullmann, L.O. Herrmann, C. Reinhardt, V. Volskiy, A. V. Silhanek, B. N. Chichkov, C. Sibilia, G. A. E. Vandenbosch, V. V. Moshchalkov, J. J. Baumberg, T. Verbiest
  Optics Letters **38**, pp. 2256 - 2258 (2013)

- *Bow-tie nano-antenna assisted generation of extreme ultraviolet radiation*
  N. Pfullmann, C. Waltermann, M. Noack, S. Rausch, T. Nagy, C. Reinhardt, M. Kovacev, V. Knittel, R. Bratschitsch, D. Akemeier, A. Huetten, A. Leitensdorfer, U. Morgner
  New Journal of Physics **15**, pp. 093027-1 - 093027-14 (2013)

- *Nano-antennae assisted emission of extreme ultraviolet radiation*
  N. Pfullmann, M. Noack, J.C. de Andrade, S. Rausch, T. Nagy, C. Reinhardt, V. Knittel, R. Bratschitsch, A. Leitensdorfer, D. Akemeier, A. Huetten, M. Kovacev, U. Morgner
  Annalen der Physik **526**, pp. 119–134 (2014)

7 Theoretical and Numerical Methods

Commonly used numerical methods to get an insight into dynamic or static electric and magnetic field distributions inside nanostructures are the finite element method (FEM) and finite-difference time-domain (FDTD) simulations, being described in the first two sections of this chapter. Both, FDTD and FEM have been applied in a commercial software package by *RSoft Design Group*, now part of *Synopsis Optical Solutions Group* since 2012 [306]. FDTD has been used for simulation of time dependent SPP excitation and propagation as well as for calculating temporal evolution of electric and magnetic fields in and around nanoparticles and nanoparticle structures. FEM has been applied to calculation of static 2D mode structures for the cross-sections of SPP waveguides.

For the case of spherical nanoparticles, field distributions and polarizabilities have been calculated using Mie theory. Its implementation is briefly outlined in the third section.

An exact formulation to calculate field distributions of electric dipole scattering from single particles is given in terms of the Green's function. Complex particles can be thought to be build up from a set of point dipoles. The corresponding theoretical formulation in the Discrete-Dipole Approximation (DDA) is introduced in the fourth section.

For the simulations of field distributions a computational cluster consisting of 5 nodes with quad core computers has been set up. Each computer runs at 2.6 GHz and is equipped with 8 GByte of RAM.

7.1 Finite-Difference Time-Domain Method

The FDTD calculations use the simulation tool *FullWAVE* by *RSoft* [307]. The vectorial Maxwell equations are discretized using the central difference scheme for the spatial and temporal partial derivatives [308].

The initial idea for finite difference schemes dates back to A. Thom in 1920, who developed the method of squaring to numerically solve differential equation in hydrodynamics [309]. A detailed description can be found in [310]. The time-dependent finite-difference schemes for second-order wave equations and stability criteria have been introduced by Courant, Friedrichs, and Lewy in [311]. The arrangement of the space grid and the temporal stepping, implementing Faraday's law, has been reported about 38 years later by Yee, which can be regarded as the starting point for modern FDTD calculations [312]. The calculation domain has to be closed by appropriate boundary conditions. Besides symmetric and antisymmetric periodic boundaries and perfect conductors, absorbing boundary conditions which are impedance matched to the calculation domain (perfectly matched layers, PML) have been used [313]. A complete mathematical description can be found in [314].

The FDTD method has been used in the context of different micro-and nanooptical problems. In all calculations, PML has been applied to the truncation of the computational domain. The grid discretization has been chosen to $\lambda/20$ for reliable simulations,

where λ is the wavelength in the material component with the highest refractive index. FDTD has been applied to the simulation of SPP field distributions and propagation in DLSPPWs and large-mode bandgap-confined waveguides [20,21]. It has been shown that this method is also capable of simulating 3D light propagation through laser fabricated microscale conical lenses with high accuracy [47]. Electric field distributions have been simulated for metallic particles located on a metal surface, showing the mode structure of the particle [32]. The SPP field distributions in plasmonic focussing devices have been compared with PEEM measurements, yielding good correlation of experimental and numerical results [6,7].

Important main contributions:

- **Design of a novel SPP Y-splitter concept**

- **Simulation of microaxicon performance**

- **Simulation of optical near-fields around nanostructures:**
  Spherical nanoparticles, chiral structures, and rod or bow-tie nanoantennas

- **3D simulation of ultrashort SPP excitation, propagation, and focussing**

- **3D simulation of ultrashort SPP-LSP interaction**

- **3D simulation of SPP propagation in bandgap-confined waveguide structures**

The relevant literature is:

- *Novel efficient design of Y-splitter for surface plasmon-polariton applications*
  S. Passinger, A. Seidel, C. Ohrt, C. Reinhardt, A. Stepanov, R. Kiyan, B.N Chichkov
  Optics Express **16**, pp. 14369 - 14379 (2008)

- *Optical properties of spherical gold mesoparticles*
  A. B. Evlyukhin, A. I. Kuznetsov, S. M. Novikov, J. Beermann, C. Reinhardt, R. Kiyan, S. I. Bozhevolnyi, B. N. Chichkov
  Applied Physics B **106**, pp. 841 - 848 (2012)

- *Closely packed hexagonal conical microlens array fabricated by direct laser photopolymerization*
  A. Zukauskas, M. Malinauskas, C. Reinhardt, B. N. Chichkov, R. Gadonas
  Applied Optics **51**, pp. 4995 - 5003 (2012)

- *Bandgap-confined large-mode waveguides for surface plasmon-polaritons*
  C. Reinhardt, A. B. Evlyukhin, W. Cheng, T. Birr, A. Markov, B. Ung, M. Skorobogatiy, B. N. Chichkov
  Journal of the Optical Society of America B **30**, pp. 2898 - 2905 (2013)

- *Spatiotemporal Characterization of SPP Pulse Propagation in Two-Dimensional Plasmonic Focussing Devices*
  C. Lemke, C. Schneider, T. Leissner, D. Bayer, J. W. Radke, A. Fischer, P. Melchior, A. B. Evlyukhin, B. N. Chichkov, C. Reinhardt, M. Bauer, M. Aeschlimann
  NANO Letters **13**, pp. 1053 - 1058 (2013)

- *The Interplay between Localized and Propagating Plasmonic Excitations Tracked in Space and Time*
  C. Lemke, T. Leissner, A. B. Evlyukhin, J. W. Radke, A. Klick, J. Fiutowski, J. Kjelstrup-Hansen, H.-G. Rubahn, B. N. Chichkov, C. Reinhardt, M. Bauer
  NANO Letters, DOI 10.1021/nl500106z (2014)

7.2 Finite Element Method

The FEM calculations use the simulation tool *FemSIM* by *RSoft* [315]. It is a modesolver for transverse and cavity modes with 2D cross sections.

The origin of this method dates back to 1943 when it has been introduced by Courant for equilibrium and vibration analysis [316]. FEM in electromagnetic problems emerged in the late 1960th [317]. The principle is based on a subdivision of the computational domain into smaller sub-domains, the finite elements. The method applies a nonuniform hybrid triangular/rectangular mesh to calculate the electric field components of the modes. The wave equations are solved on the FEM grid by minimizing the functional of the wave equation with respect to the given material distribution. In order to introduce the material distribution into the calculation the mesh is generated automatically according to the structure and it covers both, the computational domain and the PML. The complex procedure and the mathematical treatment of FEM in electrodynamics together with an implementation into Matlab can be found in [308, 318] and references therein.

The FEM modesolver has been applied to the calculation of mode structures of open core SPP waveguides with bandgap confinement [19, 20].

Important main contributions:

- **Simulation of mode structures for bandgap-confined large-mode waveguides**

The relevant literature is:

- *Photonic bandgap plasmonic waveguides*
  A. Markov, C. Reinhardt, B. Ung, A. B. Evlyukhin, W. Cheng, B. N. Chichkov, M. Skorobogatiy
  Optics Letters **36**, pp. 2468 - 2470 (2011)

- *Bandgap-confined large-mode waveguides for surface plasmon-polaritons*
  C. Reinhardt, A. B. Evlyukhin, W. Cheng, T. Birr, A. Markov, B. Ung, M. Skorobogatiy, B. N. Chichkov
  Journal of the Optical Society of America B **30**, pp. 2898 - 2905 (2013)

7.3 Mie Theory

The scattering and absorption properties of small spherical particles have already been analyzed in 1890 by L. Lorenz [319, 320]. The problem, in connection with Maxwell's equations has been treated independently in 1908 by Mie to describe the color of colloidal gold nanoparticle solutions [95]. A review on Mie theory and developments until 2012 can be found in [321]

The basis of the analysis is the consideration of the interaction of a spherical particle with radius a and refractive index $n_p = \sqrt{\epsilon_p}$, embedded inside a dielectric host medium with refractive index $n_d = \sqrt{\epsilon_d}$, subjected to an incident plane electromagnetic wave with wave vector $k_d = n_d k_0$ inside the host medium. Throughout the calculation it is assumed that the permeabilities of the particle and the host are $\mu_p = 1 = \mu_d$, as usual in the optical range.

The modes of the sphere are expressed in terms of spherical harmonics. To extract absorption and scattering cross sections as well as electric and magnetic fields inside and outside the sphere the plane wave has to be expressed in spherical coordinates. An explicit treatment of this problem can for instance be found in the textbooks of Bohren and Huffman [322] and Born and Wolf [323]. The calculation of fields and scattering and extinction cross sections within this work have been performed according to the formulas given in chapter 4 of [322].

The optical properties of nanoparticles are described in terms of the scattering and extinction cross sections c_{sca} and c_{ext}, respectively. These quantities are expressed in terms of the Mie coefficients a_l and b_l as

$$c_{sca} = \frac{2\pi}{k_d} \sum_{l=1}^{\infty} (2l+1)(|a_l|^2 + |b_l|^2) \tag{7.1}$$

$$c_{ext} = \frac{2\pi}{k_d} \sum_{l=1}^{\infty} (2l+1)\Re(a_l + b_l) \quad . \tag{7.2}$$

The absorption cross section can be obtained according to $c_{abs} = c_{ext} - c_{sca}$. The Mie coefficients are

$$a_l = \frac{m\psi_l(u)\psi_l'(v) - \psi_l(v)\psi_l'(u)}{m\psi_l(u)\xi_l'(v) - \xi_l(v)\psi_l'(u)} \tag{7.3}$$

$$b_l = \frac{\psi_l(u)\psi_l'(v) - m\psi_l(v)\psi_l'(u)}{\psi_l(u)\xi_l'(v) - m\xi_l(v)\psi_l'(u)} \quad , \tag{7.4}$$

where the following abbreviations have been introduced:

$$m = \frac{n_p}{n} \tag{7.5}$$

$$v = k_d a \tag{7.6}$$

$$u = mv \quad . \tag{7.7}$$

The functions ψ_l and ξ_l are the Ricatti-Bessel functions, which are defined as

$$\psi_l(x) \;=\; \sqrt{\frac{\pi x}{2}} J_{l+\frac{1}{2}}(x) \tag{7.8}$$

$$\xi_l(x) \;=\; \sqrt{\frac{\pi x}{2}} \left[J_{l+\frac{1}{2}}(x) + i Y_{l+\frac{1}{2}}(x) \right] \quad , \tag{7.9}$$

using the Bessel functions of first and second kind J_ν and Y_ν, respectively. These functions are conveniently available in various programming languages and computer algebra programs.

The Mie coefficients a_l and b_l are connected with the electric and magnetic scattering multipoles of the sphere, respectively [322, 324]. The coefficient a_1 represents the electric dipole of the particle, b_1 is the magnetic dipole. Correspondingly, the electric and magnetic dipole polarizabilities of the sphere are therefore

$$\alpha^E \;=\; i\frac{6\pi\epsilon_0\epsilon_d}{k_d^3} a_1 \tag{7.10}$$

$$\alpha^M \;=\; i\frac{6\pi}{k_d^3} b_1 \quad . \tag{7.11}$$

These expressions have been applied in the calculation of scattering properties of silicon particles and arrays of silicon particles [35], where the occurrence of magnetic dipole modes in the visible spectral range has been shown theoretically. The scattering properties of silicon particles predicted by these calculations have been verified experimentally [36, 37].

Field calculations using Mie theory have been performed for investigation of the optical properties of gold particles with diameters of 150 nm to 650 nm [32]. The calculations of electric and magnetic fields of resonantly driven silicon particles shows that strong magnetic fields can be obtained inside the particles. The influence of a potential oxide shell around the silicon particles has been taken into account [35] according to the formulas given in chapter 8 in [322].

Important main contributions:

- **Calculation of scattering cross sections, polariabilities, and field distributions for spherical particles**

- **Demonstration of magnetic dipole resonances in the visible spectral range for silicon nanoparticles**

The relevant literature is:

- *Optical response features of Si-nanoparticle arrays*
  A. B. Evlyukhin, C. Reinhardt, A. Seidel, B. S. Luk'yanchuk, B. N. Chichkov
  Physical Review B **82**, pp. 045404-1 - 045404-12 (2010)

- *Multipole light scattering by nonspherical nanoparticles in the discrete dipole approximation*
  A. B. Evlyukhin, C. Reinhardt, B. N. Chichkov
  Physical Review B **84**, pp. 235429-1 - 235429-8 (2011)

- *Collective resonances in metal nanoparticle arrays with dipole-quadrupole interactions*
  A. B. Evlyukhin, C. Reinhardt, U. Zywietz B. N. Chichkov
  Physical Review B **85**, pp. 245411-1 - 245411-8 (2012)

- *Optical properties of spherical gold mesoparticles*
  A. B. Evlyukhin, A. I. Kuznetsov, S. M. Novikov, J. Beermann, C. Reinhardt, R. Kiyan, S. I. Bozhevolnyi, B. N. Chichkov
  Applied Physics B **106**, pp. 841 - 848 (2012)

- *Demonstration of Magnetic Dipole Resonances of Dielectric Nanospheres in the Visible Region*
  A. B. Evlyukhin, S. M. Novikov, U. Zywietz, R. L. Eriksen, C. Reinhardt, S. I. Bozhevolnyi, B. N. Chichkov
  Nano Letters **12**, pp. 3749 - 3755 (2012)

- *Generation and patterning of Si nanoparticles by femtosecond laser pulses*
  U. Zywietz, C. Reinhardt, A. B. Evlyukhin, T. Birr, B. N. Chichkov
  Applied Physics A **114**, pp. 45 - 50 (2014)

- *Laser printing of silicon nanoparticles with resonant optical electric and magnetic responses*
  U. Zywietz, A. B. Evlyukhin, C. Reinhardt, B. N. Chichkov
  Nature Communications **5**, pp. 4402-1 - 4402-7 (2014)

7.4 The Green's Function Method in the Discrete-Dipole Approximation

If the optical properties of nonspherical particles shall be calculated, mostly numerical methods are applied. A versatile approach besides FDTD and FEM is the discrete dipole approximation (DDA). The basic idea was published in 1964 by DeVoe for determining the optical absorption and refraction properties of aggregates of monomers [325]. The DDA has been applied by Purcell and Pennycraker in 1973 for considering the scattering properties of interstellar dust particles assumed as point dipoles, where also retardation effects have been taken into account [326]. Due to substantial improvements by Draine et al. it has been evolved into a powerful technique to study light scattering by nanoparticles [327,328] and SPP scattering and excitation, see [34] and references therein. An overview about the development and the mathematical formulation can be found in [329].

The principle is based on the discretization of a homogeneous particle of arbitrary shape into a set of N point electrical dipoles $\mathbf{p}^j$ ($j = 1...N$) with polarizability α_p located at the points $\mathbf{r}_j$ of a reference system, respectively, as it is shown schematically in Fig.7.1.
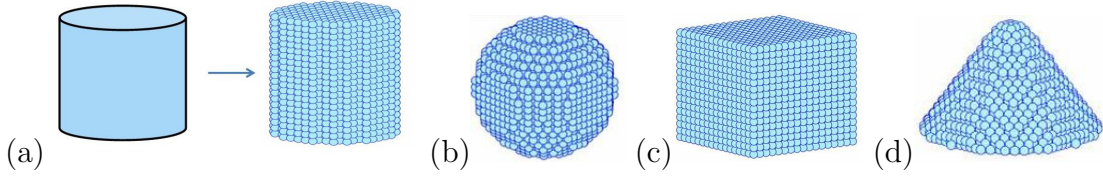
Figure 7.1:
(a) Principle of DDA: Representation of a cylindrical body as a set of point electric dipole particles. (b,c,d) Examples of a sphere, cube, and cone in DDA representation, respectively.

The reference in the simplest case can be an empty background space. Without loss of generality, α_p is the same for all point dipoles. Every dipole $\mathbf{p}^j$ at position $\mathbf{r}_j$ creates a monochromatic electric field at a point $\mathbf{r}$ so that the total electric field is the superposition

$$\mathbf{E}(\mathbf{r}) = \frac{k_0^2}{\varepsilon_0} \sum_{j=1}^{N} \hat{G}(\mathbf{r}, \mathbf{r}_j) \mathbf{p}^j \qquad (7.12)$$

of the individual fields, where k_0 is the wave number in vacuum, ε_0 is the vacuum dielectric constant, $\hat{G}(\mathbf{r}, \mathbf{r}_j)$ is the Green's function tensor, i.e. the dipole field propagator, for dipole $\mathbf{p}^j$ in the reference system without other particles. In a homogeneous dielectric medium with dielectric constant ε_d this tensor can be expressed in the analytical form

$$\hat{G}(\mathbf{r}, \mathbf{r}_j) = \left\{ \left(\frac{1}{R} + \frac{\mathrm{i}}{k_d R^2} - \frac{1}{k_d^2 R^3} \right) \hat{U} \right.$$
$$\left. + \left(-\frac{1}{R} - \frac{\mathrm{i}3}{k_d R^2} + \frac{3}{k_d^2 R^3} \right) \mathbf{e_R}\mathbf{e_R} \right\} \frac{e^{\mathrm{i}k_d R}}{4\pi} ,$$

$$(7.13)$$

where $R = |\mathbf{R}| = |\mathbf{r} - \mathbf{r}_j|$, $k_d = k_0\sqrt{\varepsilon_d}$, $\hat{U}$ is the unit tensor, and $\mathbf{e_R}\mathbf{e_R}$ is the dyadic constructed from the vector $\mathbf{e_R} = \mathbf{R}/R$. The terms in brackets represent the near-, intermediate, and far-field parts of the Green's function. Due to the dyadic $\mathbf{e_R}\mathbf{e_R}$ this tensor depends in general on all coordinates, i.e. distance, azimutal angle, and polar angle of the observation point with respect to the dipole position.

If radiated fields in the far or wave zone ($R \gg 1/k_d$) shall be considered, the tensor can be used in the far-field approximation

$$\hat{G}_{FF}(\mathbf{r}, \mathbf{r}_j) = \left(\hat{U} - \mathbf{e_R}\mathbf{e_R} \right) \frac{e^{\mathrm{i}k_d R}}{4\pi R} . \qquad (7.14)$$

If further $r \gg r'$, then $R = |\mathbf{r} - \mathbf{r}_j| = r - \mathbf{n}\mathbf{r}_j$ ($\mathbf{n}$ is the unit vector in the $\mathbf{r}$-direction), the tensor $\hat{G}_{FF}(\mathbf{r}, \mathbf{r}_j)$ can be written as

$$\hat{G}_{FF}(\mathbf{r}, \mathbf{r}_j) = \left(\hat{U} - \mathbf{e_n}\mathbf{e_n} \right) \frac{e^{\mathrm{i}k_d r}}{4\pi r} e^{-\mathrm{i}k_d (\mathbf{n}\mathbf{r}')} . \qquad (7.15)$$

The dipole moment $\mathbf{p}^j$ induced in each point $\mathbf{r}_j$ of the lattice is determined by the local electric field, being the sum of the incident external electric field $\mathbf{E}_0(\mathbf{r}_j)$ at position $\mathbf{r}_j$ of the point dipole j and the electric fields at $\mathbf{r}_j$ emanating from all other point dipoles at positions $j' \neq j$. For monochromatic fields the electric dipole moment of each point dipole is expressed in the coupled-dipole equations

$$\mathbf{p}_j = \alpha_p \mathbf{E}_0(\mathbf{r}_j) + \alpha_p \frac{k_0^2}{\varepsilon_0} \sum_{l \neq j}^{N} \hat{G}(\mathbf{r}_j, \mathbf{r}_l) \mathbf{p}^l , \tag{7.16}$$

After solving the system of equations (7.16), the total extinction cross section can be found using the optical theorem [51]

$$c_{ext} = \frac{k_d}{\varepsilon_0 \varepsilon_d |\mathbf{E}_0|^2} \operatorname{Im} \sum_{j=1}^{N} \left[\mathbf{E}_0^*(\mathbf{r}_j) \cdot \mathbf{p}^j \right] \quad , \tag{7.17}$$

where $\mathbf{E}_0^*$ is the complex conjugate of the incident field. The scattering cross section is determined by integration of the scattered electric field in the far zone given by equations 7.12 and 7.15:

$$c_{sca} = \frac{\int |\mathbf{E}(\mathbf{r})|^2 r^2 \sin\theta d\theta d\phi}{|\mathbf{E}_0|^2} \quad . \tag{7.18}$$

The absorption cross section can be calculated by $c_{abs} = c_{ext} - c_{sca}$. With this approach, only total extinction, absorption, and scattering cross sections could have been calculated, without information about separate contributions of different multipole moments, as it is possible with Mie theory.

In the theoretical work related to this thesis, a new direct method in the framework of DDA has been introduced that allows the individual multipole contributions to light extinction and scattering cross sections by nanoparticles of arbitrary shapes to be studied. In order to decompose the extinction cross section into the different multipole contributions, the expression $\mathbf{E}_0^*(\mathbf{r}_j) \cdot \mathbf{p}^j$ in equation 7.17 has been expanded into a Taylor series around a reference point $\mathbf{r}_0$ [51]. Alternatively, one could perform the multipole decomposition by expanding the δ-function in the general expression of the total induced polarization $\mathbf{P}(\mathbf{r})$ in a particle into a Taylor series. The discretization of the polarization in this case has been performed after the expansion [53]. The main idea in order to obtain a minimum number of contributing multipole moments to the extinction cross section has been to put the reference point into the center of mass for homogeneous particles [51]:

$$\mathbf{r}_c = \sum_{j=1}^{N} \frac{\mathbf{r}_j}{N} \quad . \tag{7.19}$$

An example of multipole contributions for a spherical particle with a radius of 65 nm is shown in Fig.7.2 for two different choices of the reference point for the multipole decomposition.

In Fig.7.2(a) the point is in the center of mass and only the contributions of the electric and magnetic dipoles to the extinction cross section are present. If the reference point is
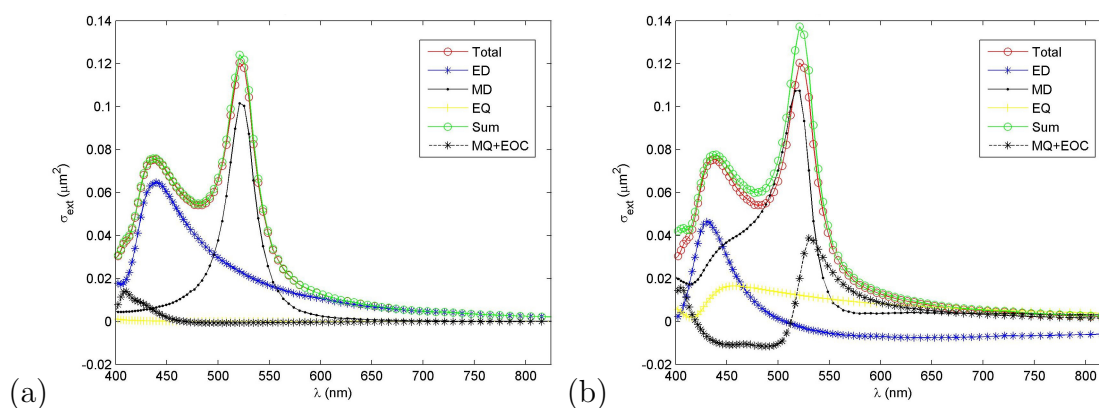
Figure 7.2:
(a) Choice of the reference point for calculating the multipole contributions for a silicon sphere with 130 nm diameter. (a) In the center of mass: Only the electric and magnetic dipoles contribute to the extinction cross section. (b) Shifted 40 nm out of the center: Higher-order multipoles with partially negative contributions appear. The total extinction cross section remains the same.

shifted, higher-order multipoles appear, although the total extinction cross section is the same, see Fig.7.2(b). This example has been compared to the results obtained with Mie theory in [51], showing an accurate agreement for the total extinction cross section and the multipole contribution, when the reference point is in the center of mass. For this novel method the name decomposed discrete dipole approximation (DDDA) has been introduced.

Important main contributions:

- **Application of DDA to plasmonic systems**

- **Introduction of the decomposition of the induced polarization in DDA to obtain contributions of individual multipole moments -** *Decomposed DDA*

- **First demonstration of decomposed scattering cross section into individual multipole moments for arbitrary shaped particles**

The relevant literature is:

- *Focussing and directing of surface plasmon polaritons by curved chains of nanoparticles*
  A. B. Evlyukhin, S. I. Bozhevolnyi, A. L. Stepanov, R. Kiyan, C. Reinhardt, S. Passinger, B. N. Chichkov
  Optics Express **15**, pp. 16668 - 16680 (2007)

- *Asymmetric and symmetric local surface plasmon-polariton excitation on chains of nanoparticles*
  A. B. Evlyukhin, C. Reinhardt, E. Evlyukhina, B. N. Chichkov
  Optics Letters **34**, pp. 2237 - 2239 (2009)

- *Laser-induced transfer of metallic nanodroplets for plasmonics and metamaterial applications*
  A. I. Kuznetsov, A. B. Evlyukhin, C. Reinhardt, A. Seidel, R. Kiyan, W. Cheng, A. Ovsianikov, B. N. Chichkov
  Journal of the Optical Society of America B **26**, pp. B130 - B138 (2009)

- *Optical response features of Si-nanoparticle arrays*
  A. B. Evlyukhin, C. Reinhardt, A. Seidel, B. S. Luk'yanchuk, B. N. Chichkov
  Physical Review B **82**, pp. 045404-1 - 045404-12 (2010)

- *Laser Fabrication of Large Scale Nanoparticle Arrays for Sensing Applications*
  A. I. Kuznetsov, A. B. Evlyukhin, M. R. Goncalves, C. Reinhardt, A. Koroleva, M. L. Arnedillo, R. Kiyan, O. Marti, B. N. Chichkov
  ACS Nano **19**, American Chemical Society, pp. 4843 - 4849 (2011)

- *Multipole light scattering by nonspherical nanoparticles in the discrete dipole approximation*
  A. B. Evlyukhin, C. Reinhardt, B. N. Chichkov
  Physical Review B **84**, pp. 235429-1 - 235429-8 (2011)

- *Collective resonances in metal nanoparticle arrays with dipole-quadrupole interactions*
  A. B. Evlyukhin, C. Reinhardt, U. Zywietz B. N. Chichkov
  Physical Review B **85**, pp. 245411-1 - 245411-8 (2012)

- *Multipole analysis of light scattering by arbitrary-shaped nanoparticles on a plane surface*
  A. B. Evlyukhin, C. Reinhardt, E. Evlyukhin, B. N. Chichkov
  Journal of the Optical Society of America B **30**, pp. 2589 - 2598 (2013)

- *Laser printing of silicon nanoparticles with resonant optical electric and magnetic responses*
  U. Zywietz, A. B. Evlyukhin, C. Reinhardt, B. N. Chichkov
  Nature Communications **5**, pp. 4402-1 - 4402-7 (2014)

8 Summary

In this habilitation treatise, novel fabrication, characterization, and simulation methods in the field of nanooptics have been introduced.

The development of a two-photon laser fabrication technology for micromechanical, microfluidic, microoptical, and photonic components has been presented, which has been turned into a commercially available product. As demonstrators for the capabilities of this technology, a readily assembled microvalve and conical microlenses have been presented. Two-photon fabrication and nanoimprint lithography have been applied to prototyping of plasmonic excitation and focussing structures, and first polymer dielectric surface plasmon-polariton waveguides have been demonstrated. Leakage radiation microscopy has been applied to spatially-resolved and Fourier-transform optical characterization of surface plasmon excitation, focussing, and waveguiding. Temporally-resolved investigations of surface plasmon focussing devices have been performed by two-photon photoelectron emission microscopy.

Laser-induced transfer has been developed for the generation of spherical gold nanoparticles and nanoparticle arrays. The method has been improved for the controlled production of silicon nanoparticles from bulk and SOI wafers. With this approach, it has become possible to experimentally demonstrate magnetic dipole scattering in the visible spectral range, in agreement with theoretical predictions on the basis of Mie theory. Scattering spectra of individual gold and silicon particles have been investigated by single particle spectroscopy. Surface enhanced Raman spectroscopy has been applied to demonstrate field enhancement in the gap of gold particle pairs. The produced particles have been discussed for use as metamaterial and metasurface building blocks. In this context, highly sensitive sensors surfaces from nanoparticle arrays have been presented.

Field enhancement and the occurrence of field hotspots in and around metallic nanostructures have been characterized by novel methods, which have been developed within this thesis, based on resonant four-photon absorption in PMMA polymer and ultrafast melt dynamics in straight and chiral metallic nanoantennas.

Besides the individual development of fabrication, prototyping, and optical near-and far-field characterization methods, the nanooptics of surface plasmon-polaritons has been combined with the optics of nanoparticles to obtain insight into the multipole structure and scattering properties of nanoparticles and time-resolved interaction between localized and propagating plasmon modes has been investigated.

The experimental observation of significant contributions of higher multipoles to the scattering behaviour of particles has initialized the development of a reformulation of the discrete dipole approximation. With a decomposition of the dipole approach into higher multipole moments, it has become possible for the first time to calculate individual multipole contributions to the total extinction cross sections for arbitrary shaped particles.

The main achievements in the different working directions with international scientific

impact can be summarized as follows:

Fabrication:

- Development of a commercially available prototyping technology for photonic and plasmonic components based on two-photon laser fabrication and nanoimprint lithography

- Demonstration of a versatile technology for the production and positioning of metallic and dielectric nanoparticles of spherical shape with determined diameters and positions

Characterization:

- Application and further development of leakage radiation microscopy for characterization of plasmonic components and waveguides

- Demonstration of different approaches for field mapping in plasmonic nanostructures

- First measurement of magnetic dipole Mie resonances in silicon nanospheres in the visible spectral range

Simulation:

- Improvement of the discrete dipole approximation method by using a decomposition approach to obtain information about individual scattering multipole moments for arbitrary shaped particles, including the influence of substrate surfaces

- Analytical proof for the interaction of silicon nanoparticles with the magnetic field component of light and calculation of the radiation-corrected polarizability using the Green's function method

The work for this professorial dissertation resulted in 44 peer reviewed contributing publications in 23 journals and one contributing book chapter. The number of publications are listed below according to the journals in the order of their journal impact factor (JIF):

1)	**2 Advanced Materials** (JIF: 14.829)
2)	**4 Nano Letters** (JIF: 13.025)
3)	**1 ACS Nano** (JIF: 12.062)
4)	**1 Nature Communications** (JIF: 10.015)
5)	**1 Langmuir** (JIF: 4.187)
6)	**1 New Journal of Physics** (JIF: 4.063)

7)	**3 Applied Physics Letter** (JIF: 3.794)
8)	**3 Physical Review B** (JIF: 3.767)
9)	**3 Optics Express** (JIF: 3.546)
10)	**1 Microporous and Mesoporous Materials** (JIF: 3.414)
11)	**4 Optics Letters** (JIF: 3.385)
12)	**1 Annalen der Physik** (JIF: 3.318)
13)	**1 Scientific Reports** (JIF: 2.927)
14)	**1 Optical Materials Express** (JIF: 2.616)
15)	**4 Journal Opt. Soc. Am. B** (JIF: 2.210)
16)	**1 IEEE Photonics Journal** (JIF: 2.038)
17)	**1 Applied Physics B** (JIF: 1.782)
18)	**1 Applied Optics** (JIF: 1.689)
19)	**1 Journal Opt. Soc. Am. A** (JIF: 1.665)
20)	**5 Applied Physics A** (JIF: 1.545)
21)	**1 Int. Jour. Advanced Manufacturing** (JIF: 1.205)
22)	**1 Journal of Material Science** (JIF: 1.198)
23)	**1 Journal of Laser Applications** (JIF: 0.570)
24)	**1 Int. Journal of Optics** (JIF: 0.520)
25)	**1 Book Chapter** (JIF: NA)

The achievements within this thesis demonstrate the huge potential of laser-based nanoengineering technologies. Together with novel characterization methods and theoretical and numerical simulations, a powerful working platform for the fields of photonics and nanooptics has been established.

9 Outlook

Two-photon fabrication and nanoimprint lithography have been demonstrated as versatile tools for prototyping of photonic and plasmonic components. In comparison to electron beam writing, the advantages are obvious: No need for expensive vacuum equipment and electron optics, numerous materials are available, fast processing speeds are possible, and arbitrary 3D structures can be generated. This technology, although being far developed, can further be improved and opened to a broader field of costumers by reducing the prices for such a system and by increasing the resolution, in order to provide the possibilities for use as an alternative to electron beam writing. One approach to fulfill these requirements could be the replacement of still cost intensive femtosecond laser oscillators by suitable semiconductor lasers. The fast development of laser diodes has already provided a broad range of available wavelength down to the ultraviolet spectrum. Recently, high speed and high frequency electronic switching circuits have enabled the generation of sub-100 ps pulses and pulse sequences with high optical power. An own streak camera measurement of the pulse durations from high speed switched green and red laser diodes, emitting at 515 nm and 635 nm, respectively is shown in Fig.9.1. Pulse durations of 360 ps for the green laser diode (multimode) and 78 ps for the red laser diode have (singlemode) been measured.

The concentration of light energy in such short pulses provides the possibility to directly initiate nonlinear processes in different polymers for use in two-photon fabrication. High output powers in the blue spectral range around 450 nm might enable the direct nonlinear illumination of standard electron beam resist, e.g. poly (methyl methacrylate). Strong focussing of the radiation together with the two-photon character of the absorption process can give the potential for reliable structuring well below 100 nm. The potential of these miniature and low cost ultrashort pulse laser sources for two-photon fabrication, prototyping, and production will be investigated in future work.

Suitable amplification schemes can be applied to boost the output power of compact semiconductor laser sources so that laser ablation processes become possible. Since the
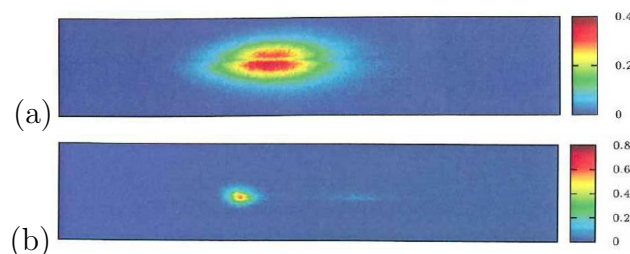

Figure 9.1:
   (a) Pulsed laser diodes at (a) 515 nm and (b) 635 nm with pulse durations of 360 ps and 78 ps, respectively.

pulses from ultrashort pulsed laser diodes are strongly chirped, a reduction of the pulse duration by optical compression can be applied. The application of amplified pulsed laser diodes for the production of nanoparticles by laser-induced transfer will be studied.

The different approaches, namely two-photon laser writing in polymers and laser-induced transfer of nanoparticles, can be merged into a low-cost structuring platform for nanophotonic components. The possibilities for combining nonlinear laser writing and nanoparticle generation for the production of photonic and plasmonic components will be investigated in future work.

The following research activities are proposed for further investigations:

- Investigation of ultrafast pulsed laser diodes for two-photon fabrication

- Investigation of suitable amplification schemes for ultrashort pulsed laser diodes

- Investigation into structuring properties of novel materials as an alternative to electron beam writing

- Development of a structuring platform combining two-photon laser writing in polymers and laser-induced transfer

The above described technological improvement of nonlinear laser fabrication can provide novel possibilities for the production of plasmonic components and waveguides as well as for the realization of metamaterial building blocks. The applicability of plasmonic waveguide components for optical data transport and processing as an alternative to electronics is still an open question. Investigations of SPPs, their amplification, and their linear and nonlinear interactions remain fields of active research. Within the work for this thesis, wide-angle high-resolution microscopy of the SPP leakage radiation for visualizing SPP excitations has been developed into a versatile technology for the characterization of surface plasmon propagation on thin metal films and in waveguides. The contributions to the development of this imaging technology have resulted in a worldwide interest, showing up in a huge number of publications, where this method has been used for characterization of SPP systems. However, in a direct comparison to two-photon photoelectron emission microscopy, which has been used in parallel to provide temporal resolution, it has not been possible up to now to obtain phase- and time-resolved imaging of SPP excitation, propagation, and their interaction with plasmonic systems. To overcome these limitations an interferometric approach is suggested to obtain both, phase information and time resolution with optical methods. In initial experiments the phase and temporally resolved propagation recording has already been achieved, as it is shown in Fig.9.2 for interferometric leakage radiation microscopy at two time steps separated by half an optical period.

Spatially- and temporally-resolved characterization by wide-angle microscopy can further be combined with spectrally resolving methods, as already applied in single particle spectroscopy. The improvements in imaging of SPP propagation and scattering properties of nanoparticles will allow precisely investigating plasmonic properties of different materials. As it has been shown in section 4.1, gold, although widely used as plasmonic material, represents not always the best choice. It is outplayed by silver and aluminium
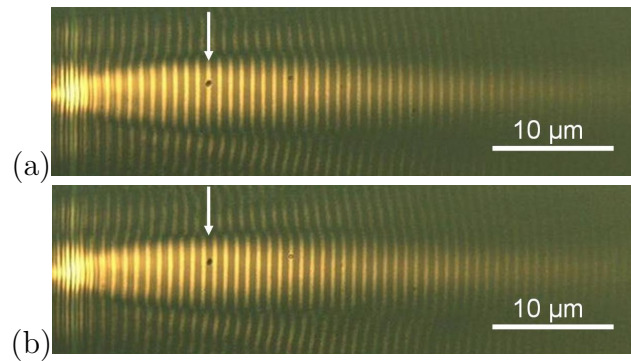
Figure 9.2:
(a) Phase and temporally resolved images of SPP leakage radiation. The phase difference between both images is $\pi/2$.

in certain spectral regions. These materials provide long propagation lengths in the visible and ultraviolet spectral ranges, where hardly any other approach for light confinement and guiding can be used other than plasmonics. In recent works, graphene has been demonstrated as plasmonic material with huge potential in the infrared and even visible spectral range. The properties of optical excitations in these materials and their linear and nonlinear interactions will be investigated. Coherent control of light and surface plasmons in nanostructures provides an additional degree of freedom, allowing the construction of all optical switches, transistors and logical gates, which confirm with the definitions given by electronics. Temporally resolved wide-angle microscopy can be applied to visualize and optimize the operation of these devices.

Silver and aluminium as low-loss plasmonic materials can further be used for the generation of nanoparticles by laser-induced transfer, as it is described above. The transfer of this technology to aluminium requires special attention due to the strong electron phonon-coupling and will be investigated in future work. The laser-based nanoparticle generation can further be extended to other materials, e.g III-V compound semiconductors gallium phosphide or gallium nitride.

Multipole excitation in these nanoparticles and nanoparticle structures leads to directional scattering which could be externally controlled by light or static electric fields. High refractive semiconductor materials can be combined with metallic nanoparticles for the creation of novel metamolecules as building blocks for metamaterials and metasurfaces. Sensors based on metamolecules will be investigated in future work for time-resolved detection of the electric and magnetic field components of light and SPPS, allowing new insights into the nature of electromagnetic phenomena at the nanoscale.

The following research activities are proposed for future investigations:

- Investigation of aluminium, silver, and graphene plasmonic properties in the visible wavelength range

- Implementation of interferometric time- and spectrally-resolved recording of SPP propagation and nanoparticle scattering

- Realization of optical and plasmonic transistors and logical elements

- Optical investigation of metamolecules as building blocks for metasurfaces

- Development of novel sensors for the electric and magnetic field components of light and SPPs

Investigation of novel material combinations for nanophotonic structures require improved numerical simulations. The discrete dipole approximation has been developed within this professorial dissertation to obtain a decomposition of scattering multipole moments. It has become a versatile tool for the calculation of optical near-fields of arbitrary shaped particles with information about the contributing multipole components. In future work, it has to be investigated how this decomposition can be accomplished for inhomogeneous particles composed of different materials.

The discrete dipole approximation has been applied in the quasi-stationary form. It can be extended to allow simulating temporal evolution of multipole excitations in nanooptical systems. The method, however, requires solving the system of coupled dipole equations, which becomes very memory intensive for large systems or high resolutions. Another way to obtain the temporal behaviour of fields inside the nanostructures to calculate the point dipoles is provided by the finite-difference time-domain method. The approach can be applied to calculate the multipoles and their individual near-and far-field contributions by applying the Green's function method, which would save considerable computational time. Both numerical techniques, the discrete dipole approximation and the finite-difference time-domain method can be combined to benefit from their individual advantages. Nonlinear interactions as well as the effect of gain media will be included to provide a unique computational platform for the calculation of fields in complex nanooptical systems.

Further possibilities for investigations are the development of this platform into a commercial product and the implementation of the software solution on graphic processing units. The increased calculation speed and memory will allow calculation of larger systems, entering the microscale.

The following research activities are proposed for future investigations:

- Definition and prescription of the decomposition procedure for inhomogeneous particles

- Development of a combined DDDA/FDTD platform

- Implementation of nonlinear and gain effects

- Increase of computational power for the reliable simulation of microscale systems

Acknowledgements

Bibliography

[1] The Nanophotonics Europe Association (NEA), *Nanophotonics - A Forward Look*, http://www.nanophotonicseurope.org/index.php/publications/ 82-nanophotonics-a-forward-look2012 (2012)

[2] Nanophotonics Europe Association, http://www.nanophotonicseurope.org

[3] The Nanophotonics Europe Association (NEA), *Nanophotonics Foresight Report 2011*, http://www.nanophotonicseurope.org/index.php/publications/ 52-nanophotonics-foresight-report (2011)

[4] Horizon2020, http://ec.europa.eu/programmes/horizon2020

[5] Photonics21, http://www.photonics21.org

[6] C. Lemke, C. Schneider, T. Leissner, D. Bayer, J. W. Radke, A. Fischer, P. Melchior, A. B. Evlyukhin, B. N. Chichkov, **C. Reinhardt**, M. Bauer, M. Aeschlimann, *Spatiotemporal Characterization of SPP Pulse Propagation in Two-Dimensional Plasmonic Focussing Devices*, Nano Letters **13**, pp. 1053–1058 (2013)

[7] C. Lemke,T. Leissner, A. B. Evlyukhin, J. W. Radke, A. Klick, J. Fiutowski, J. Kjelstrup-Hansen, H.-G. Rubahn, B. N. Chichkov, **C. Reinhardt**, M. Bauer, *The Interplay between Localized and Propagating Plasmonic Excitations Tracked in Space and Time*, Nano Letters, DOI 10.1021/nl500106z (2014)

[8] A. I. Aristov, U. Zywietz, A. B. Evlyukhin, **C. Reinhardt**, B. N. Chichkov, A. V. Kabashin, *Laser-ablative engineering of phase singularities in plasmonic metamaterial arrays for biosensing applications*, Appl. Phys. Lett. **104**, 071101 (2014)

[9] N. Pfullmann, C. Waltermann, M. Noack, S. Rausch, T. Nagy, **C. Reinhardt**, M. Kovacev, V. Knittel, R. Bratschitsch, D. Akemeier, A. Huetten, A. Leitensdorfer, U. Morgner, *Bow-tie nano-antenna assisted generation of extreme ultraviolet radiation*, New Journal of Physics **15**, 093027 (2013)

[10] N. Pfullmann, M. Noack, J. C. de Andrade, S. Rausch, T. Nagy, **C. Reinhardt**, V. Knittel, R. Bratschitsch, A. Leitensdorfer, D. Akemeier, A. Huetten, M. Kovacev, U. Morgner, *Nano-antennae assisted emission of extreme ultraviolet radiation*, Annalen der Physik **526**, pp. 119–134 (2014)

[11] **C. Reinhardt**, S. Passinger, B. N. Chichkov, C. Marquart, I. P. Radko, S. I. Bozhevolnyi, *Laser-fabricated dielectric optical components for surface plasmon polaritons*, Optics Letters **31**, pp. 1307–1309 (2006)

[12] **C. Reinhardt**, S. Passinger, R. Kiyan, A. L. Stepanov, B. N. Chichkov, *Laser-based rapid prototyping of plasmonic components*, Proc. SPIE **6323**, 63230P (2006)

[13] **C. Reinhardt**, R. Kiyan, A. Seidel, S. Passinger, A. L. Stepanov, A. B. Evlyukhin, B. N. Chichkov, *Focusing and manipulation of surface plasmon polaritons by laser fabricated dielectric structures*, Proc. SPIE **6642**, 664205 (2007)

[14] **C. Reinhardt**, S. Passinger, B. N. Chichkov, W. Dickson, G. A. Wurtz, P. Evans R. Pollard, and A. V. Zayats, *Restructuring and modification of metallic nanorod arrays using femtosecond laser direct writing*, Appl. Phys. Lett. **89**, 231117 (2006)

[15] R. Kiyan, **C. Reinhardt**, S. Passinger, A. L. Stepanov, A. Hohenau, J. R. Krenn, B. N. Chichkov, *Rapid prototyping of optical components for surface plasmon polaritons*, Optics Express **15**, pp. 4205–4215 (2007)

[16] **C. Reinhardt**, R. Kiyan, S. Passinger, A. L. Stepanov, A. Ostendorf, and B. N. Chichkov, *Rapid laser prototyping of plasmonic components*, Appl. Phys. A **89**, pp. 321–325 (2007)

[17] **C. Reinhardt**, A. Seidel, A. B. Evlyukhin, W. Cheng, R. Kiyan, B. N. Chichkov, *Direct laser-writing of dielectric-loaded surface plasmon-polariton waveguides for the visible and near infrared*, Appl. Phys. A **100**, pp. 347–352 (2010)

[18] A. Seidel, **C. Reinhardt**, T. Holmgaard, W. Cheng, T. Rosenzveig, K. Leosson, S. I. Bozhevolnyi, B. N. Chichkov, *Demonstration of Laser-Fabricated DLSPPW at Telecom Wavelength*, IEEE Photonics Journal **2**, pp. 652–658 (2010)

[19] A. Markov, **C. Reinhardt**, B. Ung, A. B. Evlyukhin, W. Cheng, B. N. Chichkov, M. Skorobogatiy, *Photonic bandgap plasmonic waveguides*, Optics Letters **36**, pp. 2468–2470 (2011)

[20] **C. Reinhardt**, A. B. Evlyukhin, W. Cheng, T. Birr, A. Markov, B. Ung, M. Skorobogatiy, B. N. Chichkov, *Bandgap-confined large-mode waveguides for surface plasmon-polaritons*, Journal of the Optical Society of America B **30**, pp. 2898–2905 (2013)

[21] S. Passinger, A. Seidel, C. Ohrt, **C. Reinhardt**, A. L. Stepanov, R. Kiyan, B. N. Chichkov, *Novel efficient design of Y-splitter for surface plasmon polariton applications*, Opt. Express **16**, 14369–14379 (2008)

[22] A. B. Evlyukhin, S. I. Bozhevolnyi, A. L. Stepanov, R. Kiyan, **C. Reinhardt**, S. Passinger, B. N. Chichkov, *Focusing and directing of surface plasmon polaritons by curved chains of nanoparticles*, Optics Express **15**, pp. 16668–16680 (2007)

[23] **C. Reinhardt**, A. Seidel, A. B. Evlyukhin, W. Cheng, B. N. Chichkov, *Mode-selective excitation of laser-written dielectric-loaded surface plasmon polariton Waveguides*, Journal of the Optical Society of America B **26**, pp. B55–B60 (2009)

[24] G. Volpe, M. Noack, S. S. Acimovic, **C. Reinhardt**, R. Quidant, *Near-Field Mapping of Plasmonic Antennas by Multiphoton Absorption in Poly(methyl methacrylate)*, Nano Letters **12**, pp. 4864–4868 (2012)

[25] V. K. Valev, D. Denkova, X. Zheng, A. I. Kuznetsov, **C. Reinhardt**, B. N. Chichkov, G. Tsutsumanova, E. J.Osley, V. Petkov, B. DeClercq, A. V. Silhanek, Y. Jeyaram, V. Volskiy, P. A. Warburton, G. A. E. Vandenbosch, S. Russev, O. A. Aktsipetrov, M. Amelo, V. M. Moshchalkov, T. Verbiest, *Plasmon-Enhanced Sub-Wavelength Laser Ablation: Plasmonic Nanojets*, Advanced Materials **24**, pp. OP29–OP35 (2012)

[26] V. K. Valev, W. Libaers, U. Zywietz, X. Zheng, M. Centini, N. Pfullmann, L. O. Herrmann, **C. Reinhardt**, V. Volskiy, A. V. Silhanek, B. N. Chichkov, C. Sibilia, G. A. E. Vandenbosch, V. V. Moshchalkov, J. J. Baumberg, T. Verbiest, *Nanostripe length-dependence of plasmon-induced material deformation*, Optics Letters **38**, pp. 2256–2258 (2013)

[27] C. Schizas, V. Melissinaki, A. Gaidukeviciute, **C. Reinhardt**, C. Ohrt, V. Dedoussis, B. N. Chichkov, C. Fotakis, M. Farsari, D. Karalekas, *On the design and fabrication by two-photon polymerization of a readily assembled micro- valve*, International Journal of Advanced Manufacturing Technology **48**, pp. 435–441 (2010)

[28] J. Koch, T. Bauer, **C. Reinhardt**, B. N. Chichkov, *Recent progress in direct write 2D and 3D photofabrication technique with femtosecond laser pulses*, in Recent Advances in Laser Material Processing, chapter **8**, Elsevier, pp. 472–495 (2006)

[29] F. Claeyssens, E. A. Hasan, A. Gaidukeviciute, D. S. Achilleos, A. Ranella, **C. Reinhardt**, A. Ovsianikov, X. Shizhou, C. Fotakis, M. Vamvakaki, B. N. Chichkov, M. Farsari, *Three-Dimensional Biodegradable Structures Fabricated by Two-Photon Polymerization*, Langmuire **25**, pp. 3219–3223 (2009)

[30] A. I. Kuznetsov, A. B. Evlyukhin, **C. Reinhardt**, A. Seidel, R. Kiyan, W. Cheng, A. Ovsianikov, B. N. Chichkov, *Laser-induced transfer of metallic nanodroplets for plasmonics and metamaterial applications*, Journal of the Optical Society of America B **26**, pp. B130–B138 (2009)

[31] A. I. Kuznetsov, A. B. Evlyukhin, M. R. Goncalves, **C. Reinhardt**, A. Koroleva, M. L. Arnedillo, R. Kiyan, O. Marti, B. N. Chichkov, *Laser Fabrication of Large Scale Nanoparticle Arrays for Sensing Applications*, ACS Nano **19**, American Chemical Society, pp. 4843–4849 (2011)

[32] A. B. Evlyukhin, A. I. Kuznetsov, S. M. Novikov, J. Beermann, **C. Reinhardt**, R. Kiyan, S. I. Bozhevolnyi, B. N. Chichkov, *Optical properties of spherical gold mesoparticles*, Applied Physics B **106**, pp. 841–848 (2012)

[33] A. Schilling, J. Schilling, **C. Reinhardt**, B. Chichkov, *A superlens for the deep ultraviolet*, Appl. Phys. Lett. **95**, 121909 (2009)

[34] A. B. Evlyukhin, C. Reinhardt, E. Evlyukhina, B. N. Chichkov, *Asymmetric and symmetric local surface plasmon-polariton excitation on chains of nanoparticles*, Optics Letters **34**, pp. 2237 - 2239 (2009)

[35] A. B. Evlyukhin, **C. Reinhardt**, A. Seidel, B. S. Luk'yanchuk, B. N. Chichkov, *Optical response features of Si-nanoparticle arrays*, Phys. Rev. B **82**, 045404 (2010)

[36] A. B. Evlyukhin, S. M. Novikov, U. Zywietz, R. L. Eriksen, **C. Reinhardt**, S. I. Bozhevolnyi, B. N. Chichkov, *Demonstration of Magnetic Dipole Resonances of Dielectric Nanospheres in the Visible Region*, Nano Lett. **12**, pp. 3749–3755 (2012)

[37] U. Zywietz, **C. Reinhardt**, A. B. Evlyukhin, T. Birr, B. N. Chichkov, *Generation and patterning of Si nanoparticles by femtosecond laser pulses*, Appl. Phys. A **114**, pp. 45–50 (2014)

[38] U. Zywietz, A. B. Evlyukhin, **C. Reinhardt**, B. N. Chichkov. *Laser printing of silicon nanoparticles with resonant optical electric and magnetic responses*, Nature Comm. **5**, p. 4402 (2014)

[39] A. B. Evlyukhin, R. L. Eriksen, W. Cheng, J. Beermann, **C. Reinhardt**, A. Petrov, S. Prorok, M. Eich, B. N. Chichkov, S. I. Bozhevolnyi, *Optical spectroscopy of single Si nanocylinders with magnetic and electric resonances*, Scientific Reports **4**, 4126 (2014)

[40] S. Passinger, R. Kiyan, A. Ovsianikov, **C. Reinhardt**, B. N. Chichkov, *3D nanomanufacturing with femtosecond lasers and applications*, Proc. SPIE **6591**, 632304 (2007)

[41] S. Passinger, M. S. Saifullah, **C. Reinhardt**, K. R. V. Subramanian, B. N. Chichkov, M. E. Welland, *Direct 3D Patterning of TiO_2 Using Femtosecond Laser Pulses*, Advanced Materials **19**, pp. 1218–1221 (2007)

[42] F. Heinroth, I. Bremer, S. Münzer, P. Behrens, **C. Reinhardt**, S. Passinger, C. Ohrt, B. Chichkov, *Microstructured templates produced using femtosecond laser pulses as templates for the deposition of mesoporous silicas*, Microporous and Mesoporous Materials **119**, pp. 104–108 (2009)

[43] F. Heinroth, S. Münzer, A. Feldhoff, S. Passinger, W. Cheng, **C. Reinhardt**, B. Chichkov, P. Behrens, *Three-dimensional titania pore structures produced by using a femtosecond laser pulse technique and a dip coating procedure*, Journal of Materials Science **44**, pp. 6490–6497 (2009)

[44] I. Sakellari, A. Gaidukeviciute, A. Giakoumaki, D. Gray, C. Fotakis, M. Farsari, M. Vamvakaki, **C. Reinhardt**, A. Ovsianikov, B. N. Chichkov, *Two-photon polymerization of titanium-containing sol-gel composites for three-dimensional structure fabrication*, Applied Physics A **100**, pp. 359–364 (2010)

[45] K. Terzaki, N. Vasilantonakis, A. Gaidukeviciute, **C. Reinhardt**, C. Fotakis, M. Vamvakaki, M. Farsari, *3D conducting nanostructures fabricated using direct laser writing*, Optical Materials Express **1**, pp. 58–597 (2011)

[46] V. Ferreras-Paz, M. Emons, K.Obata, A. Ovsianikov, S. Peterhänsel, K. Frenner, **C. Reinhardt**, B. Chichkov, U. Morgner, W. Osten*Development of functional sub-100 nm structures with 3D two-photon polymerization technique and optical methods for characterization*, Journal of Laser Application **24**, 042004 (2012)

[47] A. Zukauskas, M. Malinauskas, **C. Reinhardt**, B. N. Chichkov, R. Gadonas, *Closely packed hexagonal conical microlens array fabricated by direct laser photopolymerization*, Applied Optics **51**, pp. 4995–5003 (2012)

[48] **C. Reinhardt**, S. Passinger, V. Zorba, B. N. Chichkov, C. Fotakis, *Replica molding of picosecond laser fabricated Si microstructures*, Applied Physics A **87**, pp. 673–677 (2007)

[49] A. Seidel, C. Ohrt, S. Passinger, **C. Reinhardt**, R. Kiyan, B. Chichkov, *Nanoimprinting of dielectric loaded surface plasmon-polariton waveguides from masters fabricated by 2-photon polymerization technique*, JOSA B **26**, pp. 810–812 (2009)

[50] A. Seidel, J. Gosciniak, M. U. Gonzalez, J. Renger, **C. Reinhardt**, R. Kiyan, R. Quidant, S. I. Bozhevolnyi, B. N. Chichkov, *Fiber-Coupled Surface Plasmon Polariton Excitation in Imprinted Dielectric-Loaded Waveguides*, International Journal of Optics **2010**, 897829 (2010)

[51] A. B. Evlyukhin, **C. Reinhardt**, B. N. Chichkov, *Multipole light scattering by nonspherical nanoparticles in the discrete dipole approximation* Phys. Rev. B **84**, 235429 (2011)

[52] A. B. Evlyukhin, **C. Reinhardt**, U. Zywietz, B. N. Chichkov, *Collective resonances in metal nanoparticle arrays with dipole-quadrupole interactions*, Phys. Rev. B **85**, 245411 (2012)

[53] A. B. Evlyukhin, **C. Reinhardt**, E. Evlyukhin, B. N. Chichkov, *Multipole analysis of light scattering by arbitrary-shaped nanoparticles on a plane surface*, J. Opt. Soc. Am. A **30**, pp. 2589–2598 (2013)

[54] J. M. Enoch and V. Lakshminarayanan, *Duplication of unique optical effects of ancient Egyptian lenses from the IV/V Dynasties: lenses fabricated ca 2620–2400 BC or roughly 4600 years ago*, Ophthal. Physiol. Opt. 20, 126 (2000)

[55] H. Römer, *Theoretical Optics: An Introduction*, 2nd Edition, Wiley-VCH, Weinheim (2009)

[56] H. E. Burton, *The Optics of Euclid*, JOSA **55**, pp. 357–372 (1945)

[57] R. Rashed, *A pioneer in anaclastics: Ibn Sahl on burning mirrors and lenses*, Isis **81**, p. 464 (1990)

[58] L. C. De Wreede, *Willebrord Snellius (1580–1626): A Humanist Reshaping the Mathematical Science*, Dissertation University Uetrecht (2007)

[59] G. B. Stewart, *Microscopes*, The Kid Haven Science Library, Farmington Hills, MI, Kid Heaven Press (2003)

[60] D. Bardell, *The invention of the microscope*, BIOS, **75** (2), pp. 78–84. (2004)

[61] J. C. Maxwell, *On physical lines of force*, Philos. Mag. Series 4 **21**, pp. 161–223 (1861)

[62] J. C. Maxwell, *A dynamical theory of the electromagnetic field*, Philos. Trans. R. Soc. London **155**, pp. 459–512 (1865)

[63] P. J. Nahin, *Oliver Heaviside: the life, work, and times of an electrical genius of the Victorian age*, JHU Press, pp. 108–112 (2002)

[64] O. Heaviside, *On the Forces, Stresses, and Fluxes of Energy in the Electromagnetic Field*, Philosophical Transaction of the Royal Society A **183**, pp. 423–480 (1892)

[65] E. B. Wilson, *Vector Analysis, a text-book for the use of students of Mathematics and Physics, founded upon the Lectures of J. Willard Gibbs*, New Haven, Yale University Press, 1929 (1901)

[66] J. Z. Buchwald, *The creation of scientific effects: Heinrich Hertz and electric waves*, University of Chicago Press, p. 194 (1994)

[67] A. Einstein, *The Fundamentals of Theoretical Physics*, Washington Periodical Science, May 24 (1940)

[68] Photonics21, *Towards a Bright Future for Europe: Strategic Research Agenda in Photonics*, http://www.photonics21.org/download/sra_april.pdf (2006)

[69] T. H. Maiman, *Stimulated optical radiation in ruby*, Nature **187**, p. 493 (1960)

[70] J. Bardeen, W. H Brattain, *The Transistor: A Semi-Conductor Triode.*Physical Review **74**, pp. 230–231 (1948)

[71] M. Boerner, *Mehrstufiges Übertragungssystem für Pulscodemodulation dargestellte Nachrichten*, DE patent 1254513, issued 1967-11-16, assigned to Telefunken Patentverwertungsgesellschaft m.b.H.

[72] J. Hecht, *City of Light, The Story of Fiber Optics*, New York, Oxford University Press (1999)

[73] R. Zia, J. A. Schuller, A. Chandran, M. L. Brongersma, *Plasmonics: The next chip-scale technology*, Materials Today **9**, p. 20 (2006)

[74] R. G. Hunsperger, *Integrated Optics: Theory and Technology*, Advanced Texts in Physics 6th ed., Springer (2009)

[75] G. T. Reed, A. P. Knight, *Silicon photonics: an introduction*, John Wiley and Sons (2004)

[76] L. Pavesi, D. J. Lockwood, *Silicon photonics*, Springer (2004)

[77] M. Köhler, W. Fritzsche, *Nanotechnology*, 2nd Edition Wiley (2007)

[78] M. Madou, *Fundamentals of Microfabrication and Nanotechnology*, Boca Raton, CRC Press (2012)

[79] H. A. Bethe, *Theory of diffraction by small holes*, Phys. Rev. **66**, p. 163 (1944)

[80] C. Bouwkamp, *On Bethe's theory of diffraction by small holes*, Philips Res. Rep. **5**, p. 321 (1950)

[81] E. Abbe, *Beiträge zur Theorie des Mikroskops und der mikroskopischen Wahrnehmung*, Archiv f. Mikroskop. Anat. **9**, p. 413 (1873)

[82] L. Rayleigh, *Investigations in optics, with special reference to the spectroscope*, Phil. Mag. **8**, pp. 261–274, 403–411, 477–486 (1879)

[83] L. Novotny, B. Hecht, *Principles of Nano-Optics*, Cambridge University Press (2011)

[84] E. H. Synge, *A suggested method for extending microscopic resolution into the ultra-microscopic region*, Phil. Mag. **6**, pp. 356–362 (1928)

[85] D. W. Pohl, W. Denk, M. Lanz, *Optical stetoskopy: image recording with resolution $\lambda/20$*, Appl. Phys. Lett. **44**, pp. 658–660 (1984)

[86] S. V. Gaponenko, *Introduction to Nanophotonics*, Cambridge University Press (2010)

[87] M. Ohtsu, T. Kawazoe, M. Naruse, T. Yatsui, K. Kobayashi, *Principles of Nanophotonics*, Taylor & Francis (2008)

[88] H. Rigneault, J.-M. Lourtioz, C. Delalande, A. Levenson, *Nanophotonics*, Wiley-ISTE, Volume **102** (2010)

[89] M. Aeschlimann, M. Bauer, D. Bayer, T. Brixer, S. Cunovic, A. Fischer, P. Melchior, W. Pfeiffer, M. Rohmer, C. Schneider, C. Strüber, *Optimal open-loop near-field control of plasmonic nanostructures*, New Journal of Physics **14**, 033030 (2012)

[90] W. Pfeiffer and M. Aeschlimann, *Simultaneous spatial and temporal control of nanooptical fields*, in: Dynamics at Solid State Surfaces and Interfaces, Editors: U. Bovensiepen, H. Petek, and M. Wolf, Weinheim, Wiley-VCH, pp. 555 (2010)

[91] B. Lee, I.-M. Lee, S. Kim, D.-H. Oh, L. Hesselink, *Review on subwavelength confinement of light with plasmonics*, Journal of Modern Optics **57**, pp. 1479–1497 (2010)

[92] V. M. Agranovich, D. L. Mills, *Surface polaritons: electromagnetic waves at surfaces and interfaces*, Elsevier, New York (1982)

[93] H. Raether, *Surface Plasmons on Smooth and Rough Surfaces and on Gratings*, Springer, Berlin (1988)

[94] R. W. Wood, *On a Remarkable Case of Uneven Distribution of Light in a Diffraction Grating Spectrum*, Proc. Phys. Soc. London **18**, p. 269–275 (1902)

[95] G.A. Mie, *Beiträge zur Optik trüber Medien, speziell kolloidaler Metallösungen*, Annalen der Physik **25**, pp. 377–445 (1908)

[96] T. W. Ebbesen, H. J. Lezec, H. F. Ghaemi, T. Thio, and P. A. Wolff, *Extraordinary optical transmission through sub-wavelength hole arrays*, Nature **391**, pp. 667–669 (1998)

[97] M. J. Mendes, S. Morawiec, F. Simone, F. Prioloabc, I. Crupia, *Colloidal plasmonic back reflectors for light trapping in solar cells*, Nanoscale **391**, pp. 4796–4805 (2014)

[98] J. A. Fan, K. Bao, C. Wu, J. Bao, R. Bardhan, N. J. Halas, V. N. Manoharan, G. Shvets, P. Nordlander, F. Capasso, *Fano-like Interference in Self-Assembled Plasmonic Quadrumer Clusters*, Nano Lett. **10**, pp. 4680–4685 (2010)

[99] A. G. Curto, G. Volpe, T. H. Taminiau, M. P. Kreuzer, R. Quidant, N. F. van Hulst, *Unidirectional Emission of a Quantum Dot Coupled to a Nanoantenna*, Science **329**, pp. 930–933 (2010)

[100] G. Lozano, D. J. Louwers, S. R. K. Rodríguez, S. Murai, O. T. A. Jansen, M. A Verschuuren, J. G. Rivas, *Plasmonics for solid-state lighting: enhanced excitation and directional emission of highly efficient light sources*, Light: Science & Applications **2**, p. e66 (2013)

[101] M. L. Brongersma, P. G. Kik, Editors, *Surface Plasmon Nanophotonics*, Springer Series in Optical Sciences **131**, Springer (2007)

[102] W. Cai, V. Shalaev, *Optical Metamaterials*, Springer (2010)

[103] M. L. Brongersma, J. W. Hartman, H. H. Atwater, *Plasmonics: electromagnetic energy transfer and switching in nanoparticle chain-arrays below the diffraction limit*, Molecular Electronics Symposium, 29 Nov. until 2 Dec. 1999, Boston, MA, USA. 1999: Warrendale, PA, USA: Mater. Res. Soc. (2001)

[104] Z. Han, S. I. Bozhevolnyi, *Radiation guiding with surface plasmon polaritons*, Rep. Prog. Phys. **76**, 016402 (2013)

[105] M. Z. Alam, J.S. Aitchinson, M. Mojahedi, *A marriage of convenience: Hybridization of surface plasmon and dielectric waveguide modes*, Laser and Photonics Reviews, DOI: 10.1002/lpor.201300168, Wiley (2014)

[106] Berini, *Long-range surface plasmon-polaritons*, Advances in Optics and Photonics, **1**, pp. 484–588 (2009)

[107] T. W. Ebbesen, C. Genet, S. I. Bozhevolnyi, *Surface Plasmon Circuitry*, Physics Today **61**, pp. 44–50 (2008)

[108] A. Dereux, J.-C. Weeber, S. I. Bozhevolnyi, E. Kriezis, N. Pleros, T. Tekin, M. Baus, H. Avramopoulos, *Surface Plasmon Circuitry in Opto-Electronics*, Conference Paper Quantum Electronics and Laser Science Conference San Jose, California United States May 6-11 (2012)

[109] A.. Olivieri, A. Akbari, P. Berini, *Surface plasmon waveguide Schottky detectors op erating near breakdown*, Physica Status Solidi - Rapid Research Letters, Special Issue: Plasmonics and Nanophotonics **4**, pp. 283–285 (2010)

[110] J. P. Colinge, *Silicon-on-Insulator Technology: Materials to VLSI*, Springer, Berlin (1991)

[111] G. K. Celler, S. Cristoloveanu, *Frontiers of silicon-on-insulator*, J. Appl. Phys. **93**, p. 4955 (2003)

[112] D. Kalavrouziotis, S. Papaioannou, K. Vyrsokinos, A. Kumar, S. Bozhevolnyi, L. Markey, J.-C. Weeber, A. Dereux, G. Giannoulis, D. Apostolopoulos, H. Avramopoulos, N. Pleros, *First demonstration of active plasmonic device in true data traffic conditions: ON/OFF thermo-optic modulation using a hybrid silicon-plasmonic asymmetric MZI*, onference Paper Optical Fiber Communication Conference Los Angeles, California United States March 4-8 (2012)

[113] S. A. Maier, *Plasmonics: fundamentals and applications*, Springer, Berlin (2007)

[114] P. Bharadwaj, B. Deutsch, L. Novotny, *Optical Antennas*, Advances in Optics and Photonics **1**, pp. 438–483 (2009)

[115] Q. Park, *Optical antennas and plasmonics*, Contemporary Physics **50**, pp. 407–423 (2009)

[116] L. Novotny, N. van Hulst, *Antennas for light*, Nature Photonics **5**, pp. 83–90 (2011)

[117] P. Biagioni, J.-S. Huang, B. Hecht, *Nanoantennas for visible and infrared radiation*, Rep. Prog. Phys. **75**, 024402 (2011)

[118] P. Mühlschlegel, H.-J. Eisler, O. J. F. Martin, B. Hecht, D. W. Pohl, *Resonant Optical Antennas*, Science **308**, pp. 1607–1609 (2005)

[119] L. Novotny, *Effective Wavelength Scaling for Optical Antennas*, Phys. Rev. Lett. **98**, 266802 (2007)

[120] D. P. Fromm, A. Sundaramurthy, P. J. Schuck, G. Kino, W. E. Moerner, *Gap-Dependent Optical Coupling of Single "Bowtie" Nanoantennas Resonant in the Visible*, Nano Letters **4**, pp. 957–961 (2004)

[121] S. Kim, J. Jin, Y.-J. Kim, Y. Park, Y. Kim, S.-W. Kim, *High-harmonic generation by resonant plasmon field enhancement*, Nature **453**, pp. 757–760 (2008)

[122] S. Kim, J. Jin, Y.-J. Kim, Y. Park, Y. Kim, S.-W. Kim, *High-harmonic generation by resonant plasmon field enhancement*, Nature **453**, pp. 757–760 (2008)

[123] A. Husakou, S.-J. Im, J. Herrmann, *Theory of plasmon-enhanced high-order harmonic generation in the vicinity of metal nanostructures in noble gases*, Phys. Rev. A **83**, 043839 (2011)

[124] S. Kim, J. Jin, Y.-J. Kim, Y. Park, Y. Kim, S.-W. Kim, *Kim et al. reply*, Nature **485**, pp. E1–E3 (2012)

[125] T. Shaaran, M. F. Ciappina, R. Guichard, J. A. Pérez-Hernández, L. Roso, M. Arnold, T. Siegel, A. Zaïr, M. Lewenstein, *High-order-harmonic generation by enhanced plasmonic near-fields in metal nanoparticles*, Phys. Rev. A **87**, 041402(R) (2013)

[126] M. Sivis, M. Duwe, B. Abel, C. Ropers, *Bow-tie nano-antenna assisted generation of extreme ultraviolet radiation*, New Journal of Physics **15**, 093027 (2013)

[127] M. Agio, A. Alu, *Optical Antennas*, Cambridge University Press (2013)

[128] M. I. Stockman, *Nanoplasmonics: past, present, and glimpse into future*, Optics Express **19**, pp. 22029–22106 (2013)

[129] D. R. Smith, W. J. Padilla, D. C. Vier, S. C. Nemat-Nasser, S. Schultz, *Composite medium with simultaneously negative permeability and permittivity*, Phys. Rev. Lett. **84**, pp. 4184–4187 (2000)

[130] J. C. Bose, *On a Remarkable Case of Uneven Distribution of Light in a Diffraction Grating Spectrum*, Proc. Phys. Soc. London 18, pp. 269–275 (1902)

[131] L V. Lindell, A. H. Sihvola, and J. Kurkijarvi, *Karl F. Lindman: The Last Hertzian, and a Harbinger of Electromagnetic Chirality*, IEEE Antennas and Propagation Magazine, Vol. **34**, pp. 24–30 (1992)

[132] W. E. Kock, *Metallic Delay Lenses*, Bell Systems Technical Journal, Vol. **27**, pp. 58–82 (1948)

[133] J. Brown, *Artificial dielectrics having refractive indices less than unity*, Proc. IEE **100**, pp. 51–62 (1953)

[134] L. D. Landau, E. M. Liftshitz, L. P. Pitaevskii, *Electrodynamics of continuous media*, Chapter 79, Pergamon, New York (1984)

[135] W. N. Hardy, L. A. Whitehead, *Split-ring resonator for use in magnetic-resonance from 200-2000 MHz*, Rev. Sci. Instrum. **52** pp. 213–216 (1981)

[136] V. G. Veselago, *Electrodynamics of substances with simultaneously negative values of sigma and mu*, Sov. Phys. Usp. **10**,pp. 509–514 (1968)

[137] B. Lahiri, S. G. McMeekin, A. Z. Khokhar, R. M. De La Rue, N. P. Johnson, *Magnetic response of split ring resonators (SRRs) at visible frequencies*, Optics Express **18**, pp. 3210–3218 (2010)

[138] L. Y. M. Tobing, L.Tjahjana, D. H. Zhang, Q. Zhang, Q, Xiong, *Sub-100-nm Sized Silver Split Ring Resonator Metamaterials with Fundamental Magnetic Resonance in the Middle Visible Spectrum*, Advanced Optical Materials **2**, pp. 280–285 (2014)

[139] A. N. Grigorenko, A. K. Geim, H. F. Gleeson, Y. Zhang, A. A. Firsov, I. Y. Khrushchev, J. Petrovic, *Nanofabricated media with negative permeability at visible frequencies*, Nature **438**, p. 335 (2005)

[140] T. Pakizeh, M. S. Abrishamian, N. Granpayeh, A. Dmitriev, M. Käll, *Magnetic-field enhancement in gold nanosandwiches*, Opt. Express **14**, p. 8240 (2006)

[141] Y. Ekinci, A. Christ, M. Agio, O. J. F. Martin, H. H. Solak, J. F. Löffler, *Electric and magnetic resonances in arrays of coupled gold nanoparticle in-tandem pairs*, Opt. Express **16**, 13287 (2008)

[142] A. Melikyan, H. Minassian, *On surface plasmon damping in metallic nanoparticles*, Applied Physics B **78**, pp. 453–455 (2004)

[143] K. Kolwas, A. Derkachova, *Damping rates of surface plasmons for particles of size from nano- to micrometers; reduction of the nonradiative decay*, Journal of Quantitative Spectroscopy & Radiative Transfer **114**, 45–55 (2013)

[144] J. Grandidier, S. Massenot, G. Colas des Francs, A. Bouhelier, J.-C. Weeber, L. Markey, A. Dereux, J. Renger, M. U. González, R. Quidant, *Dielectric-loaded surface plasmon polariton waveguides: Figures of merit and mode characterization by image and Fourier plane leakage microscopy*, Phys. Rev. B **78**, 245419 (2008)

[145] A. Fang, Z. Huang, T. Koschny, C. M. Soukoulis, *Overcoming the losses of a split ring resonator array with gain*, Opt. Express **19**, pp. 12688–12699 (2011)

[146] M. S. Miller, *Loss compensation in a plasmonic nanoparticle array*, University of Texas, Digital Repository, PhD Thesis (2013)

[147] M. A. Noginov, G. Zhu, M. Mayy, B. A. Ritzo, N. Noginova, V. A. Podolskiy, *Stimulated emission of surface plasmon polaritons*, Phys. Rev. Lett. **101**, 226806 (2013)

[148] J. Grandidier, G. Colas des Francs, S. Massenot, A. Bouhelier, L. Markey, J.-C. Weeber, C. Finot, A. Dereux, *Gain-Assisted Propagation in a Plasmonic Waveguide at Telecom Wavelength*, Nano Lett. **9**, pp. 2935–2939 (2009)

[149] M. C. Gather, K. Meerholz, N. Danz, K. Leosson, *Net optical gain in a plasmonic waveguide embedded in a fluorescent polymer*, Nature Photonics **4**, p. 457 (2010)

[150] D. J. Bergman and M. I. Stockman, *Surface plasmon amplification by stimulated emission of radiation: quantum generation of coherent surface plasmons in nanosystems*, Phys. Rev. Lett. **90**, 027402 (2003)

[151] J. Seidel, S. Grafström, and L. Eng, *Stimulated emission of surface plasmons at the interface between a silver film and an optically pumped dye solution*, Phys. Rev. Lett. **94**, 177401 (2005)

[152] M. A. Noginov, G. Zhu, A. M. Belgrave, R. Bakker, V. M. Shalaev, E. E. Narimanov, S. Stout, E. Herz, T. Suteewong, U. Wiesner, *Demonstration of a spaser-based nanolaser*, Nature **460**, pp. 1110–1112 (2009)

[153] A. V. Zayats, S. A. Maier, *Active Plasmonics and Tuneable Plasmonic Metamaterials*, Wiley-Science Wise Publishing Co-Publication (2013)

[154] C. Rockstuhl, F. Lederer, C. Etrich, T. Pertsch, T. Scharf, *Design of an Artificial Three-Dimensional Composite Metamaterial with Magnetic Resonances in the Visible Range of the Electromagnetic Spectrum*, Phys. Rev. Lett. **99**, 017401 (2007)

[155] Q. Zhaoa, J. Zhoua, F. Zhangc, D. Lippens, *Mie resonance-based dielectric metamaterials*, Materials Today **12**, pp. 60–69 (2009)

[156] M. S. Wheeler, J. S. Aitchison, M. Mojahedi, *Three-dimensional array of dielectric spheres with an isotropic negative permeability at infrared frequencies*, Phys. Rev. B **72**, 193103 (2005)

[157] J. A. Schuller, R. Zia, T. Taubner, M. L. Brongersma, *Dielectric Metamaterials Based on Electric and Magnetic Resonances of Silicon Carbide Particles*, Phys. Rev. Lett. **99**, 107401 (2007)

[158] A. Ahmadi, H. Mosallaei, *Physical configuration and performance modeling of all-dielectric metamaterials*, Phys. Rev. B **77**, 045104 (2008)

[159] B.-I. Popa, S. A. Cummer, *Compact Dielectric Particles as a Building Block for Low-Loss Magnetic Metamaterials*, Phys. Rev. Lett. **100**, 207401 (2008)

[160] P. Moitra, Y. Yang, Z. Anderson, I. I. Kravchenko, D. P. Briggs J. Valentine, *Realization of an all-dielectric zero-index optical metamaterial*, Nature Photonics **7**, pp. 791–795 (2013)

[161] J. C. Ginn, I. Brener, D. W. Peters, J. R. Wendt, J. O. Stevens, P. F. Hines, L. I. Basilio, L. K. Warne, J. F. Ihlefeld, P. G. Clem, M. B. Sinclair, *Realizing Optical Magnetism from Dielectric Metamaterials*, Phys. Rev. Lett. **108**, 097402 (2012)

[162] E. Kallos, I. Chremmos, V. Yanopapas, *Resonance Properties of Optical All-Dielectric Metamaterials Using Two-Dimensional Multipole Expansion*, Phys. Rev. B. **86**, 245108 (2012)

[163] G. Shvets, C. Wu, N. Arju, G. Kelp, B. Neuner, G. T. Eyck, M. B. Sinclair, I. Brener, *All-Dielectric Metamaterials: Path to Low Losses and High Spectral Selectivity*, Conference Paper CLEO: QELS, Fundamental Science San Jose, California United States June 9-14 (2013)

[164] L. Khriachtchev, *Silicon Nanophotonics: Basic Principles, Current Status and Perspectives*, eBook, PDF (2012)

[165] Y. A. Vlasov, IBM T. J. Watson Research Center, *Silicon CMOS-Integrated Nano-Photonics for Computer and Data Communications Beyond 100G*, IEEE Communications Magazine, pp. 67–72 (2012)

[166] S. Assefa, S. Shank, W. Green, M. Khater, E. Kiewra, C. Reinholm, S. Kamlapurkar, A. Rylyakov, C. Schow, F. Horst, H. Pan, T. Topuria, P. Rice, D. M. Gill, J. Rosenberg, T. Barwicz, M. Yang, J. Proesel, J. Hofrichter, B. Offrein, X. Gu, W. Haensch, J. Ellis-Monaghan, Y. Vlasov, *A 90nm CMOS Integrated Nano-Photo nics Technology for 25Gbps WDM Op tical Communications Applications*, IEEE International Electron Devices Meeting (IEDM), postdeadline session 33.8, December 10-12 (2012)

[167] B. Fay, *Advanced optical lithography development, from UV to EUV*, Microelectron. Eng. **61-2**, p. 11 (2002)

[168] William B. Glendinning, Franco Cerrina, *X-Ray Lithography*, in: Helbert Helbert, *Handbook of VLSI Microlithography: Principles, Tools, Technology and Applications*, 2nd Edition William Andrew Inc, ISBN 0815514441, pp. 856–956 (2001)

[169] A. N. Broers, A. C. F. Hoole, J. M. Ryan, *Electron Beam Lithography - Resolution Limits*, Microelectron. Eng. **32**, p. 131 (1996)

[170] F. Watt, A. A. Bettiol, J. A. van Kan, E. J. Teo, M. B. H. Breese, *Ion Beam Lithography and Nanofabrication: A Review*, Int. J. Nanosci. **04**, p. 269 (2005)

[171] D. J. Resnick, W. J. Dauksher, D. Mancini, K. J. Nordquist, T. C. Bailey, S. Johnson, N. Stacey, J. G. Ekerdt, C. G. Willson, S. V. Sreenivasan, N. Schumaker, *Imprint lithography for integrated circuit fabrication*, J. Vac. Sci. Tech. B, **21**, pp. 2624–2631 (2003)

[172] C. W. Hull, *Apparatus for Production of Three-Dimensional Objects by Stereolithography*, U.S. Patent 4,575,330 (1982)

[173] J.-W. Choi, E. MacDonald, R. Wicker, *Multi-material microstereolithography*, International Journal of Advanced Manufacturing Technology **49**, pp: 543–551 (2010)

[174] M. Göppert Mayer, *Über Elementarakte mit zwei Quantensprüngen*, Dissertation, Univ. Göttingen (1930)

[175] M. Göppert Mayer, *Über Elementarakte mit zwei Quantensprüngen*, Annalen der Physik **9**, p. 273 (1931)

[176] W. Kaiser and C. G. B. Garrett, *Two-photon excitation in CaF2:Eu2+*, Phys. Rev. Lett. **7**, p. 229 (1961)

[177] J. H. Strickler, W. W. Webb, *2-photon excitation in laser scanning fluorescence microscopy*, Proceedings Article, Proc. SPIE **1398**, p. 107 (1991)

[178] E.-S. Wu, J. H. Strickler, W. R. Harrell, W. W. Webb, *Two-photon lithography for microelectronic application*, Proceedings Article, Proc. SPIE **1674**, p. 776 (1992)

[179] S. R. Desai, C. S. Feigerle, J. C. Miller, *Laser-induced polymerization within carbon-disulfide clusters*, J. Phys. Chem. **99**, p. 1786 (1995)

[180] O. K. Song, J. N Woodford, and C. H. Wang, Effects of two-photon fluorescence and polymerization on the first hyperpolarizability of an azobenzene dye, J. Phys. Chem. A 101, 3222 (1997)

[181] P. F. Moulton, *Ti-doped Sapphire: Tunable Solid-state Laser*, Optics News **8**, pp. 9–13 (1982)

[182] P. F. Moulton, *Spectroscopic and laser characteristics of Ti:Al2O3*, J. Opt. Soc. Am. B **3**, p. 125 (1986)

[183] S. Maruo, O. Nakamura, S. Kawata, *Three-dimensional microfabrication with two-photon-absorbed photopolymerization*, Optics Letters **22**, pp. 132–134 (1997)

[184] J. Serbin, A. Egbert, A. Ostendorf, B. N. Chichkov, R. Houbertz, G. Domann, J. Schulz, C. Cronauer, L. Fröhlich, M. Popall, *Femtosecond laser-induced two-photon polymerization of inorganic organic hybrid materials for applications in photonics*, Opt. Lett. **28**, p. 301–303 (2003)

[185] M. Deubel, G. von Freymann, M. Wegener, S. Pereira, K. Busch, C. M. Soukoulis, *Direct laser writing of three-dimensional photonic-crystal templates for telecommunications*, Nature Materials **3**, p. 444–447 (2004)

[186] J. Serbin. A. Ovsianikov, B. N. Chichkov, *Fabrication of woodpile structures by two-photon polymerization and investigation of their optical properties*, Opt. Express **12**, pp. 5221–5228 (2004)

[187] H.-B. Sun, S. Kawata, *Two-Photon Photopolymerization and 3D Lithographic Microfabrication,* Apvances in Polymer Science **170**, pp. 169–273 (2004)

[188] M. Malinauskas, M. Farsari, A. Piskarskas, S. Juodkazis, *Ultrafast laser nanostructuring of photopolymers: a decade of advances*, Phys. Rep. **533**, pp. 1–31 (2013)

[189] W. Hesse, *Phenolic Resins*, Ullmann's Encyclopedia of Industrial Chemistry, Wiley-VCH (2002), see also http://en.wikipedia.org/wiki/Phenol_formaldehyde_resin

[190] Microchem, *Shipley Microposit S1800 Series Photo Resists*, http://www.microchem.com/PDFs_Dow/S1800.pdf

[191] microresist technologies GmbH, *ma-P 1200-Positive Tone Photoresist Series*, http://www.microresist.de/products/positive_photoresists/pdf/pi_map_1200_en_07062201_ls_neu.pdf

[192] S. Uchino, T. Tanaka, T. Ueno, T. Iwayanagi, Nobuaki Hayashi, *Azide novolak resin negative photoresist for i line phase shifting lithography*, Journal of Vac Sci Technol B **9**, p. 3162 (1991)

[193] D. Roy, P. K. Basu, P. Raghunathan, S. V. Eswaran, *Photo induced cross-linking mechanism in azide-novolac negative photoresists: molecular level investigation using NMR spectroscopy*, Magnetic Resonance in Chemistry **41**, pp. 671–678 (2003)

[194] microresist technologies GmbH, *ma-N 400 and ma-N 1400-Negative Tone Photoresists*, http://www.microresist.de/products/negative_photoresists/pdf/po_pi_1400_400_man_08041003_en_ls.pdf

[195] Microchem, *NANO^{TM} SU8 Negative Tone Photoresist*, http://www.microchem.com/pdf/SU8_50-100.pdf

[196] H. Lorenz, M. Despont, N. Fahrni, N. LaBianca, P. Renaud, P. Vettiger, *SU-8: a low-cost negative resist for MEMS* , J. Micromech. Microeng. **7**, p. 121 (1997)

[197] E. H. Conradie, D. F. Moore, *SU-8 thick photoresist processing as a functional material for MEMS applications*, J. Micromech. Microeng. **12**, p. 368 (2002)

[198] N.-T. Nguyen, S. T. Wereley, *Fundamentals and Applications of Microfluidics*, Wereley Artech House (2002)

[199] microresist technologies GmbH, *mr-NIL 6000E–High performance resist with decreased imprint temperature*, http://www.microresist.de/produkte/polymere_nil/pdf/6000e_en.pdf

[200] microresist technologies GmbH, *Inorganic-Organic Hybrid Polymers (ORMOCER®s)*, http://www.microresist.de/produkte/ormocer/ormocer_en.htm

[201] J. J. Serbin, *Fabrication of Photonic Structures by Two-Photon Polymerization*, Dissertation Univ. Hannover, Cuvillier Göttingen (2004)

[202] Irgacure 369, http://www.xtgchem.cn/upload/20110629045432.PDF

[203] http://www.mufong.com.tw/Ciba/ciba_guid/photo_uv_2.pdf

[204] W. Michler, *Synthese aromatischer Ketone mittelst Chlorkohlenoxyd*, Berichte der deutschen chemischen Gesellschaft **9**, pp. 716–718 (1876), see also http://en.wikipedia.org/wiki/Michler%27s_ketone

[205] R. O. Kan, *Organic Photochemistry*, McGraw-Hill, New York (1966)

[206] E. J. J. Groenen, W. N. Koelman, *Spectroscopic study of Michler's ketone. Part 1: Absorption*, J. Chem. Soc., Faraday Trans. **2**, pp. 58–68 (1979)

[207] K. J. Schafer, J. M Hales, M. Balu, K. D. Belfield, E. W. Van Strylandb, D. J, Hagan, *Two-photon absorption cross-sections of common photoinitiators*, Journal of Photochemistry and Photobiology A **162**, pp. 497–502 (2004)

[208] U. Fano, *The Theory of Anomalous Diffraction Gratings and of Quasi-Stationary Waves on Metallic Surfaces (Sommerfeld's Waves)*, JOSA **31**, pp. 213–222 (1941)

[209] A. Sommerfeld, *Über die Ausbreitung der Wellen in der drahtlosen Telegraphie*, Annalen der Physik **333**, p. 665 (1909)

[210] J. Zenneck, *Über die Fortpflanzung ebener elektromagnetischer Wellen längs einer ebenen Leiterfläche und ihre Beziehung zur drahtlosen Telegraphie*, Annalen der Physik **328**, p. 846 (1906)

[211] D. Bohm and D. Pines, *A collective description of electron interactions. 2. Collective vs individual particle aspects of the interactions*, Phys. Rev. **85**, p. 338 (1952)

[212] D. Bohm and D. Pines, *A collective description of electron interactions .3. Coulomb interactions in a degenerate electron gas*, Phys. Rev. **92**, p. 609 (1953)

[213] E. Le Ru, P. Etchegoin, *Principles of Surface-Enhanced Raman Spectroscopy and related plasmonic effects*, Elsevier (2008)

[214] H. Watanabe, *Experimental Evidence for the Collective Nature of the Characteristic Energy Loss of Electrons in Solids - Studies on the Dispersion Relation of Plasma Frequency*, J. Phys. Soc. Jpn. **11**, p. 112 (1955)

[215] D. Pines, *Collective Energy Losses in Solids* Rev. Mod. Phys. **28**, p. 184 (1956)

[216] R. H. Ritchie, *Plasma Losses by Fast Electrons in Thin Films*, Phys. Rev. **106**, p. 874 (1957)

[217] C. J. Powell, J. B. Swan, *Origin of the Characteristic Electron Energy Losses in Aluminum*, Phys. Rev. **115**, pp. 869–875 (1959)

[218] E. A. Stern and R. A. Ferrell, *Surface Plasma Oscillations of a Degenerate Electron Gas*, Phys. Rev. **120**, p. 130 (1960)

[219] D. L. Mills, E. Burstein, *Polaritons: the electromagnetic modes of media*, Rep. Prog. Phys. **37**, p. 817 (1974)

[220] A. Otto, *Excitation of Nonradiative Surface Plasma Waves in Silver by the Method of Frustrated Total Reflection*, Zeitschrift f. Physik **216**, p. 398 (1968)

[221] E. Kretschmann, H. Raether, *Radiative decay of non radiative surface plasmons excited by light*, Z. Naturf. A **23**, p. 2135 (1968)

[222] E. Kretschmann, *Die Bestimmung optischer Konstanten von Metallen durch Anregung von Oberflächenplasmonschwingungen*, Zeitschrift f. Physik **241**, p. 333 (1971)

[223] F. Abeles, *Surface Electromagnetic Waves Ellipsometry*, Surface Sci. 56, p. 237 (1976)

[224] I. Pockrand *Surface Plasma Oscillations At Silver Surfaces With Thin Transparent And Absorbing Coatings*, Surface Sci. **72**, p. 577 (1978)

[225] J. G. Gordon II, J. D. Swalen *The Effect Of Thin Organic Films On The Surface Plasma Resonance On Gold*, Opt. Commun. **22**, p. 374 (1977)

[226] I. Pockrand, J. D. Swalen, J. G. Gordon II, M. R. Philpott, *Surface plasmon spectroscopy of organic monolayer assemblies*, Surface Sci. **74**, pp. 237–244 (1978)

[227] X. Guo, *Surface plasmon resonance based biosensor technique: a review*, Journal of biophotonics **5**, No. 7, (2012)

[228] H. Raether, *Physics of Thin Films* **9**, p. 145 (1977)

[229] P. B. Johnson, R. W. Christy, *Optical constants of noble metals*, Phys. Rev. B **6**, pp. 4370–4379 (1972)

[230] http://www.wave-scattering.com/drudefit.html

[231] P. R. West, S. Ishii, G. V. Naik, N. K. Emani, V. M. Shalaev, A. Boltasseva, *Searching for better plasmonic materials*, Laser & Photonics Reviews **4**, pp. 795–808 (2010)

[232] E. N. Economou, *Surface Plasmons in Thin Films*, Phys. Rev. **182**, p. 539 (1969)

[233] A. Hohenau, J. R. Krenn, A. L. Stepanov, A. Drezet, H. Ditlbacher, B. Steinberger, A. Leitner, F. R. Aussenegg, *Dielectric optical elements for surface plasmons*, Opt. Lett. **30**, pp. 893–895 (2005)

[234] J. Takahara, S. Yamagishi, H. Taki, A. Morimoto, T. Kobayashi, *Guiding of a one-dimensional optical beam with nanometer diameter*, Opt. Lett. **22**, p. 475 (1997)

[235] J.-C.Weeber, A. Dereux, C. Girard, J. R. Krenn, J.-P. Goudonnet, *Plasmon polaritons of metallic nanowires for controlling submicron propagation of light*, Phys. Rev. B **60**, pp. 9061–9068 (1999)

[236] H. Ditlbacher, A. Hohenau, D. Wagner, U. Kreibig, M. Rogers, F. Hofer, F. R. Aussenegg, and J. R. Krenn, *Silver Nanowires as Surface Plasmon Resonators*, Phys. Rev. Lett. **95**, 257403 (2005)

[237] E. Verhagen, M. Spasenovic, A. Polman, L. Kuipers, *Nanowire Plasmon Excitation by Adiabatic Mode Transformation*, Phys. Rev. Lett. **102**, 203904 (2009)

[238] M. Quinten, A. Leitner, J. R. Krenn, F. R. Aussenegg, *Electromagnetic energy transport via linear chains of silver nanoparticles*, Opt. Lett. **23**, p. 1331 (1998)

[239] S. A. Maier, P. G. Kik, H. A. Atwater, S. Meltzer, E. Harel, B. E. Koel, and A. A. G. Requicha, *Local detection of electromagnetic energy transport below the diffraction limit in metal nanoparticle plasmon waveguides*, Nat. Mat. **2**, pp. 229–232 (2003)

[240] S. C. Kitson, W. L. Barnes, and J. R. Sambles, *Full Photonic Band Gap for Surface Modes in the Visible*, Phys. Rev. Lett. **77**, pp. 2670–2673 (1996)

[241] S. I. Bozhevolnyi, J. Erland, K. Leosson, P. M. W. Skovgaard, and J. M. Hvam, *Waveguiding in Surface Plasmon Polariton Band Gap Structures*, Phys. Rev. Lett. **86**, pp. 3008–3011 (2001)

[242] J.-C. Weeber, J. R. Krenn, A. Dereux, B. Lamprecht, Y. Lacroute, and J. P. Goudonnet, *Near-field observation of surface plasmon polariton propagation on thin metal stripes* Phys. Rev. B **64**, 045411 (2001)

[243] P. Berini, *Plasmon-polariton waves guided by thin lossy metal films of finite width: Bound modes of symmetric structures*, Phys. Rev. B **61**, 10484 (2000)

[244] R. Zia, M. D. Selker, M. L. Brongersma, *Leaky and bound modes of surface plasmon waveguides*, Phys. Rev. B **71**, 165431 (2005)

[245] J. Jung, T. Sondergaard, S. I. Bozhevolnyi, *Theoretical analysis of square surface plasmon-polariton waveguides for long-range polarization-independent waveguiding*, Phys. Rev. B **76**, 035434 (2007)

[246] J.-C. Weeber, J. R. Krenn, A. Dereux, B. Lamprecht, Y. Lacroute, J. P. Goudonnet, *Near-field observation of surface plasmon polariton propagation on thin metal stripes*, Phys. Rev. B **64**, 045411 (2001)

[247] T. Nikolajsen, K. Leosson, I. Salakhutdinov, S. I. Bozhevolnyi, *Polymerbased surface-plasmon-polariton stripe waveguides at telecommunication wavelengths*, Appl. Phys. Lett. **82**, pp. 668–670 (2003)

[248] J.-C. Weeber, Y. Lacroute, A. Dereux, E. Devaux, T. Ebbesen, C. Girard, M. U. Gonzcalez, A.-L. Baudrion, *Near-field characterization of Bragg mirrors engraved in surface plasmon waveguides*, Phys. Rev. B **70**, 235406 (2004)

[249] P. Berini, R. Charbonneau, N. Lahoud, *Long-Range Surface Plasmons on Ultrathin Membranes*, Nano Lett. **7**, p. 1376 (2007)

[250] H. J. Lezec, J. A. Dionne1, H, A. Atwater, *Negative Refraction at Visible Frequencies*, Science **316**, pp. 430–432 (2007)

[251] J. A. Dionne, E. Verhagen, A. Polman, H. A. Atwater, *Are negative index materials achievable with surface plasmon waveguides? A case study of three plasmonic geometries*, Opt. Expr. **16**, 19001 (2008)

[252] I. V. Novikov, A. A. Maradudin, *Channel polaritons*, Phys. Rev. B **66**, 035403 (2002)

[253] D. K. Gramotnev, D. F. P. Pile, *Single-mode subwavelength waveguide with channel plasmon-polaritons in triangular grooves on a metal surface*, Appl. Phys. Lett. **85**, p. 6323 (2004)

[254] S. I. Bozhevolnyi, V. S. Volkov, E. Devaux, J.-Y. Laluet, T. W. Ebbesen, *Channel plasmon subwavelength waveguide components including interferometers and ring resonators*, Nature **440**, 508–511 (2006)

[255] V. S. Volkov, S. I. Bozhevolnyi, E. Devaux, J.-Y. Laluet, T. W. Ebbesen, *Wavelength selective nanophotonic components utilizing channel plasmon polaritons*, Nano Lett. **7**, pp. 880–884 (2007)

[256] C. Manolatou, S. G. Johnson, S. Fan, P. R. Villeneuve, H. A. Haus, and J. D. Joannopoulos, *High-density integrated optics*, J. Lightwave Technol. **17**, p. 1682 (1999)

[257] B. Steinberger, A. Hohenau, H. Ditlbacher, A. L. Stepanov, A. Drezet, F. R. Aussenegg, A. Leitner, J. R. Krenn, *Dielectric stripes on gold as surface plasmon waveguides*, Appl. Phys. Lett. **88**, 094104 (2006)

[258] H. Kogelnik, *Theory of Dielectric Waveguides In Integrated Optics*, T. Tamir Editor, Springer (1979)

[259] A. B. Buckman, *Guided-Wave Photonics*, 1st Edition, Saunders College Publishing (1992)

[260] T. Holmgaard, S. I. Bozhevolnyi, L. Markey, A. Dereux, A. V. Krasavin, P. Bolger, A. V. Zayats, *Effcient excitation of dielectric-loaded surface plasmonpolariton waveguide modes at telecommunication wavelengths*, Phys. Rev. B **78**, 165431 (2008)

[261] T. Holmgaard, Z. Chen, S. I. Bozhevolnyi, L. Markey, and A. Dereux, *Design and characterization of dielectric-loaded plasmonic directional couplers*, J. Lightwave Technol. **27**, pp. 5521–5528 (2009)

[262] T. Holmgaard, S. I. Bozhevolnyi, L. Markey, A. Dereux, *Dielectric-loaded surface plasmon-polariton waveguides at telecommunication wavelengths: Excitation and characterization*, Appl. Phys. Lett. **92**, 011124 (2008)

[263] T. Holmgaard, Z. Chen, S. I. Bozhevolnyi, L. Markey, A. Dereux, *Dielectric-loaded plasmonic waveguide-ring resonators*, Opt. Express **17**, pp. 2968–2975 (2009)

[264] J. Gosciniak, L. Markey, A. Dereux, S. I. Bozhevolnyi, *Thermo-optic control of dielectric-loaded plasmonic Mach-Zehnder interferometers and directional coupler switches*, Nanotechnology **23**, 444008 (2012)

[265] S. I. Bozhevolnyi, Editor, *Plasmonic Nanoguides and Circuits*, Pan Stanford Publishing (2009)

[266] T. Holmgaard, J. Gosciniak, S. I. Bozhevolnyi, *Long-range dielectric-loaded surface plasmon-polariton waveguides*, Opt. Express **18**, pp. 23009–23015 (2010)

[267] H. A. Jamid, M. N. Akram, *Analysis of antiresonant reflecting optical waveguide gratings by use of the method of lines*, Appl. Opt. **42**, pp. 3488–3494 (2003)

[268] M. A. Duguay, Y. Kokubun, T. L. Koch, L. Pfeiffer, *Antiresonant reflecting optical waveguides in SiO2-Si multilayer structures*, Appl. Phys. Lett. **49**, pp. 13–15 (1986)

[269] R. A. Zsigmondy, *Über wässrige Lösungen metallischen Goldes*, Justus Liebig's Annalen der Chemie **301**, p. 29 (1898)

[270] B. Auguie, W. L. Barnes, *Collective Resonances in Gold Nanoparticle Arrays*, Phys. Rev. Lett. **101**, 143902 (2008)

[271] A. Lovera, B. Gallinet, P. Nordlander, O. J. F. Martin, *Mechanisms of Fano Resonances in Coupled Plasmonic Systems*, ACS Nano **7**, American Chemical Society, pp. 4527–4536 (2013)

[272] K. Thyagarajan, J. Butet, O. J. F. Martin, *Augmented Second Harmonic Generation Using Fano Resonances in Plasmonic Systems*, Nano Lett. **13**, 1847–1851 (2013)

[273] J. Bohandy, B. Kim, F. Adrian, *Metal deposition from a supported metal film using an excimer laser*, J. Appl. Phys. **60**, pp. 1538–1539 (1986)

[274] P. Papakonstantinou, N. A. Vainos, C. Fotaki, *Microfabrication by UV femtosecond laser ablati on of Pt, Cr and indium oxide thin films*, Appl. Surf. Sci. **151**, pp. 159–170 (1999)

[275] F. Korte, J. Koch, and B. N. Chichkov, *Formation of microbumps and nanojets on gold targets by femtosecond laser pulses*, Appl. Phys. A **79**, pp. 879–881 (2004)

[276] D. A. Willis and V. Grosu, *Microdroplet deposition by laser-induced forward transfer*, Appl. Phys. Lett. **86**, 244103 (2005)

[277] D. P. Banks, C. Grivas, J. D. Mills, R. W. Eason, I. Zergioti, *Nanodroplets deposited in micro arrays by femtosecond Ti:sapphire laser-induced forward transfer*, Appl. Phys. Lett. **89**, 193107 (2006)

[278] L. Yang, C. Wang, X. Ni, Z. Wang, W. Jia, L. Chai, *Microdroplet deposition of copper film by femtosecond laser-induced forward transfer*, Appl. Phys. Lett. **89**, 161110 (2006)

[279] J. Koch, F. Korte, T. Bauer, C. Fallnich, A. Ostendorf, B. N. Chichkov, *Nanotexturing of gold films by femtosecond laser-induced melt dynamics*, Appl. Phys. A **81**, pp. 325–328 (2005)

[280] E. Palik, *Handbook of Optical Constant of Solids*, Academic, San Diego, CA (1985)

[281] RefractiveIndex.INFO, *Refractive Index Database*, http://refractiveindex.info (2014)

[282] E.H. Synge, *An application of piezoelectricity to microscopy*, Phil. Mag. **13**, p. 297 (1932)

[283] D. W. Pohl, *Optical near field scanning microscope*, US-Patent Nr. 4604520 (1982)

[284] M. Sandtke, R. J. Engelen, H. Schoenmaker, I. Attema, H. Dekker, I. Cerjak, J. P. Korterik, F. B. Segerink, L. Kuipers, *Novel instrument for surface plasmon polariton tracking in space and time*, Rev. Sci. Instrum. **79**, 013704 (2008)

[285] C. Marquart, *Scanning Near-Field Microscopy of Surface Plasmon Polariton Scattering in Structures of Gold Nano-Particles*, Institute of Physics, Aalborg University, http://projekter.aau.dk/projekter/files/61061127/1086802030.pdf (2004)

[286] E. Kröger, H. Raether, *Light emission from non radiative plasmons excited by electrons on smooth surfaces*, Z. Phys. **224**, p. 1 (1971)

[287] H.J. Simon, J.K. Guha, *Directional surface plasmon scattering from silver films*, Opt. Comm. **18**, pp. 391–394 (1976)

[288] B. Hecht, H. Bielefeldt, L. Novotny, Y. Inouye, D. W. Pohl, *Local Excitation, Scattering, and Interference of Surface Plasmons*, Phys. Rev. Lett. **77**, p. 1889 (1996)

[289] A. Drezet, A. Hohenau, A. L. Stepanov, H. Ditlbacher, B. Steinberger, N. Galler, F. R. Aussenegg, A. Leitner, J. R. Krenn, *How to erase surface plasmon fringes*, Appl. Phys. Lett. **89**, 091117 (2006)

[290] A. Drezet, A. Hohenau, D. Koller, A. Stepanov, H. Ditlbacher, B. Steinberger, F. R. Aussenegg, A. Leitner, J. R. Krenn, *Leakage radiation microscopy of surface plasmon polaritons*, Materials Science and Engineering B **149**, pp. 220–229 (2008)

[291] E. Brüche, *Elektronenmikroskopische Abbildung mit lichtelektrischen Elektronen*, Z. Phys. **86**, pp. 448–450 (1933)

[292] H. Lüth, *Surfaces and Interfaces of Solid Materials*, 3rd Edition, Springer: Berlin / Heidelberg, p. 556 (1995)

[293] R. Fowler, *The Analysis of Photoelectric Sensitivity Curves for Clean Metals at Various Temperatures*, Phys. Rev. **38**, pp. 45–56 (1931)

[294] L. A. DuBridge, *Theory of the Energy Distribution of Photoelectrons*, Phys. Rev. **43**, pp. 727–741 (1933)

[295] J. H. Bechtel, W. L. Smith, N. Bloembergen, *Two-photon photoemission from metals induced by picosecond laser pulses*, Phys. Rev. B **15**, pp. 4557–4563 (1977)

[296] A. Kubo, N. Pontius, H. Petek, *Femtosecond microscopy of surface plasmon polariton wave packet evolution at the silver/vacuum interface*, Nano Lett.**7**, p. 470-5 (2007)

[297] H. Skriver, N. Rosengaard, *Surface energy and work function of elemental metals*, Phys. Rev. B **46**, pp. 7157–7168 (1992)

[298] M. Bauer, *Real-time Investigations of the Lifetime of Electronic Excitations at Clean and Adsorbate-covered Metal Surfaces*, Dissertation, ETH Zürich (1997)

[299] W. Swiech, G. Fecher, C. Ziethen, O. Schmidt, G. Schönhense, K. Grzelakowski, C. M. Schneider, R. Frömter, H. Oepen, J. Kirschner, *Recent progress in photoemission microscopy with emphasis on chemical and magnetic sensitivity*, J. Electron Spectroscopy and Related Phenomena **84**, pp. 171–188 (1997)

[300] C. Lemke, *Orts- und zeitaufgelöste Charakterisierung ultrakurzer Wellenpakete in plasmonischen Nanostrukturen*, Dissertation, Christian-Albrechts-University Kiel (2014)

[301] L. Zhang, A. Kubo, L. Wang, H. Petek, T. Seideman, *Imaging of surface plasmon polariton fields excited at a nanometer-scale slit*, Phys. Rev.B **84**, 245442 (2011)

[302] T. Leißner, *Plasmonische Wellenleitung an Gold/para-Hexaphenyl-Grenzflächen*, Dissertation, Christian-Albrechts-University Kiel (2013)

[303] V. K. Valev, A. V. Silhanek, Y. Jeyaram, D. Denkova, B. De Clercq, V. Petkov, X. Zheng, V. Volskiy, W. Gillijns, G. A. E. Vandenbosch, O. A. Aktsipetrov, M. Ameloot, V. V. Moshchalkov, T. Verbiest, *Hotspot Decorations Map Plasmonic Patterns with the Resolution of Scanning Probe Techniques*, Phys. Rev. Lett. **106**, 226803 (2011)

[304] V. K. Valev, A. V. Silhanek, N. Smisdom, B. De Clercq, W. Gillijns, O. A. Aktsipetrov, M. Ameloot, V. V. Moshchalkov, T. Verbiest, *Linearly polarized second harmonic generation microscopy reveals chirality*, Optics Express **18**, pp. 8286–8293 (2010)

[305] C. Hubert, A. Rumyantseva, G. Lerondel, J. Grand, S. Kostcheev, L. Billot, A. Vial, R. Bachelot, P. Royer, S. H. Chang, S. K. Gray, G. P. Wiederrecht, G. C. Schatz, *Near-Field Photochemical Imaging of Noble Metal Nanostructures*, Nano Lett. **5**, pp. 615–619 (2005)

[306] http://optics.synopsys.com

[307] http://optics.synopsys.com/RSoft/ RSoft-passive-device-fullwave.html

[308] M. N. O. Sadiku, *Numerical Techniques in Electromagnetics with MATLAB*, Taylor & Francis Group, CRC Press (2009)

[309] D. C. Heggie, *Alexander Thom, 26 March 1894 - 7 November 1985*, Quarterly Journal of the Royal Astronomical Society **28**, pp. 178–182 (1987)

[310] A. Thom, C. J. Apelt, *Field Computations in Engineering and Physics*, London, D. Van Nostrand (1961)

[311] R. Courant, K. O. Friedrichs, H. Lewy, *Über die partiellen Differenzengleichungen der mathematischen Physik*, Mathematische Annalen **100**, pp. 32–74 (1928)

[312] K. Yee, *Numerical solution of initial boundary value problems involving maxwell's equations in isotropic media*, IEEE Transactions on Antennas and Propagation **14**, pp. 302–307 (1966)

[313] J.-P. Berenger, *A perfectly matched layer for the absorption of electromagnetic waves*, Journal of Computational Physics **114**, pp. 185–200 (1994)

[314] A. Taflove, S. C. Hagness, *Computational Electrodynamics: The Finite-Difference Time-Domain Method*, 3rd. Edition, Artech House (2005)

[315] http://optics.synopsys.com/RSoft/ RSoft-passive-device-femsim.html

[316] R. Courant, *Variational methods for the solution of problems of equilibrium and vibrations*, Bull. Am. Math. Soc. **49**, pp. 1–23 (1943)

[317] P. Silvester, *A general high-order finite element waveguide analysis program*, IEEE Trans. Microw. Theory Tech. **17**, pp. 204–210 (1969)

[318] M. K. Haldar, *Introducing the Finite Element Method in electromagnetics to undergraduates using MATLAB*, International Journal of Electrical Engineering Education **43**, pp. 232–244 (1969)

[319] L. Lorenz *Lysbevaegelsen i og uden for en af plane Lysbolger belyst Kugle*, Det Kongelige Danske Videnskabernes Selskabs Skrifter. 6. Raekke, 6. Bind, pp. 1–62 (1890)

[320] L. Lorenz, *Sur la lumiere reflechie et refractee par une sphere (surface) transparente*, Œuvres scientifiques de L. Lorenz, revues et annotees par H. Valentiner. Tome Premier, Libraire Lehmann & Stage, Kopenhagen, pp. 403–529 (1898)

[321] W. Hergert, T. Wriedt, Editors *The Mie Theory*, Springer Series in Optical Sciences **169**, Springer (2012)

[322] C. F. Bohren, D. R. Huffman, *Absorption and Scattering of Light by Small Particles*, Wiley-VCH (2007)

[323] M. Born, E. Wolf, *Principles of Optics: Electromagnetic Theory of Propagation, Interference and Diffraction of Light*, 7th Edition, Cambride University Press (2007)

[324] H. C. Van de Hulst, *Light Scattering by Small Particles*, Dover, New York (1981)

[325] H. DeVoe, *Optical Properties of Molecular Aggregates. I. Classical Model of Electronic Absorption and Refraction*, The Journal of Chemical Physics **41**, 393–400 (1964)

[326] E. M. Purcell, C. R. Pennypacker, *Scattering and adsorption of light by nonspherical dielectric grains*, Astrophys Journal **186**, pp. 705–714 (1973)

[327] B. T. Draine, *The Discrete Dipole Approximation and its Application to Interstellar Graphite Grains*, Astrophys. Journal **333**, pp. 848–872 (1988)

[328] B. T. Draine, P.J. Flatau, *Discrete-dipole appr oximation for scattering calculations*, J. Opt. Soc. Am. A **11**, pp. 1491–1499 (1994)

[329] M. A. Yurkin, A. G. Hoekstra, *The discrete dipole approximation: an overview and recent developments*, J. Quant. Spectrosc. Radiat. Transf. **106**, p. 558 (2007)

Contributing Original Publications

The original publication contributing to this habilitation treatise will be given in chronological order of the publication dates. The publications, which are provided subsequently, are:

1. **C. Reinhardt**, S. Passinger, B. N. Chichkov, C. Marquart, I. P. Radko, S. I. Bozhevolnyi, *Laser-fabricated dielectric optical components for surface plasmon polaritons*, Optics Letters **31**, pp. 1307–1309 (2006) (Number in references list: [11])

2. **C. Reinhardt**, S. Passinger, B. N. Chichkov, W. Dickson, G. A. Wurtz, P. Evans R. Pollard, and A. V. Zayats, *Restructuring and modification of metallic nanorod arrays using femtosecond laser direct writing*, Appl. Phys. Lett. **89**, 231117 (2006) (Number in references list: [14])

3. J. Koch, T. Bauer, **C. Reinhardt**, B. N. Chichkov, *Recent progress in direct write 2D and 3D photofabrication technique with femtosecond laser pulses*, in Recent Advances in Laser Material Processing, chapter **8**, Elsevier, pp. 472–495 (2006) (Number in references list: [28])

4. R. Kiyan, **C. Reinhardt**, S. Passinger, A. L. Stepanov, A. Hohenau, J. R. Krenn, B. N. Chichkov, *Rapid prototyping of optical components for surface plasmon polaritons*, Optics Express **15**, pp. 4205–4215 (2007) (Number in references list: [15])

5. S. Passinger, M. S. Saifullah, **C. Reinhardt**, K. R. V. Subramanian, B. N. Chichkov, M. E. Welland, *Direct 3D Patterning of TiO_2 Using Femtosecond Laser Pulses*, Advanced Materials **19**, pp. 1218–1221 (2007) (Number in references list: [41])

6. **C. Reinhardt**, S. Passinger, V. Zorba, B. N. Chichkov, C. Fotakis, *Replica molding of picosecond laser fabricated Si microstructures*, Applied Physics A **87**, pp. 673–677 (2007) (Number in references list: [48])

7. **C. Reinhardt**, R. Kiyan, S. Passinger, A. L. Stepanov, A. Ostendorf, and B. N. Chichkov, *Rapid laser prototyping of plasmonic components*, Appl. Phys. A **89**, pp. 321–325 (2007) (Number in references list: [16])

8. A. B. Evlyukhin, S. I. Bozhevolnyi, A. L. Stepanov, R. Kiyan, **C. Reinhardt**, S. Passinger, B. N. Chichkov, *Focusing and directing of surface plasmon polaritons by curved chains of nanoparticles*, Optics Express **15**, pp. 16668–16680 (2007) (Number in references list: [22])

9. S. Passinger, A. Seidel, C. Ohrt, **C. Reinhardt**, A. L. Stepanov, R. Kiyan, B. N. Chichkov, *Novel efficient design of Y-splitter for surface plasmon polariton applications*, Opt. Express **16**, 14369–14379 (2008) (Number in references list: [21])

10. F. Claeyssens, E. A. Hasan, A. Gaidukeviciute, D. S. Achilleos, A. Ranella, **C. Reinhardt**, A. Ovsianikov, X. Shizhou, C. Fotakis, M. Vamvakaki, B. N. Chichkov, M. Farsari, *Three-Dimensional Biodegradable Structures Fabricated by Two-Photon Polymerization*, Langmuire **25**, pp. 3219–3223 (2009) (Number in references list: [29])

11. F. Heinroth, I. Bremer, S. Münzer, P. Behrens, **C. Reinhardt**, S. Passinger, C. Ohrt, B. Chichkov, *Microstructured templates produced using femtosecond laser pulses as templates for the deposition of mesoporous silicas*, Microporous and Mesoporous Materials **119**, pp. 104–108 (2009) (Number in references list: [42])

12. A. Seidel, C. Ohrt, S. Passinger, **C. Reinhardt**, R. Kiyan, B. Chichkov, *Nanoimprinting of dielectric loaded surface plasmon-polariton waveguides from masters fabricated by 2-photon polymerization technique*, JOSA B **26**, pp. 810–812 (2009) (Number in references list: [49])

13. A. B. Evlyukhin, C. Reinhardt, E. Evlyukhina, B. N. Chichkov, *Asymmetric and symmetric local surface plasmon-polariton excitation on chains of nanoparticles*, Optics Letters **34**, pp. 2237 - 2239 (2009) (Number in references list: [34])

14. A. Schilling, J. Schilling, **C. Reinhardt**, B. Chichkov, *A superlens for the deep ultraviolet*, Appl. Phys. Lett. **95**, 121909 (2009) (Number in references list: [33])

15. **C. Reinhardt**, A. Seidel, A. B. Evlyukhin, W. Cheng, B. N. Chichkov, *Mode-selective excitation of laser-written dielectric-loaded surface plasmon polariton Waveguides*, Journal of the Optical Society of America B **26**, pp. B55–B60 (2009) (Number in references list: [23])

16. A. I. Kuznetsov, A. B. Evlyukhin, **C. Reinhardt**, A. Seidel, R. Kiyan, W. Cheng, A. Ovsianikov, B. N. Chichkov, *Laser-induced transfer of metallic nanodroplets for plasmonics and metamaterial applications*, Journal of the Optical Society of America B **26**, pp. B130–B138 (2009) (Number in references list: [30])

17. F. Heinroth, S. Münzer, A. Feldhoff, S. Passinger, W. Cheng, **C. Reinhardt**, B. Chichkov, P. Behrens, *Three-dimensional titania pore structures produced by using a femtosecond laser pulse technique and a dip coating procedure*, Journal of Materials Science **44**, pp. 6490–6497 (2009) (Number in references list: [43])

18. A. Seidel, J. Gosciniak, M. U. Gonzalez, J. Renger, **C. Reinhardt**, R. Kiyan, R. Quidant, S. I. Bozhevolnyi, B. N. Chichkov, *Fiber-Coupled Surface Plasmon Polariton Excitation in Imprinted Dielectric-Loaded Waveguides*, International Journal of Optics **2010**, 897829 (2010) (Number in references list: [50])

19. C. Schizas, V. Melissinaki, A. Gaidukeviciute, **C. Reinhardt**, C. Ohrt, V. Dedoussis, B. N. Chichkov, C. Fotakis, M. Farsari, D. Karalekas, *On the design and fabrication by two-photon polymerization of a readily assembled micro- valve*, International Journal of Advanced Manufacturing Technology **48**, pp. 435–441 (2010) (Number in references list: [27])

20. **C. Reinhardt**, A. Seidel, A. B. Evlyukhin, W. Cheng, R. Kiyan, B. N. Chichkov, *Direct laser-writing of dielectric-loaded surface plasmon-polariton waveguides for the visible and near infrared*, Appl. Phys. A **100**, pp. 347–352 (2010) (Number in references list: [17])

21. A. B. Evlyukhin, **C. Reinhardt**, A. Seidel, B. S. Luk'yanchuk, B. N. Chichkov, *Optical response features of Si-nanoparticle arrays*, Phys. Rev. B **82**, 045404 (2010) (Number in references list: [35])

22. I. Sakellari, A. Gaidukeviciute, A. Giakoumaki, D. Gray, C. Fotakis, M. Farsari, M. Vamvakaki, **C. Reinhardt**, A. Ovsianikov, B. N. Chichkov, *Two-photon polymerization of titanium-containing sol-gel composites for three-dimensional structure fabrication*, Applied Physics A **100**, pp. 359–364 (2010) (Number in references list: [44])

23. A. Seidel, **C. Reinhardt**, T. Holmgaard, W. Cheng, T. Rosenzveig, K. Leosson, S. I. Bozhevolnyi, B. N. Chichkov, *Demonstration of Laser-Fabricated DLSPPW at Telecom Wavelength*, IEEE Photonics Journal **2**, pp. 652–658 (2010) (Number in references list: [18])

24. A. I. Kuznetsov, A. B. Evlyukhin, M. R. Goncalves, **C. Reinhardt**, A. Koroleva, M. L. Arnedillo, R. Kiyan, O. Marti, B. N. Chichkov, *Laser Fabrication of Large Scale Nanoparticle Arrays for Sensing Applications*, ACS Nano **19**, American Chemical Society, pp. 4843–4849 (2011) (Number in references list: [31])

25. K. Terzaki, N. Vasilantonakis, A. Gaidukeviciute, **C. Reinhardt**, C. Fotakis, M. Vamvakaki, M. Farsari, *3D conducting nanostructures fabricated using direct laser writing*, Optical Materials Express **1**, pp. 58–597 (2011) (Number in references list: [45])

26. A. B. Evlyukhin, A. I. Kuznetsov, S. M. Novikov, J. Beermann, **C. Reinhardt**, R. Kiyan, S. I. Bozhevolnyi, B. N. Chichkov, *Optical properties of spherical gold mesoparticles*, Applied Physics B **106**, pp. 841–848 (2012) (Number in references list: [32])

27. A. Markov, **C. Reinhardt**, B. Ung, A. B. Evlyukhin, W. Cheng, B. N. Chichkov, M. Skorobogatiy, *Photonic bandgap plasmonic waveguides*, Optics Letters **36**, pp. 2468–2470 (2011) (Number in references list: [19])

28. A. B. Evlyukhin, **C. Reinhardt**, B. N. Chichkov, *Multipole light scattering by nonspherical nanoparticles in the discrete dipole approximation* Phys. Rev. B **84**, 235429 (2011) (Number in references list: [51])

29. V. K. Valev, D. Denkova, X. Zheng, A. I. Kuznetsov, **C. Reinhardt**, B. N. Chichkov, G. Tsutsumanova, E. J.Osley, V. Petkov, B. DeClercq, A. V. Silhanek, Y. Jeyaram, V. Volskiy, P. A. Warburton, G. A. E. Vandenbosch, S. Russev, O. A. Aktsipetrov, M. Amelo, V. M. Moshchalkov, T. Verbiest, *Plasmon-Enhanced*

Sub-Wavelength Laser Ablation: Plasmonic Nanojets, Advanced Materials **24**, pp. OP29–OP35 (2012) (Number in references list: [25])

30. V. Ferreras-Paz, M. Emons, K.Obata, A. Ovsianikov, S. Peterhänsel, K. Frenner, **C. Reinhardt**, B. Chichkov, U. Morgner, W. Osten*Development of functional sub-100 nm structures with 3D two-photon polymerization technique and optical methods for characterization*, Journal of Laser Application **24**, 042004 (2012) (Number in references list: [46])

31. A. B. Evlyukhin, S. M. Novikov, U. Zywietz, R. L. Eriksen, **C. Reinhardt**, S. I. Bozhevolnyi, B. N. Chichkov, *Demonstration of Magnetic Dipole Resonances of Dielectric Nanospheres in the Visible Region*, Nano Lett. **12**, pp. 3749–3755 (2012) (Number in references list: [36])

32. A. B. Evlyukhin, **C. Reinhardt**, U. Zywietz, B. N. Chichkov, *Collective resonances in metal nanoparticle arrays with dipole-quadrupole interactions*, Phys. Rev. B **85**, 245411 (2012) (Number in references list: [52])

33. A. Zukauskas, M. Malinauskas, **C. Reinhardt**, B. N. Chichkov, R. Gadonas, *Closely packed hexagonal conical microlens array fabricated by direct laser photopolymerization*, Applied Optics **51**, pp. 4995–5003 (2012) (Number in references list: [47])

34. G. Volpe, M. Noack, S. S. Acimovic, **C. Reinhardt**, R. Quidant, *Near-Field Mapping of Plasmonic Antennas by Multiphoton Absorption in Poly(methyl methacrylate)*, Nano Letters **12**, pp. 4864–4868 (2012) (Number in references list: [24])

35. C. Lemke, C. Schneider, T. Leissner, D. Bayer, J. W. Radke, A. Fischer, P. Melchior, A. B. Evlyukhin, B. N. Chichkov, **C. Reinhardt**, M. Bauer, M. Aeschlimann, *Spatiotemporal Characterization of SPP Pulse Propagation in Two-Dimensional Plasmonic Focussing Devices*, Nano Letters **13**, pp. 1053–1058 (2013) (Number in references list: [6])

36. V. K. Valev, W. Libaers, U. Zywietz, X. Zheng, M. Centini, N. Pfullmann, L. O. Herrmann, **C. Reinhardt**, V. Volskiy, A. V. Silhanek, B. N. Chichkov, C. Sibilia, G. A. E. Vandenbosch, V. V. Moshchalkov, J. J. Baumberg, T. Verbiest, *Nanostripe length-dependence of plasmon-induced material deformation*, Optics Letters **38**, pp. 2256–2258 (2013) (Number in references list: [26])

37. N. Pfullmann, C. Waltermann, M. Noack, S. Rausch, T. Nagy, **C. Reinhardt**, M. Kovacev, V. Knittel, R. Bratschitsch, D. Akemeier, A. Huetten, A. Leitensdorfer, U. Morgner, *Bow-tie nano-antenna assisted generation of extreme ultraviolet radiation*, New Journal of Physics **15**, 093027 (2013) (Number in references list: [9])

38. A. B. Evlyukhin, **C. Reinhardt**, E. Evlyukhin, B. N. Chichkov, *Multipole analysis of light scattering by arbitrary-shaped nanoparticles on a plane surface*, J. Opt. Soc. Am. A **30**, pp. 2589–2598 (2013) (Number in references list: [53])

39. **C. Reinhardt**, A. B. Evlyukhin, W. Cheng, T. Birr, A. Markov, B. Ung, M. Skorobogatiy, B. N. Chichkov, *Bandgap-confined large-mode waveguides for surface plasmon-polaritons*, Journal of the Optical Society of America B **30**, pp. 2898–2905 (2013) (Number in references list: [20])

40. U. Zywietz, **C. Reinhardt**, A. B. Evlyukhin, T. Birr, B. N. Chichkov, *Generation and patterning of Si nanoparticles by femtosecond laser pulses*, Appl. Phys. A **114**, pp. 45–50 (2014) (Number in references list: [37])

41. U. Zywietz, A. B. Evlyukhin, **C. Reinhardt**, B. N. Chichkov. *Laser printing of silicon nanoparticles with resonant optical electric and magnetic responses*, Nature Comm. **5**, p. 4402 (2014) (Number in references list: [38])

42. A. B. Evlyukhin, R. L. Eriksen, W. Cheng, J. Beermann, **C. Reinhardt**, A. Petrov, S. Prorok, M. Eich, B. N. Chichkov, S. I. Bozhevolnyi, *Optical spectroscopy of single Si nanocylinders with magnetic and electric resonances*, Scientific Reports **4**, 4126 (2014) (Number in references list: [39])

43. N. Pfullmann, M. Noack, J. C. de Andrade, S. Rausch, T. Nagy, **C. Reinhardt**, V. Knittel, R. Bratschitsch, A. Leitensdorfer, D. Akemeier, A. Huetten, M. Kovacev, U. Morgner, *Nano-antennae assisted emission of extreme ultraviolet radiation*, Annalen der Physik **526**, pp. 119–134 (2014) (Number in references list: [10])

44. A. I. Aristov, U. Zywietz, A. B. Evlyukhin, **C. Reinhardt**, B. N. Chichkov, A. V. Kabashin, *Laser-ablative engineering of phase singularities in plasmonic metamaterial arrays for biosensing applications*, Appl. Phys. Lett. **104**, 071101 (2014) (Number in references list: [8])

45. C. Lemke, T. Leissner, A. B. Evlyukhin, J. W. Radke, A. Klick, J. Fiutowski, J. Kjelstrup-Hansen, H.-G. Rubahn, B. N. Chichkov, **C. Reinhardt**, M. Bauer, *The Interplay between Localized and Propagating Plasmonic Excitations Tracked in Space and Time*, Nano Letters, DOI 10.1021/nl500106z (2014) (Number in references list: [7])